Cyclisation Cascades via Reactive Iminium Intermediates

A thesis submitted in partial fulfilment of the requirement for the degree of Doctor of Philosophy (D.Phil.)

Alex W. Gregory

Supervisor: Prof. Darren J. Dixon

Wadham College

University of Oxford

Trinity Term 2014

Contents

1. Chapter 1: Enantioselective chiral-BINOL-phosphoric acid catalysed reaction cascade ..... - 1 -
1.1. Introduction ..... - 1 -
1.2. Cascade catalysis ..... - 6 -
1.3. Aim ..... - 9 -
1.4. Synthesis of starting materials ..... - 11 -
1.5. Gold(I) catalysed cyclisation cascade ..... - 12 -
1.6. Chiral BPA catalysed cyclization ..... - 13 -
1.7. Gold and BINOL-phosphoric acid catalyzed enantioselective hydroamination/*N*-sulfonyliminium cyclisation cascade ..... - 17 -
1.7.1. Reaction scope ..... - 22 -
1.7.2. Determination of absolute stereochemistry ..... - 25 -
1.7.3. Scope expansion: *N*-acyliminium analogues ..... - 26 -
1.7.4. *N*-acyliminium cyclisation scope ..... - 28 -
1.7.5. Absolute stereochemistry determination for the *N*-acyliminium cyclisation cascade ..... - 29 -
1.8. Reaction mechanism ..... - 30 -
1.9. Conclusion ..... - 31 -
2. Chapter 2: Iridium catalysed nitro-Mannich cyclisation ..... - 32 -
2.1. Introduction ..... - 32 -
2.1.1. Metal catalysed silane reduction ..... - 32 -
2.1.2. Partial amide reduction and amide activation ..... - 35 -
2.1.3. Nitro-Mannich reaction ..... - 38 -
2.2. Aims ..... - 41 -
2.3. Synthesis of model substrate and proof of principle ..... - 42 -
2.4. Reductive method screen ..... - 43 -
2.5. Optimisation of $IrCl(CO)(PPh_3)_2$ and TMDS conditions ..... - 45 -
2.6. Reaction scope ..... - 48 -
2.6.1. Synthesis of starting materials ..... - 48 -
2.6.2. Synthesis of starting material with an aryl linked nitroalkane tether ..... - 51 -
2.6.3. Iridium catalysed nitro-Mannich cyclisation reaction scope ..... - 53 -
2.7. Reaction Mechanism ..... - 55 -
2.8. Total synthesis of (±)-*epi*-epiquinamide ..... - 57 -

2.9. Proof of relative stereochemistry. ..... - 58 -
2.10. Conclusion ..... - 60 -
3. Chapter 3: Iridium Catalysed Reductive interrupted Pictet-Spengler Cyclisation ..... - 61 -
3.1. Aims ..... - 61 -
3.2. Proof of principal and model substrate synthesis ..... - 61 -
3.3. Reaction optimization ..... - 64 -
3.4. Synthesis of substrates for the reaction scope ..... - 66 -
3.4.1. Kornblum oxidation ..... - 66 -
3.4.2. Optimization of the Fischer indolisation ..... - 67 -
3.5. Scope of the reaction methodology on lactam derived substrates ..... - 69 -
3.6. Acyclic amide examples ..... - 73 -
3.7. Reaction mechanism and diastereoselectivity ..... - 79 -
3.8. Scope expansion: 2-substituted indole tethered lactams ..... - 83 -
3.8.1. Synthesis of starting material. ..... - 83 -
3.9. Conclusion ..... - 87 -
4. Summary and Future Work. ..... - 88 -
5. Bibliography ..... - 93 -
6. Experimental ..... - 100 -
6.1. Chapter 1: Experimental ..... - 102 -
6.2. Chapter 2: Experimental ..... - 154 -
6.3. Chapter 3: Experimental ..... - 176 -
7. Appendicies ..... - 231 -
8. Experimental References ..... - 258 -

Abstract

Thesis overview

The aim of this D.Phil was to develop a range of cyclisation cascades, which initially form a reactive iminium intermediates that can then be attacked by a pendant nucleophile resulting in novel polycyclic structures.

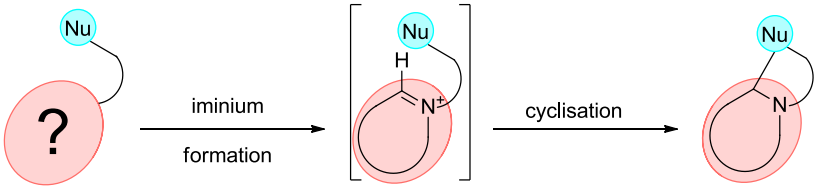

This concept has been applied to the development of three methodologies and has resulted in the discovery of new reactivity as well as the synthesis of a wide range of interesting novel structures

Chapter 1: Enantioselective chiral-BINOL-phosphoric acid catalysed reaction cascade

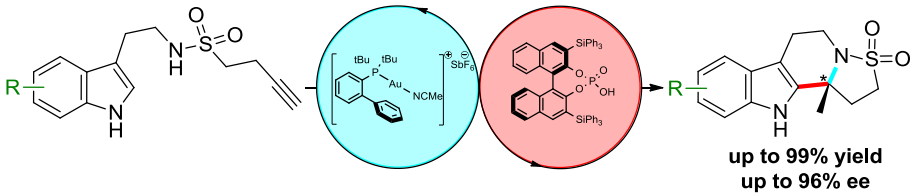

A highly enantioselective hydroamination / *N*-sulfonyliminium cyclisation cascade using a combination of Au(I) and chiral phosphoric acid catalysts has been developed. Proceeding by an initial 5-*exo*-dig hydroamination and a subsequent phosphoric acid catalysed Pictet-Spengler cyclisation, the reaction provides access to complex sulfonamide scaffolds in excellent yields and with high levels of enantiocontrol. The scope can be extended to lactam derivatives, with excellent yields and enantiomeric excesses of up to 93% ee.

Chapter 2: Iridium catalysed nitro-Mannich cyclisation

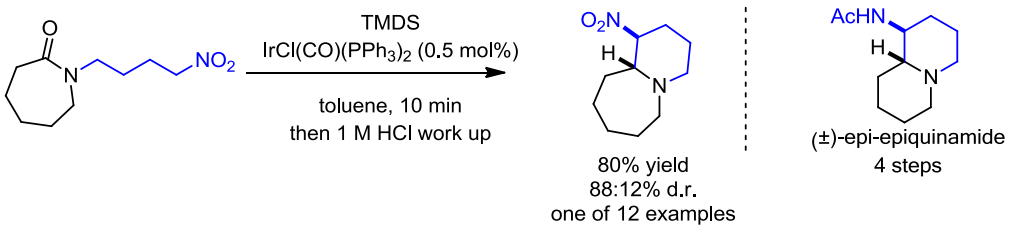

A new chemoselective reductive nitro-Mannich cyclisation reaction sequence of nitroalkyl-tethered lactams has been developed. An initial rapid and chemoselective iridium(I) catalysed reduction of lactams to the corresponding enamine is subsequently followed by intra molecular nitro-Mannich cyclisation. This methodology provides direct access to important alkaloid, natural product-like structures in yields up to 81% and in diastereoselectivities that are typically good to excellent. An in-depth understanding of the reaction mechanism has been gained through NMR studies and characterisation of reaction intermediates. The new methodology has been applied to the total synthesis of (±)-*epi*-epiquinamide in 4 steps.

Chapter 3: Iridium catalysed reductive interrupted Pictet-Spengler cyclisation

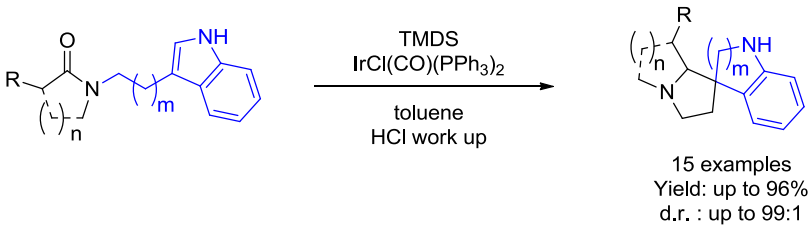

A novel reductive interrupted Pictet-Spengler cyclisation reaction cascade has been created. An iridium(I) catalyzed partial reduction of lactams/amides to the corresponding iminium is subsequently trapped by a pendant indole nucleophile. Interruption of the Pictet-Spengler reaction by indolium reduction provides a wide range of novel spirocyclic indoline moieties in excellent yield and diastereoselectivity.

Declaration and Copyright

I declare that thesis has been written by me, that it is the record of work carried out by me and that it has not been submitted in any previous application for a higher degree at this or any other university or institute of learning. Any work done in collaboration with a research colleague has been fully acknowledged and referenced within the text.

I was admitted as a probationary research student in October 2010 and as a candidate for the degree of Doctor of Philosophy in October 2011; the higher study for which this is a record was carried out in the University of Oxford between 2010 and 2014.

Alex W. Gregory

Date Signature of candidate

In submitting this thesis to the University of Oxford, I understand that I am giving permission for it to be made available for use in accordance with the regulations of the University Library for the time being in force, subject to any copyright vested in the work not being affected thereby. I also understand that the title and the abstract will be published, and that a copy of the work may be made and supplied to any *bona fide* library or research worker, that this thesis will be electronically accessible for personal or research use, and that the library has the right to migrate this thesis into new electronic forms as required to ensure continued access to the thesis. I have obtained any third-party copyright permissions that may be required in order to allow such access and migration.

Acknowledgements

Firstly I would like to Professor Darren Dixon for giving me the opportunity to work in his group in this fantastic city. I would also like to thank him for his seemingly limitless supply of ideas, energy, enthusiasm and continual support throughout my D.Phil.

I must also give a huge amount of thanks to Doctor Pavol Jakubec, under his tuition I have learnt more chemistry than I could ever have done alone as well as what it really takes to be an organic chemist. I also thank him for taking an interest in my work and helping to guide me along the rocky road that is synthetic methodology.

I would like to thank all the Oxford NMR, Mass Spec and X-ray staff for all their hard work and dedication to the oxford students. Without them this thesis would not have been possible.

I would like to thank the DJD group both past and present for providing the most interesting working environment I will ever experience. The range of "intellectual" conversations throughout the years has opened my eyes to the world around me: from the similarities between D.Phil students and Birds of Paradise to "many, many" anatomical facts few would wish to know. I must also thank them for their friendship and in some cases "colleagueship" making this experience truly enjoyable.

I would like to thank Alistair, Anna, Matt, Jin Chao, Allegra, Pengwen and Gerard for proof reading duties.

Finally I would like to thank my family for all their love and support throughout my life, for always believing in me and giving me the opportunity to be whatever I wanted to be.

Abbreviations

ºC: degrees Celsius

Å: angstrom

Ac: acetyl

Alk: alkyl

Ar: aryl, aromatic group, heteroaromatic group

BINOL: 1,1′-binaphthalene-2,2′-diol

Bn: benzyl

Boc: di-*tert*-butyl dicarbonate

BPA: BINOL phosphoric acid

br: broad

Bu: butyl

cm: centimetre

conv.: conversion

COSY: correlation spectroscopy

d: doublet

dd: doublet of doublets

dec.: decomposed

DCM: dichloromethane

DMF: *N*,*N*-dimethylformamide

DMSO: dimethylsulfoxide

EDG: electron-donating group

ee or e.e.: enantiomeric excess

e.g.: *exempli gratia* = for example

EI: electron impact

eq.: equivalent(s)

ES: electrospray

ESI: electrospray ionisation

Et: ethyl

Et_2O: diethyl ether

et al.: *et alii* = and others

EWG: electron-withdrawing group

g: gram(s)

h: hour(s)

HPLC: high performance liquid chromatography

HRMS: high resolution mass spectrometry

HSQC: heteronuclear single-quantum coherence experiment

Hz: Hertz

i or ^{i}: iso

IPA: propan-2-ol

IR: infra-red

LDA: lithium diisopropylamide

Lit.: literature

M: molar

m: meta

m: multiplet

max: maximum

m/z: mass-to-charge ratio

Me: methyl

mg: milligram

MHz: megaHertz

min: minute(s)

mL: millilitre

µL: microlitre

mmol: millimole

mol: mole

m.p.: melting point

m.r. = membered ring

MS: mass spectrometry

M.S.: molecular sieves

n: normal, linear chain

nm: nanometre

NMR: nuclear magnetic resonance

NOE: nuclear overhauser effect

NOESY: nuclear overhauser effect spectroscopy

Nu: nucleophile

N.R.: no reaction

o: ortho

p: para

Ph: phenyl

ppm: parts per million

Pr: propyl

q: quartet

quat: quaternary

R: any group (alkyl, aryl, H *etc*.)

r.t.: room temperature

s: singlet

t: triplet

TBAF: tetrabutylammonium fluoride

^{t}Bu: *tert*-butyl

Temp.: temperature

TFA: trifluoroacetic acid

THF: tetrahydrofuran

TLC: Thin Layer Chromatography

TPS: triphenylsilyl

*p*TSA: *para*-toluenesulfonic acid

General Introduction

Catalysis provides a tool to enable the formation of carbon-carbon bonds that would otherwise be inaccessible due to the relatively inert nature of the chosen starting materials. As a large amount of chemical space is taken up by chiral molecules, catalysts that induce asymmetry are of vital importance in modern chemistry. Whilst transition metal catalysts that induce enantioselectivity have been present for the majority of the second half of the 20th century, their use can result in trace amounts of toxic metal by-products being detectable in the final product. Since the turn of the century a lot of attention has been paid to organocatalysis. Organocatalysis describes reactions catalysed by carbon based molecules. They can offer mild reaction conditions, require non-stringent reaction conditions and crucially do not leave behind metal contamination. Organocatalysis was first reported by Liebig in 1860, when he demonstrated the use of acetaldehyde as a catalyst for the hydration of cyanogen to form oxamide (Scheme 0.1).[1]

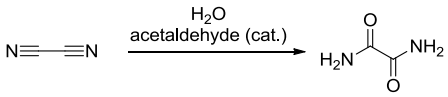

Scheme 0.1. First reported organocatalysed reaction by Liebig in 1860

However, further reactions that employ organocatalysis were not forthcoming and interestingly there are only a few other reports of organocatalysis throughout the 20th century.[2,3,4] The term itself wasn't coined until 2000 by MacMillan *et al* after their groundbreaking discovery of using chiral imidazolidinone compounds **1** to catalyse a range of Diels-Alder reactions.[5] They were also able to extend this methodology to accommodate 1,3-dipolar cycloadditions as well as Friedel-Crafts alkylations, all proceeding with excellent yield and enantioselectivity (Figure 0.1).[6,7,8]

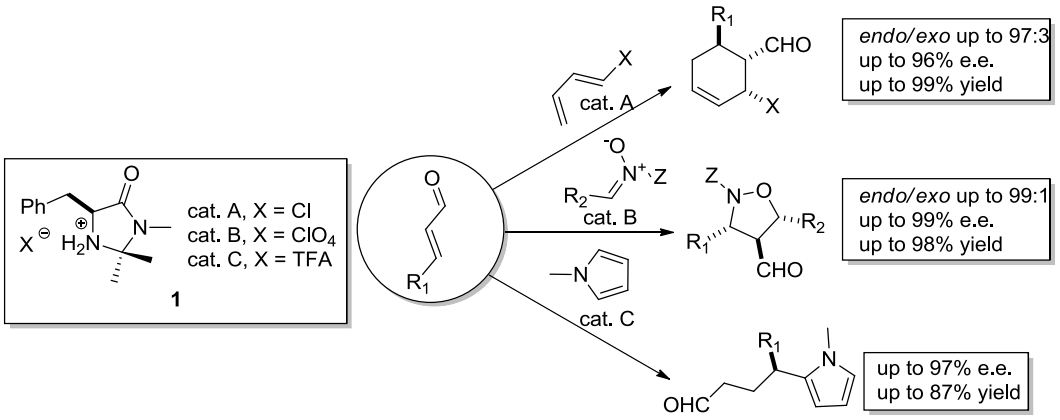

Figure 0.1. Enantioselective imidazolidinone catalysed reactions *via* iminium intermediates by MacMillan *et al*.

Since then organocatalysis has been extensively investigated and is now dominated by two main classes of catalysts: amine- and Brønsted acid-based catalysis.[9] The activation methods can involve the formation of a transient intermediate such as the transformation of a carbonyl to an iminium intermediate, which can perform the desired reaction before being hydrolysed back to the carbonyl as in MacMillan's methodology. Alternatively, organocatalysts can catalyse reactions via non-covalent interactions: hydrogen bonding can increase the electron deficiency of an electrophile as well as increase the nucleophilicity of a nucleophile, this subsequently lowers the activation energy of the reaction leading to bond formation.

With the wide variety of modern chemistry methodologies now available almost any compound can now be made by a synthetic chemist. However the number of steps to make the molecule, as well as the number of reagents used, can affect its enviromental impact.[10] Cascade reactions can offer a partial solution to this problem as they reduce the total number of steps and purification points in a synthesis. This allows the formation of complex molecules with increased efficiency and speed. Cascade reactions can also be used to avoid the isolation of reactive intermediates and therefore can lead to bond forming events that would otherwise be very difficult to carry out in a single step.[11] An impressive example of a

reaction cascade was reported by Paterson *et al* in the synthesis of a fragment of etheromycin. Di-epoxide **2** was synthesised with the hope that upon treatment with acid the diethylisopropylsilyl ether (DEIPS) would hydrolyse and trigger the cascade reaction shown in Scheme 0.2. Incredibly, when **2** was treated with 0.5 M HCl in THF the desired epoxide opening cascade proceeded to form the three new oxygen containing heterocycles, furnishing **3** in 30% yield.[12]

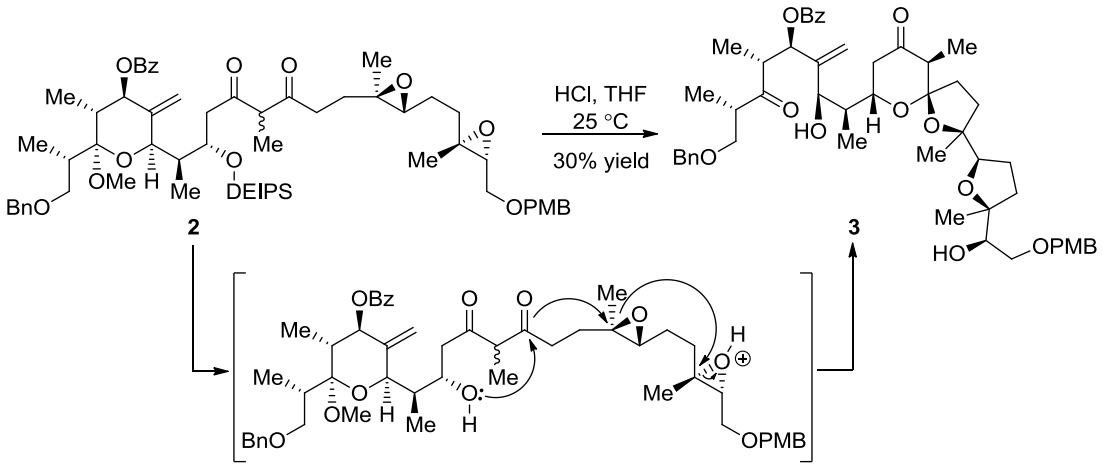

Scheme 0.2. Epoxide opening cascade towards etheromycin

A classic example of a carbon-carbon bond forming cascade reaction was reported by Johnson and co-workers in 1973 (Scheme 1).[13] The polyene cyclisation cascade allows the synthesis of steroid cores *via* a four bond forming cascade reaction. The reaction is initiated with TFA and ethylene carbonate and passes through intermediates **4a** and **4b**, resulting in the formation of polycycle **5** in 65% yield. The process is highly selective, with only one out of a possible 64 diastereomers being formed.

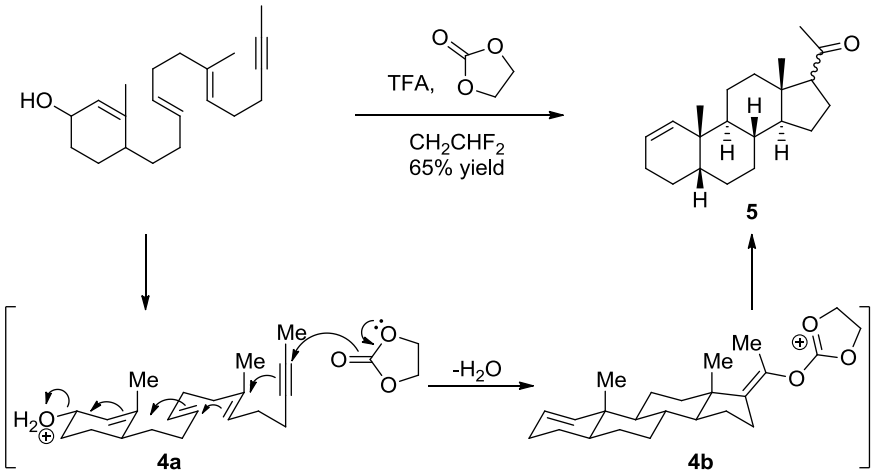

Scheme 0.3. Polyene cyclisation cascade of steroid cores.

Inspired by the potential complexity that can be built up in a single reaction, we hypothesised that a range of useful methodologies could be developed around the *in situ* formation of reactive iminium intermediates, the formation of which could be brought about by a range of modern catalytic methods. The subsequent reaction of the iminium intermediate with a pendant nucleophile would hopefully provide a wide range of complex structures in an efficient atom economic manner (Figure 0.2).

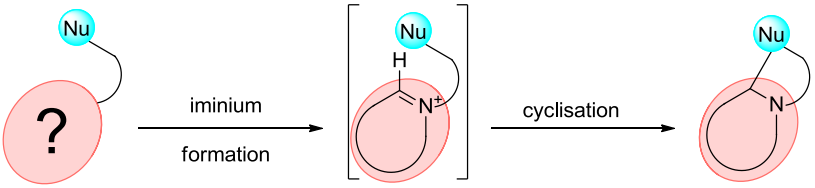

Figure 0.2. D.Phil cascade reaction hypothesis.

1. Chapter 1: Enantioselective chiral-BINOL-phosphoric acid catalysed reaction cascade

1.1. Introduction

Brønsted acid catalysis is one of the largest areas of organocatalysis. The catalysts themselves can range from hydrogen bond donor catalysts such as Schreiner's thiourea **6**[14] to the highly acidic BINSA sulfonic acid catalyst **7**[15] (Figure 1.1).

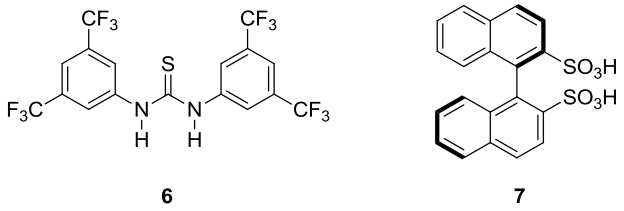

Figure 1.1. Schreiner's thiourea and BINSA catalysts

However, herein we are mostly concerned with chiral BINOL phosphoric acids (BPA) (Figure 1.1), which were independently and simultaneously discovered by Terada (Scheme 1.2, A) and Akiyama (Scheme 1.2, B) in 2004. [16,17]

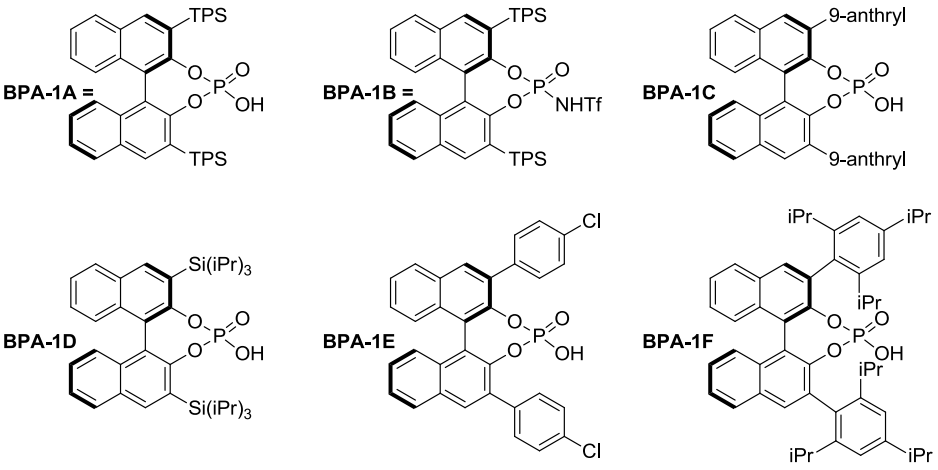

Figure 1.1. A selection of BINOL phosphoric acids.

Both groups demonstrated that BPA catalysts were able to impart excellent enantioselectivity on Mannich type reactions: preformed imine starting materials **8** and **9** were shown to react with acetylacetone **10** and silyl enol ethers **11** respectively with excellent enantioselectivity and yield (Scheme 1.2).

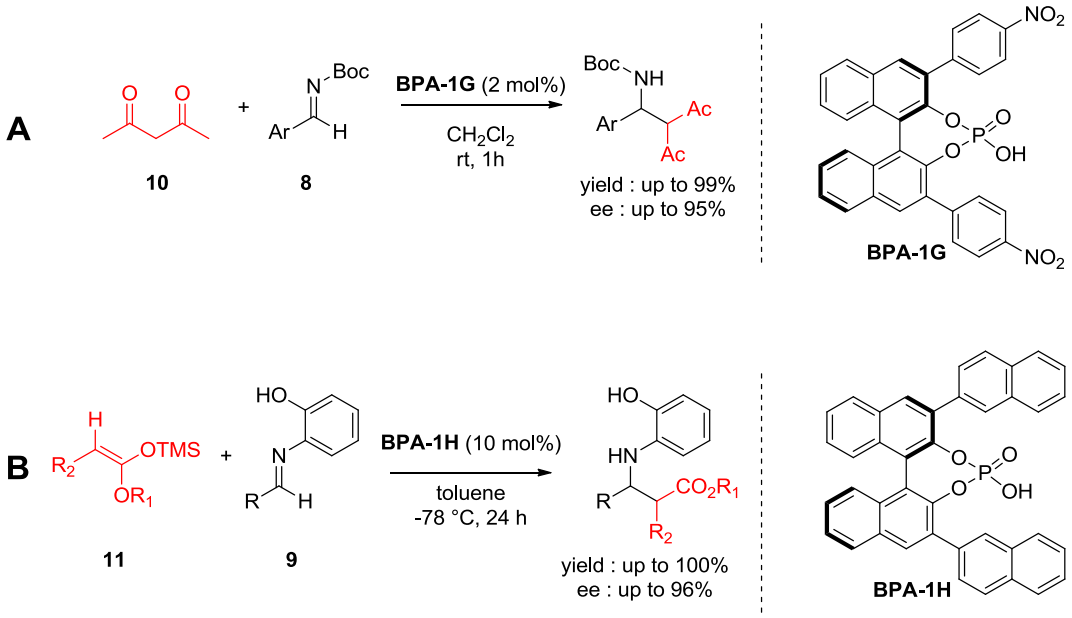

Scheme 1.2. Seminal use of BINOL phosphoric acids in organocatalysis.

Following this discovery, BINOL phosphoric acids have been used in a vast range of Mannich type reactions.[18] Imine starting materials have been shown to react with a range of carbon centred nucleophiles *via* iminium intermediates (Figure **1.2**), for example enamine attack and subsequent hydrolysis allows the formation of ketones,[19] Danishefsky dienes react to form piperidone structures[20] and a range of heterocycles are able to attack by Friedel-Crafts reaction (for example indole and furan).[21] Hantzsch esters have also been shown to provide a hydride source for enantioselective transfer hydrogenation (Figure 1.2). [22]

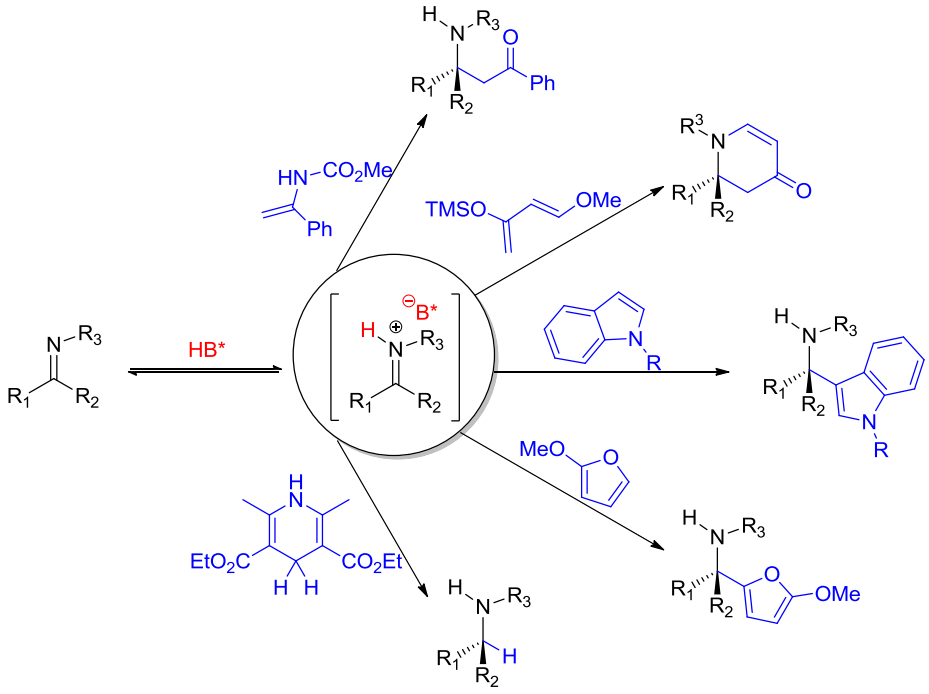

Figure 1.2. BPA catalysed Mannich type reactions from imine starting materials.

A substantial amount of work has been carried out on the mechanism of BPA catalysed reactions. Goodman and co-workers have created a set of general guidelines using computational techniques which can explain the enantioselectivity of a range of chiral BPA catalysed reactions.[23] BPA catalysts are not only Brønsted acids, they can be thought of as bifunctional catalysts with hydrogen bond donor and acceptor positions as shown in Figure 1.3. Goodman uses a three point interaction model with the phosphoric acid as a hydrogen bond donor and acceptor with the electrophile and nucleophile respectively. The third point of interaction comes from the steric bulk associated with the *ortho*-substitution on the napthyl ring and provides us with a simplified BPA model (Figure 1.3).

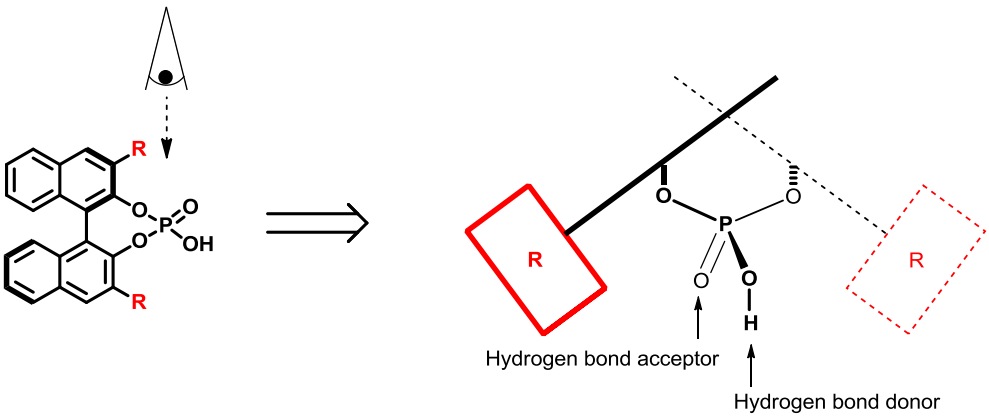

Figure 1.3. Goodman BPA model.

There are two possible transition state models that can be used when predicting the stereochemistry of a BPA catalysed reaction. These can be either *type I* or *type II* (Figure 1.4): *Type I* is favoured when R^3 is larger than R^2 and a symmetrical nucleophile is used such as a Hantzsch ester or acetylacetone (Scheme 1.3, *Type I*). *Type II* is favoured when an unsymmetrical nucleophile is used, for example indole or enamine nucleophiles, with substrates where R^3 is comparable or smaller than R^2 (Scheme 1.3, *Type II*). For these models to work the geometry of the imine must be in an orientation where R^2 and R^3 are larger than R^1, which in most cases is the most favourable isomer.

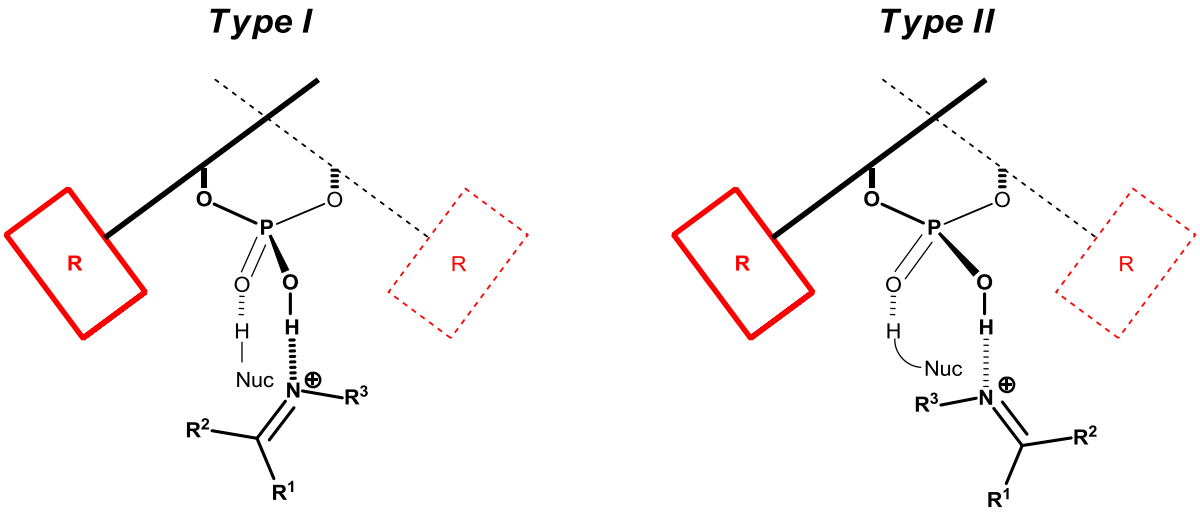

Figure 1.4. The two possible transition states proposed by Goodman

A selection of reactions that fit the Goodman model can be seen in Scheme 1.3: Reactions using Hantzsch ester[24] and acetylacetone[25] proceed via a *type I* model transition state and therefore are controlled by the nature of the imine starting material. The R^3 groups, which in these cases are acetyl (**11**) and Boc (**12**) groups respectively are placed away from the bulky ortho-substituent on the BPA catalyst. This allows the electrophilic iminium carbon to line up with the central nucleophilic centre in the lowest energy conformation.

When the nucleophiles used are indole[26] or enamine[27] the nucleophilic centre is skewed to the right (when using (*R*)-BPA catalysts), this is to minimise the steric clash of the indole-benzene ring or Cbz group respectively with the BPA catalyst. This therefore requires the iminium (**13** and **14** respectively) electrophilic carbon to also be skewed to the right of the model and therefore a *type II* orientation is adopted to minimise the energy of the transition state.

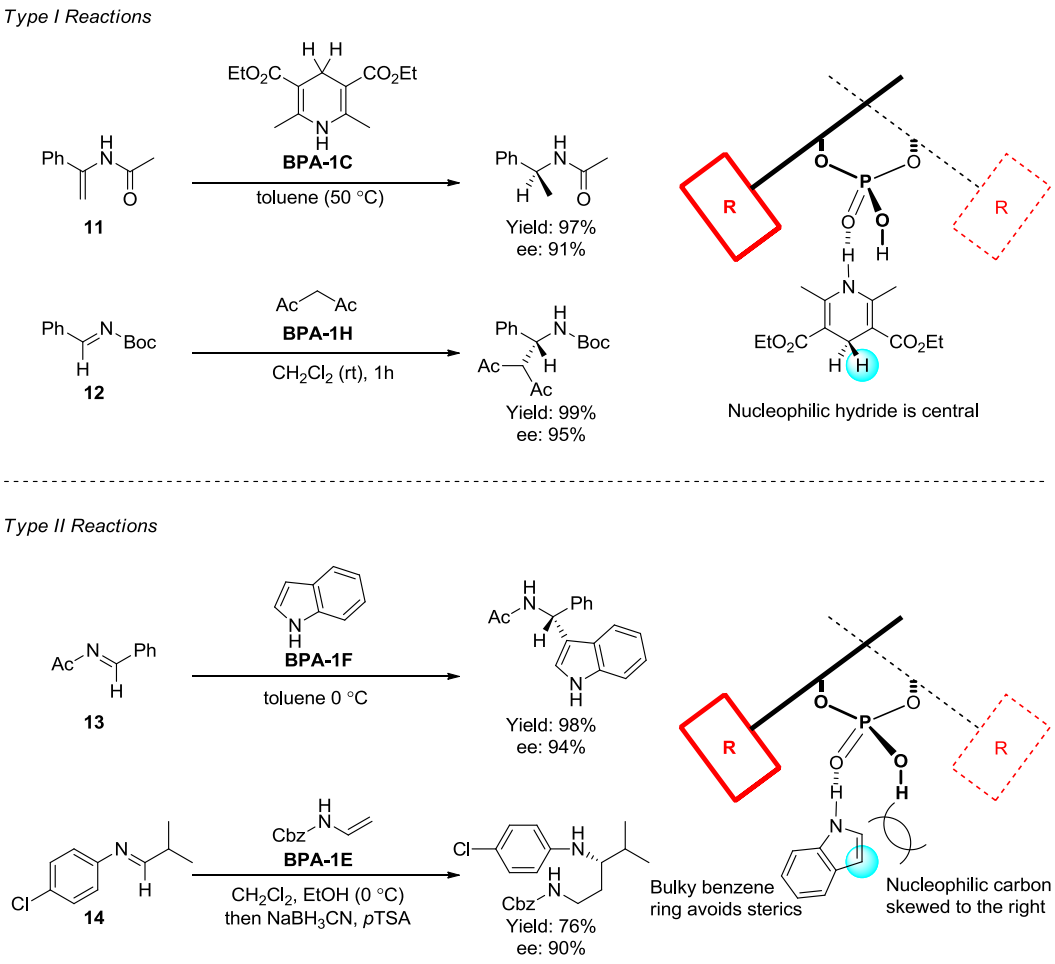

Scheme 1.3. A selection of examples that follow the Goodman model.

1.2. Cascade catalysis

In the past decade, cascade reactions employing the combined use of metal- and organocatalysis have become popular.[28] This approach was first used by Cordova *et al* in the α-allylic alkylation of aldehydes and cyclic ketones, a reaction that otherwise would be difficult due to self-aldolisation, Cannizzaro or *O*-alkylation by-products (Scheme 1.4).[29]

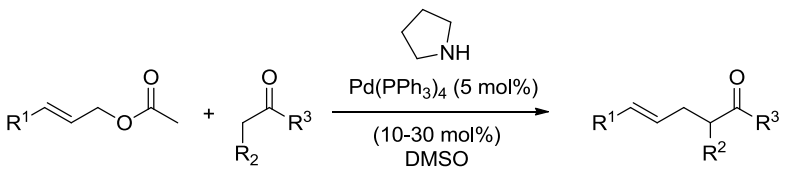

Scheme 1.4. α-Allylic alkylation of aldehydes and cyclic ketones.

The beauty of this work can be attributed to the compatibility of the two sequential catalytic cycles shown in Figure 1.5. Pyrrolidine **15** activates the carbonyl **16** to the nucleophilic enamine intermediate **17**, which is able to react with the palladium π-allyl complex **18** to allow selective α-allylic alkylation forming iminium **19**; subsequent hydrolysis allows the generation of the desired alkylation product **20** .

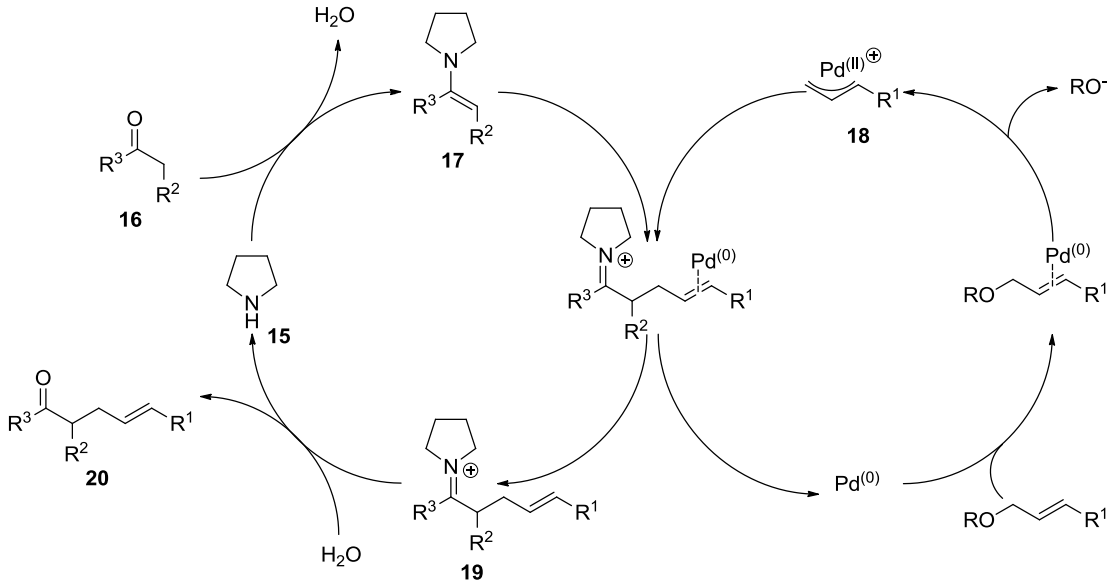

Figure 1.5. Cascade catalysis mechanism for α-allylic alkylation

Since the publication of this work, a plethora of methods have been developed using a combination of transition metals and organocatalysts.[28]

With the advent of homogenous Au(I) catalysis,[30] special attention has been paid to the use of Au(I) complexes in combination with organocatalysts. Enantioselective gold catalysed reactions have remained limited due to the linear nature of the Au(I) complexes.[30] Cascade catalysis provides a route to enantioselective reactions using Au(I) catalysts and an appropriate organocatalyst. Che,[31] Gong[32] and Dixon independently discovered the compatibility of Au(I) complexes and Brønsted acid catalysts. Che and Gong both developed reactions proceeding *via* two sequential catalytic cycles: initial gold catalysed hydroamination

is followed by BPA catalysed transfer hydrogenation. Specifically, Gong's method involves the initial hydroamination of aniline **21** to form enamine intermediates **22**, protonation by the catalytic chiral Brønsted acid then forms the reactive iminium **23** in the chiral environment induced by presence of the conjugate base of the chiral acid. Subsequent reduction with superstoichiometric quantities of Hantzsch ester provided the desired chiral amine product **24** in excellent yield and enantioselectivity (Scheme 1.5).

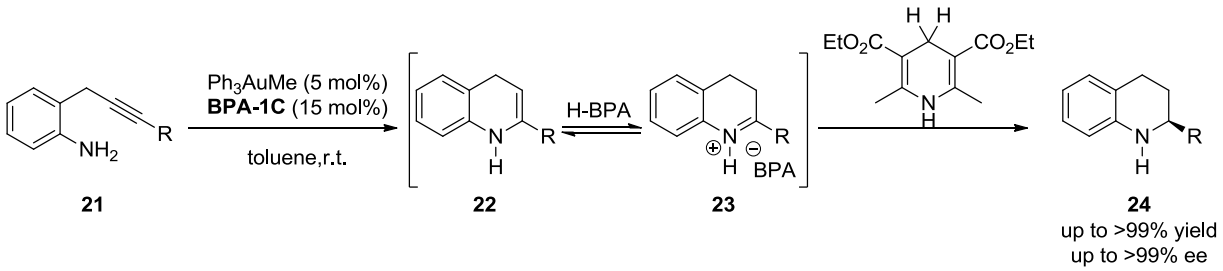

Scheme 1.5. Intramolecular hydroamination and transfer hydrogenation by Gong *et al*.

The Dixon group took a different approach to employing Au(I) and Brønsted acid catalysts. $(PPh_3)AuOTf$ was used to bring about an intramolecular hydro-carboxylation of but-3-ynoic acid derivative **25** to form their respective angelica lactone analogues **26.** The subsequent nucleophilic attack from tryptamine derivative **27** provided the indole tethered amido-ketone **28**. BPA acid-catalysed condensation reveals a reactive *N*-acyliminium intermediate **29**, which in the presence of the chiral conjugate base of the chosen **BPA-1A** is able to undergo an enantioselective Pictet-Spengler cyclisation forming tetracycle **30** in excellent yields and enantioselectivities (Scheme 1.6).[33]

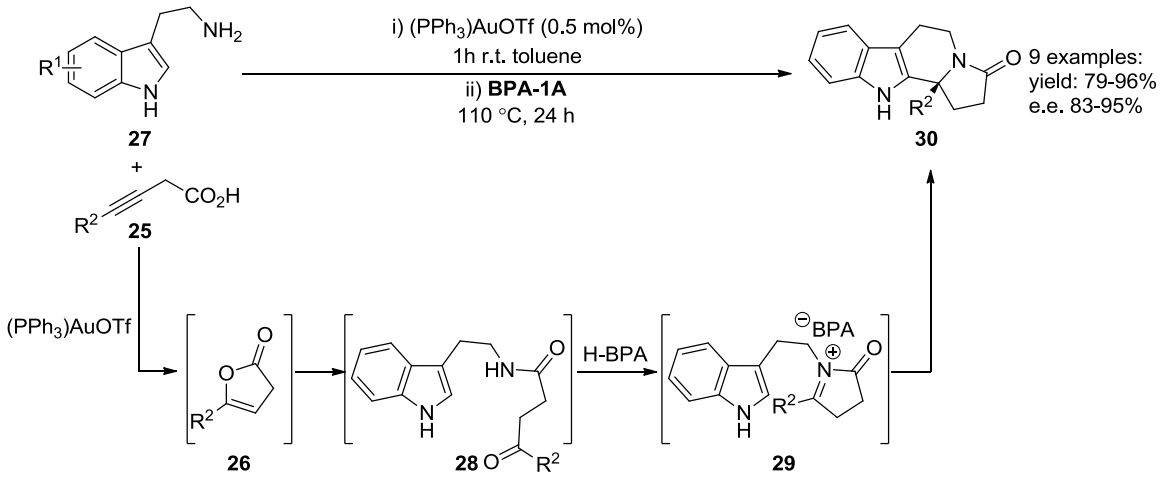

Scheme 1.6. Au(I) and BPA catalysed Pictet-Spengler cascade.

This reaction cascade provided the initial inspiration to develop a reaction cascade that proceeds through a reactive iminium based intermediate to generate polycyclic structures.

1.3. Aim

The aim was to extend this methodology from the Dixon group and develop a novel reaction cascade following an analogous concept. Specifically, we intended to develop an enantioselective *N*-sulfonyliminium Pictet-Spengler reaction forming polycyclic isothiazolidine-1,1-dioxide moieties of type **31** from a pro-iminium starting material **32** *via* an *N*-sulfonyliminium intermediate **33** (Scheme 1.7).

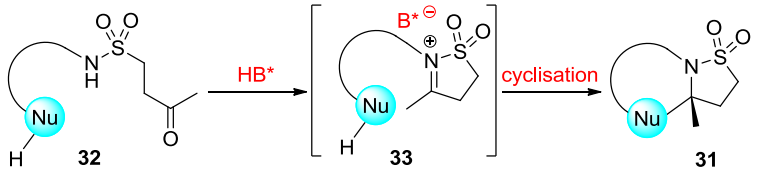

Scheme 1.7. *N*-sulfonyliminium cascade reaction concept.

The choice of sulfonamide was influenced in part by their abundance in medicinally relevant compounds[34] (Figure 1.6 shows 4 of the top 52 drugs sold in the United States of America in 2012),[35] but also by the lack of such motifs present in the enantioselective cascade literature.

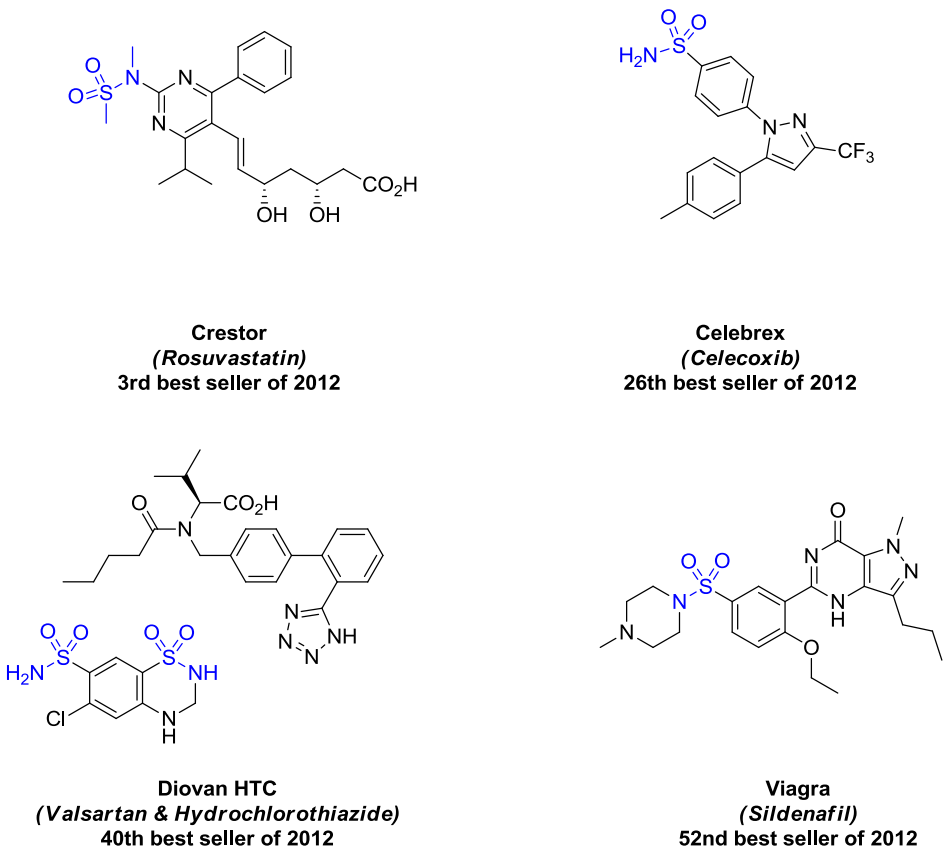

Figure 1.6. 4 of the top selling drugs in the USA in 2012.[35]

Two potential strategies to generate the *N*-sulfonyliminium intermediate **34** were proposed (Scheme 1.8): 1) condensation of the sulfonamide with a tethered ketone **35**; 2) hydroamination of a tethered alkyne **36** to generate an ene-sulfonamide **37** which can be protonated to the *N*-sulfonyl iminium intermediate **34** under acidic conditions.

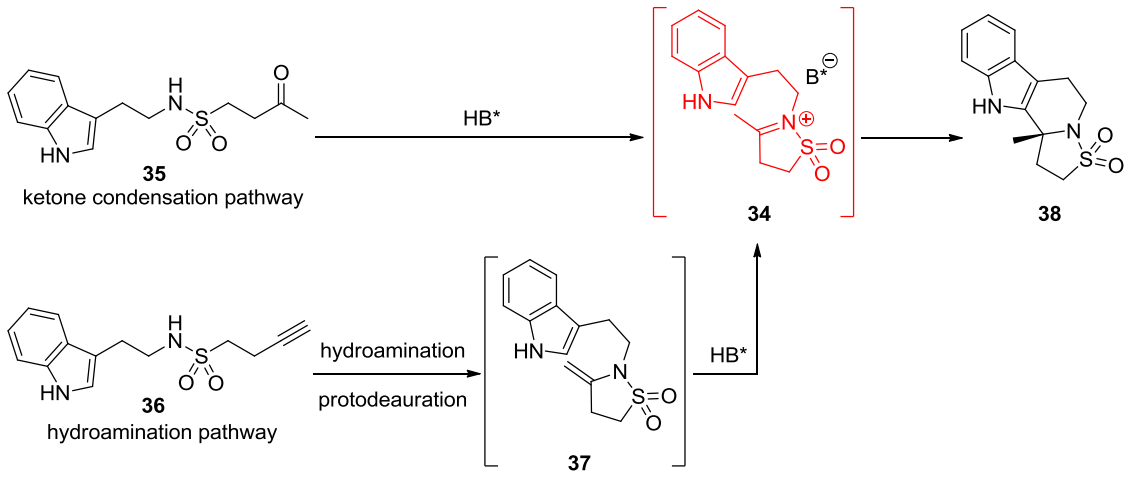

Scheme 1.8. Approaches to the *N*-sulfonyliminium intermediate.

1.4. Synthesis of starting materials

Alkyne **36a** was synthesised from commercial tryptamine and but-3-ynol (Scheme 1.9 and 1.10). Mesylation of but-3-ynol gives **39**, which was substituted with thioacetic acid yielding the pungent thioester **40**. Oxidation of **40** allows the formation of sulfonate salt **41**, however, this oxidation reaction is very capricious; over oxidation led to alkyne cleavage, resulting in the corresponding carboxylic acid,[36] It was found after some optimisation that quenching the hydrogen peroxide using an aqueous sodium sulfite solution (1.5 M) followed by concentration *in vacuo* provided a reliable method to sodium sulfonate **41** albeit as an inseparable mixture with sodium sulfite and sulfate salts.

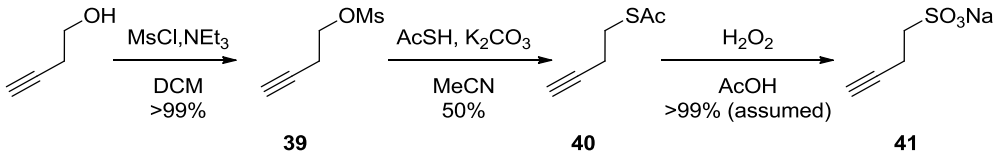

Scheme 1.9. Synthesis of alkyne sulfonate moiety **41**.[37]

Due to the presence of the undesired inorganic salts, we assumed the reaction was quantitative when carrying the crude material through to the next step. The salts present in **41** were shown to have little effect on the chlorination step to form sulfonyl chloride **42** when compared to pure **41** (Scheme 1.10). Coupling with tryptamine at –78 °C gave sulfonamide **36a** in 32% yield over 3 steps.

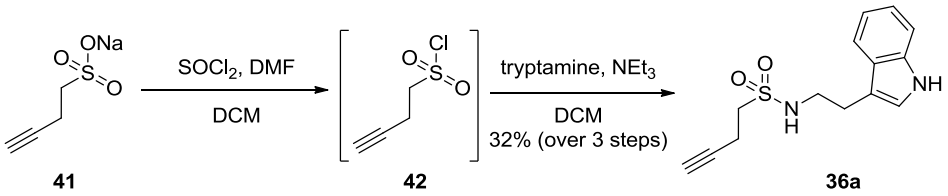

Scheme 1.10. Synthesis of alkyne **36a** from sulfonate **41**.

1.5. Gold(I) catalysed cyclisation cascade

Proof of principle was first established by adding $[P(OPh)_3]AuCl$ (5 mol%) and AgOTf (5 mol%) in one portion to a mixture of sulfonamide **36a** and **BPA-1A** (10 mol%) in toluene at 50 °C (Scheme 1.11). The reaction proceeded at a faster rate than previously reported in *N*-acyliminium cyclisation cascades and furnished the cascade products **38a** and **43a** (5-*exo* and 6-*endo* respectively in 9:1 ratio) with quantitative mass return. Subsequent analysis of **38a** using chiral HPLC revealed no enantioselectivity was observed.

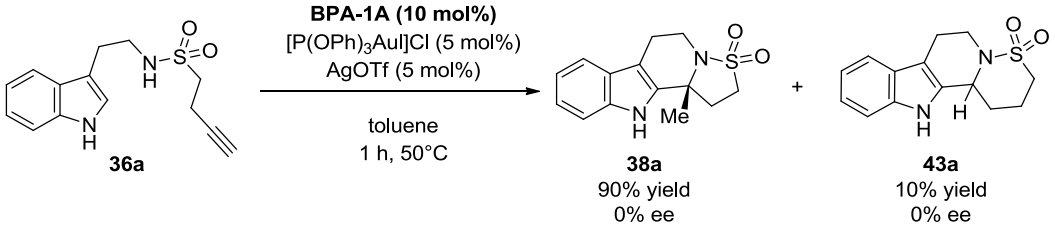

Scheme 1.11. Reaction cascade proof of principle.

We later confirmed the reason for this was a competing gold-catalysed background reaction; treatment of sulfonamide **36a** in the absence of any phosphoric acid with $[P(OPh)_3]AuCl$ (3 mol%) and AgOTf (3 mol%) at 60 °C in toluene afforded the cyclisation products **38a** and **43a** in quantitative yield as a 9:1 mixture of regioisomers respectively.[*]

Optimisation of this novel acid-free, Au(I)-catalysed cascade was carried out to gain an understanding of the hydroamination/cyclisation steps of the cascade and also provide a new methodology towards racemic polycyclic isothiazolidine-1,1-dioxide moieties **38**. Attempts were made to lower the gold catalyst loading from 5 mol % to 2 mol % (Table 1.1, entries 1-3), which resulted in a steady decrease in yield due to the reaction stalling[†]. This we presumed was due to the slow degradation of the gold catalyst leaving unreacted starting

[*] Further evidence for this background gold catalysed reaction was also provided by using catalyst **E** under the same reaction conditions, which again cyclised to **38a** and **43a** in good yield.
[†] The reaction was monitored by ^{1}HNMR and showed that no further conversion was taking place.

material. Increasing the concentration of the reaction (Table 1.1, entries 4-5) improved the yield due to the increased rate of reaction therefore the reaction is able to reach completion before the gold complex is poisoned. Degassing of the reaction mixture before the addition of gold catalyst improved the yield from 56% to 99% presumably by increasing the lifespan of the catalyst (Table 1.1, entry 6). Degassing and increasing the concentration allowed the loading of the catalyst to be lowered to 2 mol % and still maintain full conversion albeit at a lower yield. Lowering the gold catalyst equivalents further to 1 mol % failed to provide full conversion (Table 1.1, entry 7-8).

Table 1.1. Optimisation of the Au(I) catalysed cyclisation cascade.

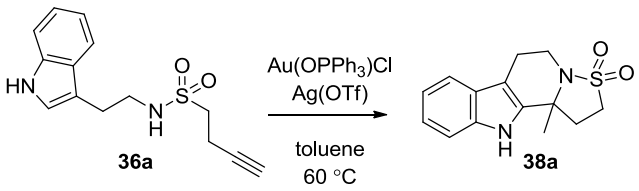

Entry[a]	Catalyst (mol%)	Conc (mM)	Degassing[b]	Yield[c] (%)
1	4	12	No	99
2	3	12	No	56
3	2	12	No	0
4	3	24	No	99
5	3	120	No	99
6	3	12	Yes	99
7	2	60	Yes	75
8	1	60	Yes	53

[a] The reaction was allowed to progress until it was deemed to have stalled or until complete consumption of starting material was seen by TLC. [b]After addition of solvent, the flask was put under vacuum, then filled with nitrogen. This process was repeated three times. [c] Isolated yield as a mixture regioisomers (9:1, 5-exo, 6-endo).

1.6. Chiral BPA catalysed cyclisation

Due to the lack of enantioselectivity in the Au(I) and BPA catalysed cyclisation cascade due to the Au(I) catalysed background reaction our focus shifted to a process that avoids the

formation of a ketone-type intermediate **35/37**. This would result in reactions that only require BPA catalysis.

Using alkyne **36a** as a masked ketone, attempts were made to hydrolyse the alkyne group to the corresponding ketone **35**. A selection of gold-catalysed hydrolysis methods[38] failed to provide any of the desired ketone due to a lack of reactivity. However, following hydroamination conditions developed by Jacobi and co-workers[39] using TBAF as a promotor for hydroamination ene-sulfonamides **37** and **44** were formed in a 82:17 ratio of 5-*exo* and 6-*endo* products respectively (Scheme 1.12). The reaction is proposed to proceed with fluoride activating the sulfonamide nucleophile in a general basic manner along with activation of the alkyne by induction from the *tert*-butylammonium ion.[40]

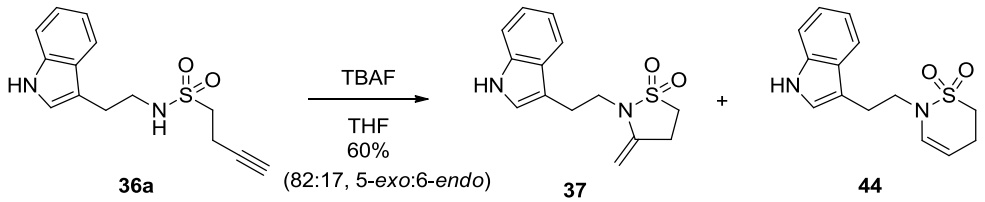

Scheme 1.12. Hydroamination of **36a** using TBAF.

Pleasingly, these products are closely related to our desired *N*-sulfonyliminium intermediate **34**. In fact protonation of **37** with a chiral acid would hopefully provide the *N*-sulfonyliminium intermediate **34** that could cyclise enantioselectively to generate our desired product **38a** (Scheme 1.13).

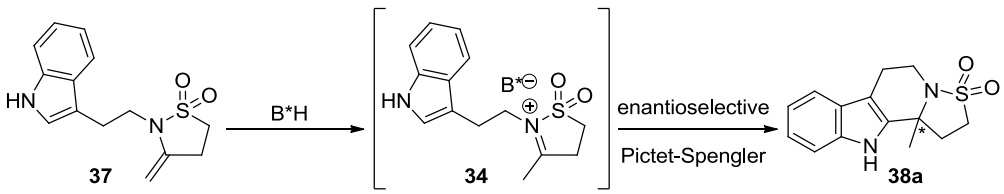

Scheme 1.13. BPA catalysed Pictet-Spengler cyclisation of enesulfonamide **37**

Unfortunately, purification of this enesulfonamide **37** proved difficult as it was unstable on silica, triethylamine-doped silica and alumina; recrystallisation and trituration techniques also failed to improve purity. Enesulfonamide **37** was therefore used in the next step as a 82:17 mixture of regioisomers after being passed rapidly through a plug of silica.

To obtain a proof of principle for the proposed enantioselective *N*-sulfonyliminium Pictet-Spengler reaction, enesulfonamide **37** was treated with **BPA-1A** in toluene at room temperature (Table 1.2, entry 2). Very pleasingly, the desired tetracycle **38a** was afforded in 70% yield and 89% ee. This indeed provided an excellent proof of principle for our concept and attempts to optimise this result were subsequently undertaken.

Decreasing the temperature to 0 and -20 °C in an attempt to improve the enantioselectivity (Table 1.2, entries 1-2) interestingly led to reduced enantioselectivity. However, increasing the temperature up to 60 °C had no deleterious effect on the enantioselectivity (Table 1.2, Entries 4-5). A possible explanation is that the phosphoric acid catalyst readily forms dimers or other aggregates which are less effective at inducing enantioselectivity than the free monomer, and therefore performing the reaction at higher temperatures reduces the amount of dimers.

Table 1.2. Temperature screen for BPA catalysed enesulfonamide cyclisation

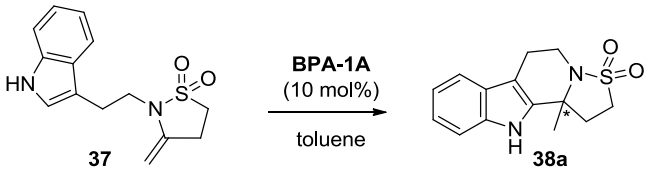

Entry[a]	Temperature (°C)	Yield[b] (%)	e.e. (%)
1	-20	75	72
2	0	82	82
3	20	70	89
4	40	67	89
5	60	70	88

[a] Reactions were performed on a 28 mg scale [b] isolated yield of a mixture 5-exo and 6-endo (85:15) of regioisomers.

A solvent screen (Table 1.3) showed that toluene was the best solvent for achieving high enantioselectivity and yield. This is most probably due to its non-polar nature maintaining the tight ion pair interactions between the sulfonyliminium intermediate and the conjugate base of BPA, thereby maximising catalyst control.[41]

Table 1.3. Solvent screen for BPA catalysed enesulfonamide cyclisation

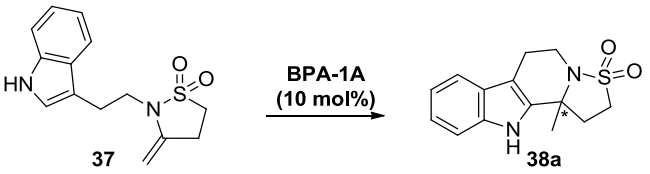

Entry[a]	Solvent	Yield[b] (%)	e.e. (%)
1	toluene	80	89
2	CH_2Cl_2	80	66
3	chloroform	69	55
4[c]	hexane	0	-
5	MeCN	34	48
6	ethanol	64	21
7	ether	54	79
8	THF	45	73

[a] Reactions were performed on a 28 mg scale at 20 (°C) [b] isolated yield of a mixture 5-exo and 6-endo (85:15) of regioisomers [c] No reaction due to poor solubility.

When testing the reaction of enesulfonamide **37** in water the ketone **35** was isolated after purification. In fact the ketone can be synthesised directly from the sulfonamide alkyne **36a** via TBAF catalysed hydroamination, followed by stirring in water for 20 mins; purification provides ketone **35** in 25% yield (Scheme 1.14).

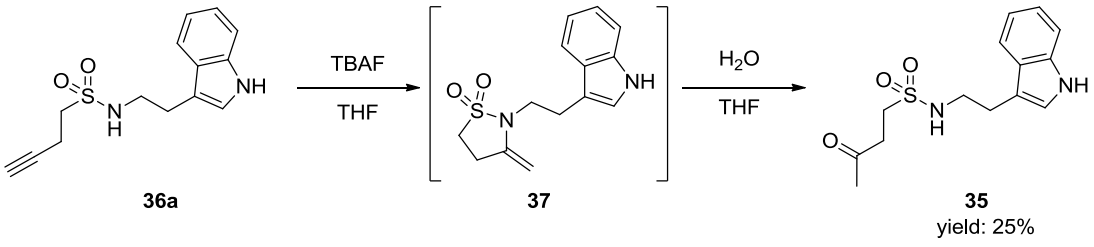

Scheme 1.14. ketone formation from hydrolysis of ene-sulfonamide

When ketone **35** was subjected to the optimised conditions for enesulfonamide **37** cyclisation, the desired product was obtained in quantitative yield and good e.e. (Table 1.4, Entry 1).

Raising the temperature of the reaction (Table 1.4, Entries 2-3) resulted in an increase in the enantioselectivity, fully consistent with the results of enesulfonamide **37a** cyclisation (breakup of aggregates at higher temperature).

Table 1.4. Temperature screen for BPA catalysed ketone cyclisation cascade

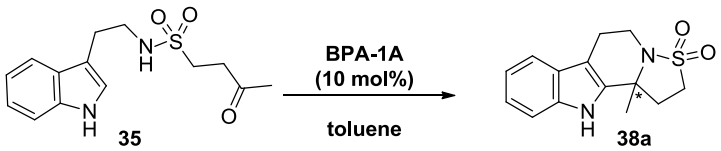

Entry[a]	Time (h)	Temp (°C)	Yield[b] (%)	e.e. (%)
1	6	20	<99	81
2	6	60	<99	90
3	1	100	<99	92

[a] Reactions were performed on a 28 mg scale. [b] isolated yield.

From this series of reactions it can be concluded that the hydroamination catalyst or its by-products must be associated with the poor enantioselectivity witnessed in our initial trials.

1.7. Gold and BINOL-phosphoric acid catalyzed enantioselective hydroamination/*N*-sulfonyliminium cyclisation cascade

The above investigations provided good insights into both the racemic Au(I) catalysed cyclisation cascade and the enantioselective BPA catalysed cyclisation cascade. This knowledge gave us the confidence to return to the initially proposed enantioselective hydroamination cyclisation cascade. By slowing the background Au(I) catalysed cascade we hoped to be facilitate an enantiofacially selective BPA catalysed cyclisation (Scheme 1.15).

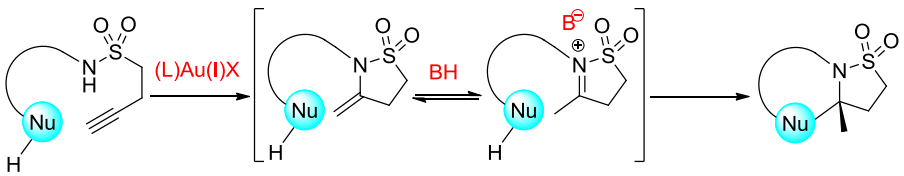

Scheme 1.15. Enantioselective hydroamination/*N*-sulfonyliminium cascade.

Therefore our attention turned to finding an appropriate hydroamination catalyst that would allow efficient hydroamination, but crucially, have limited reactivity in the Pictet-Spengler cyclisation process. Our initial trial was carried out using reduced loadings of the previously tested Lewis acid catalyst ([$P(OPh)_3$]AuCl) and AgOTf (Table 1.5, entry 1). Pleasingly, this gave an e.e. of 17% which provided a good proof of principal for our concept. We then tested a range of Lewis acid catalysts (Table 1.5/Figure 1.7), concentrating mainly on Au(I) complexes. Triphenylphosphine-derived complexes **B** and **C** (Figure 1.7) failed to react with our alkyne (Table 1.5, entry 2-3). However, both *N*-heterocyclic carbene Au(I) complex **D** and Echavarren's biphenyl complex **E** proved to work with good enantioselectivity and in good yield (Table 1.5, entries 4-5), with complex **E** showing a higher reaction rate (completion in 1h). Cu(II) catalyst **F** gave only limited enantioselectivity, however, this may have been due to the high catalyst loadings used in an attempt to increase the rate of reaction. (Table 1.7, entry 6). Due to the higher enantioselectivity and faster reaction rate we chose to proceed with complex **E** for further optimisation.

Table 1.5. Metal complex screen for dual catalysed cyclisation cascade

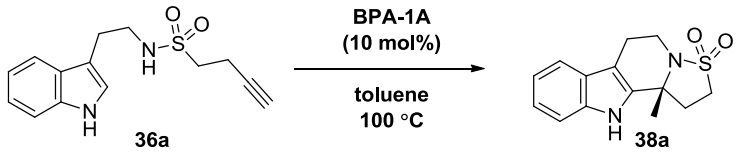

Entry[a]	Scale (mg)	Cat	Initial LA charge (mol%)	2nd LA charge (mol%)	Yield[b](%)	e.e. (%)
1	56	A	2	0	29	17
2	42	B	5	2	0	-
3	42	C	5	2	0	-
4	56	D	2	5	79	52
5[c]	42	E	5	0	62	73
6	42	F	20	0	60	17

[a] All reactions proceeded for 52 h at 7 mM concentration (with respect to 36a) unless otherwise stated. No change in regioselectivity (9:1, 6a:7a) was witnessed throughout optimisation. [b] Isolated yield. [c] Reaction complete after 1 h.

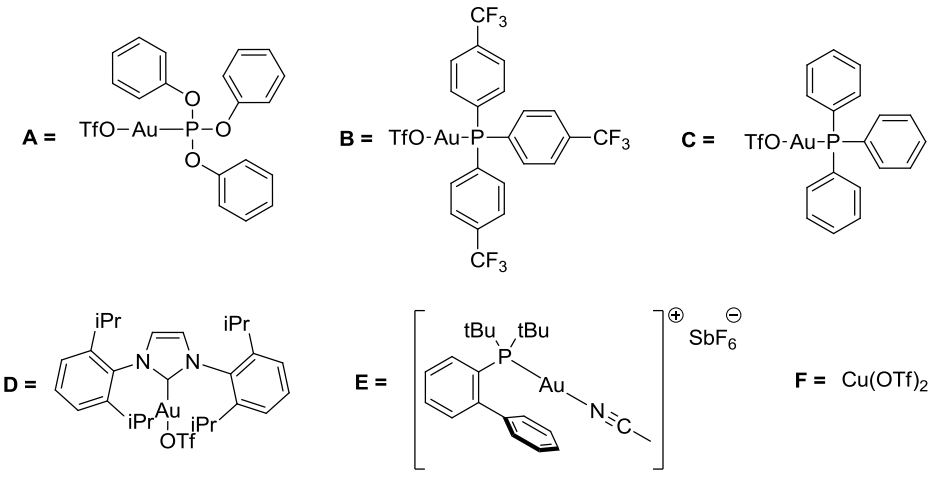

Figure 1.7. Metal complexes

To confirm that toluene was the optimal solvent for the cascade reaction a brief solvent screen was undertaken (Table 1.6). It can be seen that enantioselectivity is affected by using other solvents whereas there is very little effect on the yield of the reaction (with the exception of hexane due to poor solubility of **36a**) (Table 1.6, entries 1-5)[*].

[*] The loadings of the gold catalyst were reduced from 5 mol% to 2 mol% in an attempt to slow the background reaction.

Table 1.6. Solvent screen for dual catalytic cyclisation cascade

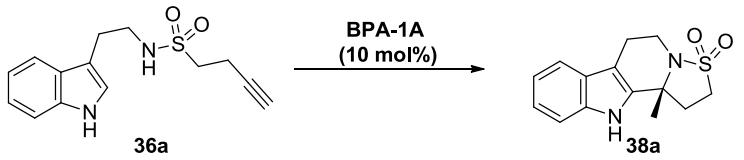

Entry[a]	Cat	Gold (mol%)	Solvent	Temp (°C)	Yield[b] (%)	e.e. (%)
1	E	2	Toluene	60	90	79
2	E	2	DCE	60	92	46
3	E	2	MeCN	60	85	53
4	E	2	Hexane	60	15	27
5	E	2	THF	60	92	0

[a] All reactions were performed on a 42 mg scale and proceeded for 24 h at 7 mM concentration (with respect to 36a). No change in regioselectivity (9:1, 6a:7a) was witnessed throughout optimisation. [b] Isolated yield

Raising the temperature from 60 °C to 110 °C (Table 1.7, Entries 1-4) we can see a potential trend towards improved e.e. which may be due to the breakup of dimers (as mentioned in section 1.6). However, the yield is inversely affected by the increased temperature; when the reaction was performed at 95 and 110 °C the reaction mixture often turned dark brown. This colouration may be an indicator for an increased proportion of side reactions that result in a decreased yield, however, no by-products were ever isolated or seen by TLC.

Table 1.7. Temperature screen for dual catalytic cyclisation cascade

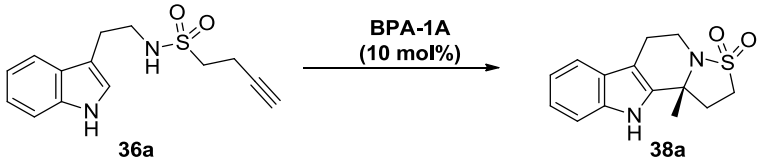

Entry[a]	Cat	Gold (mol%)	Temp (°C)	Yield[b] (%)	e.e. (%)
1	E	2	60	91	81
2	E	2	80	92	78
3	E	2	95	75	85
4	E	2	110	75	87

[a] All reactions were performed on a 42 mg scale and proceeded for 24 h at 7 mM concentration (with respect to 36a). No change in regioselectivity (9:1, 6a:7a) was witnessed throughout optimisation. [b] Isolated yields.

When the reaction was performed at 60 °C, we were able to lower the gold catalyst loading even further to 1.0 mol% and then 0.5 mol%, both of which proved beneficial to reaction yield and enantioselectivity (Table 1.8, Entries 2 and 3). However, the reaction failed to reach

completion when gold catalyst loading was below 0.5 mol%, with 0.1 mol% providing **38a** in only 23% yield after the reaction stalled (Table 1.8, Entry 4). Interestingly, 0.1 mol% loading allows the enantioselectivity to reach that obtained for the cyclisation of ketone **35** (Table 1.4, Entry 3), which we assume is the maximum enantioselectivity with no background cyclisation.

Table 1.8. Gold loading screen for dual catalytic cyclisation cascade at optimum temperature

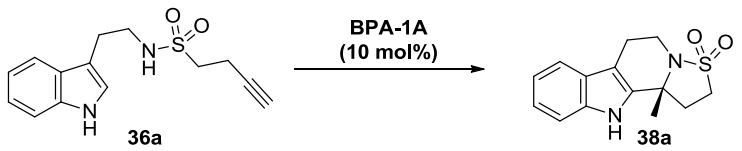

Entry[a]	Cat (%)	Gold (%)	Acid (%)	Temp (°C)	Yield[b] (%)	e.e. (%)
1	E	2	10	60	91	81
2	E	1	10	60	93	88
3	E	0.5	10	60	93	88
4	E	0.1	10	60	23	92

[a] All reactions were performed on a 42 mg scale and proceeded for 24 h at 7 mM concentration (with respect to 36a). No change in regioselectivity (9:1, 6a:7a) was witnessed throughout optimisation. [b] Isolated yield.

A screen of chiral BPA derivatives bearing different substituents and functionalities provided no enhancement in enantioselectivity (Table 1.9, entries 1-4) and confirmed that **BPA-1A** was optimal for the enantioselective cascade process.

Table 1.9. BPA screen for optimised dual catalytic cyclisation cascade.

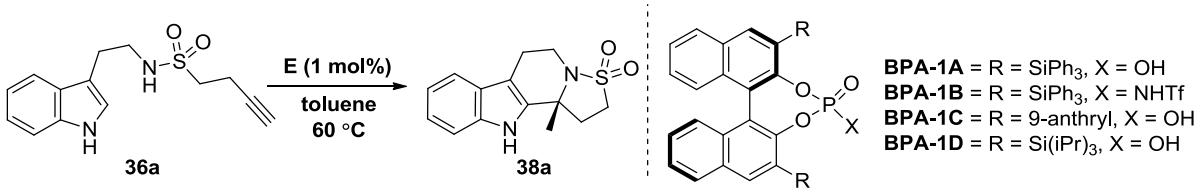

Entry[a]	Acid Cat (mol%)	BPA Cat (mol%)	Yield[b] (%)	e.e. (%)
1	10	1A	92	88
2	10	1B	92	45
3	10	1C	94	71
4	10	1D	88	45

[a] All reactions were performed on a 42 mg scale and proceeded for 24 h at 7 mM concentration (with respect to 36a). No change in regioselectivity (9:1, 6a:7a) was witnessed throughout optimisation. [b] Isolated yield.

1.7.1. **Reaction scope**

With the reaction optimisation complete, we wanted to assess the scope of the reaction: substitution of the indole would provide readily available structures that would explore the reactivity of the indole nucleophile by varying the electron donating/withdrawing abilities of the substituents. Substituted tryptamine analogues were either synthesised from the corresponding commercial indole (scheme 1.16)[33] or purchased from commercial sources (Figure 1.8).

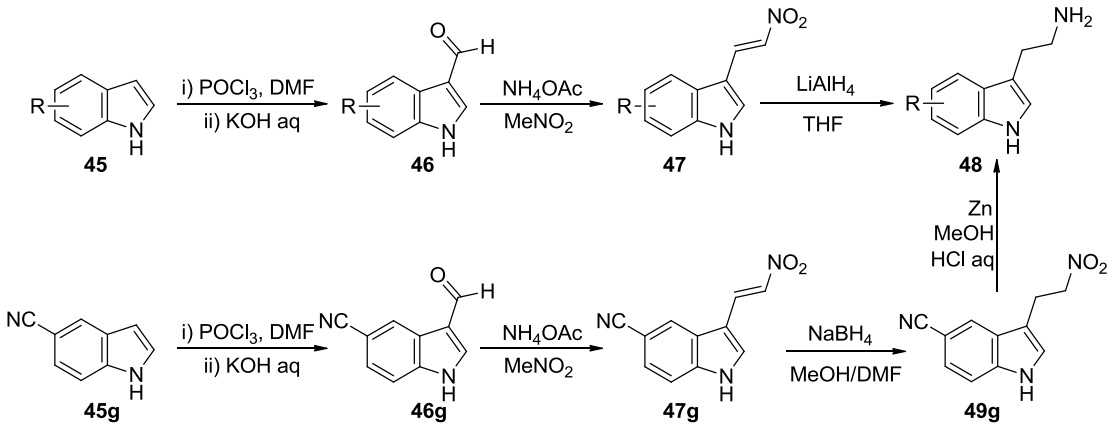

Scheme 1.16. Tryptamine synthesis

Indoles **45** were converted into the corresponding indole-3-carboxaldehyes **46** following Vilsmeier-Haack conditions in good yield. Henry reaction, using ammonium acetate in

refluxing nitromethane afforded the equivalent nitro-olefins **47**. Reduction of the nitro-olefins using lithium aluminium hydride provided the corresponding tryptamine derivative **48** in all cases except the 6-nitrile-tryptamine analogue **48g**, which was synthesised via a two stage reduction process, because of the reactive nitrile group. The double bond was initially reduced using sodium borohydride to give nitroalkane **49g** and dissolving zinc reduction allowed chemoselective reduction of the nitro group.

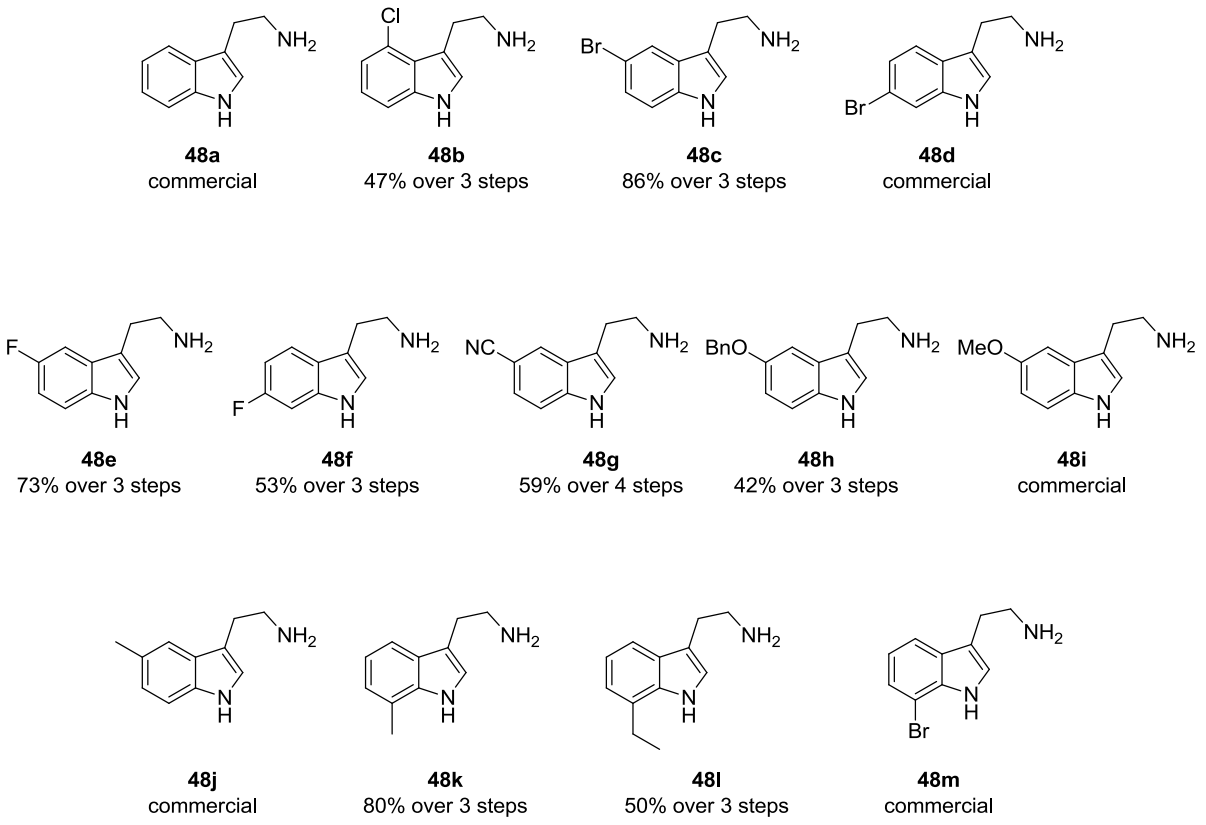

Figure 1.8. Synthesis of substituted-tryptamines.

This library of tryptamine analogues was coupled with the alkyne-tethered sulfonyl chloride **42** in a rapid reaction (5 – 10 mins) at -78 °C in the presence of triethylamine in CH_2Cl_2 to generate the desired alkyne tethered sulfonamides **36** (Figure 1.9).

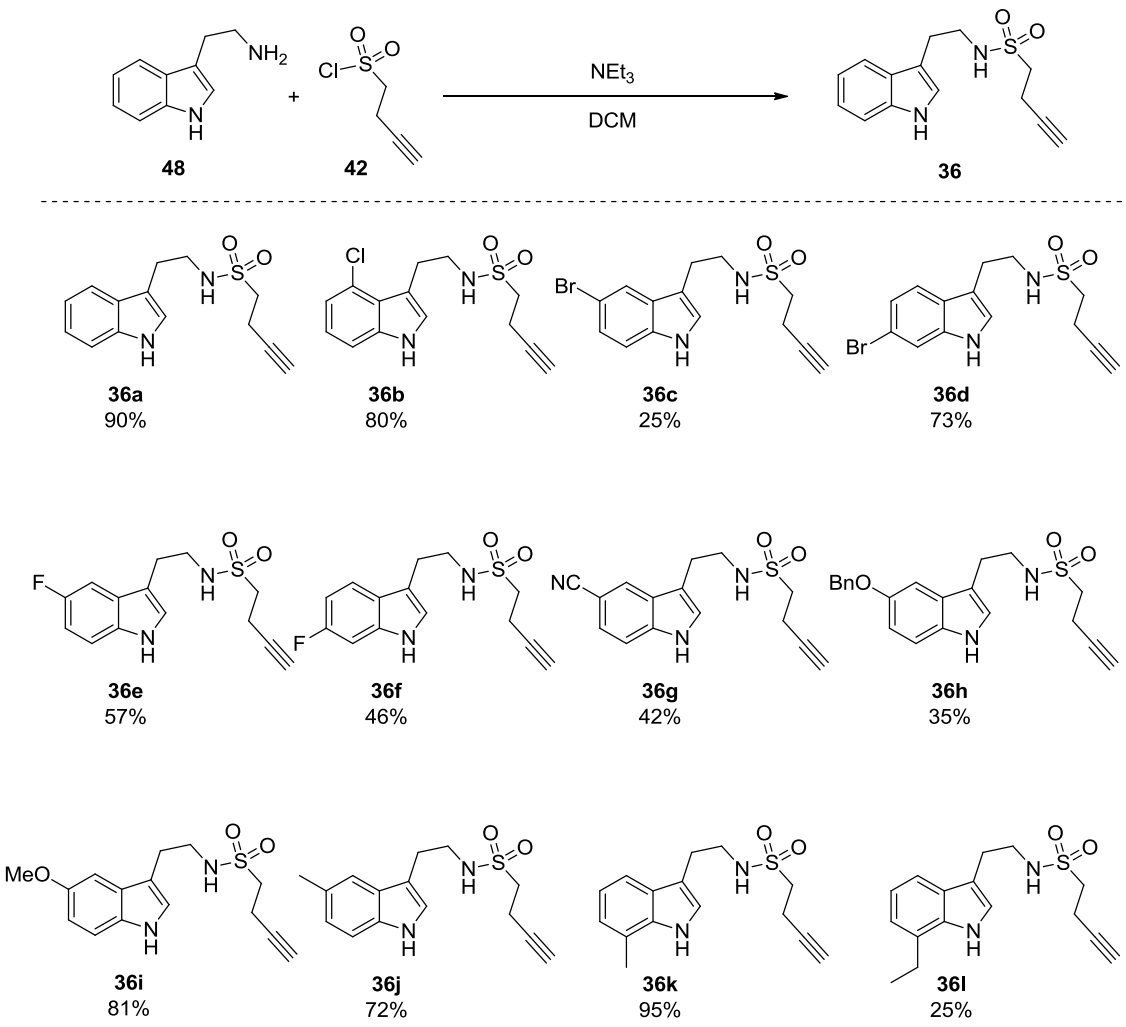

Figure 1.9. Synthesis of indole-sulfonamides.

With the substituted indole-sulfonamides in hand we exposed our library of substituted indole tethered sulfonamides to the reaction conditions (Figure 1.10). The reaction was found to tolerate electron-withdrawing halides at various positions around the ring (**38b** to **38f**) as well as the electron deficient 6-nitrile derivative (**38g**), albeit at slower reaction rate (60 h) in the latter case due to its poor solubility in the reaction solvent. Substrates containing electron donating groups (**38i** to **38l**) were also found to be well-tolerated. However, the benzyloxy-substituted indole **36h** derivative provided **38h** in lower enantioselectivity than the other analogues. This may be due to the bulky benzyl group disrupting the transition state of the cyclisation. These derivatives demonstrated that all the available positions around the

carbocycle of the indole ring could be substituted without significant detriment to enantioselectivity or yield. In all the examples the 5-*exo*-cyclisation product **38** was separated from the 6-*endo* cyclisation regioisomer **44** (which was always present in a 9:1 ratio by crude ^{1}H NMR analysis) and the yields represent the isolated quantity of **38**.

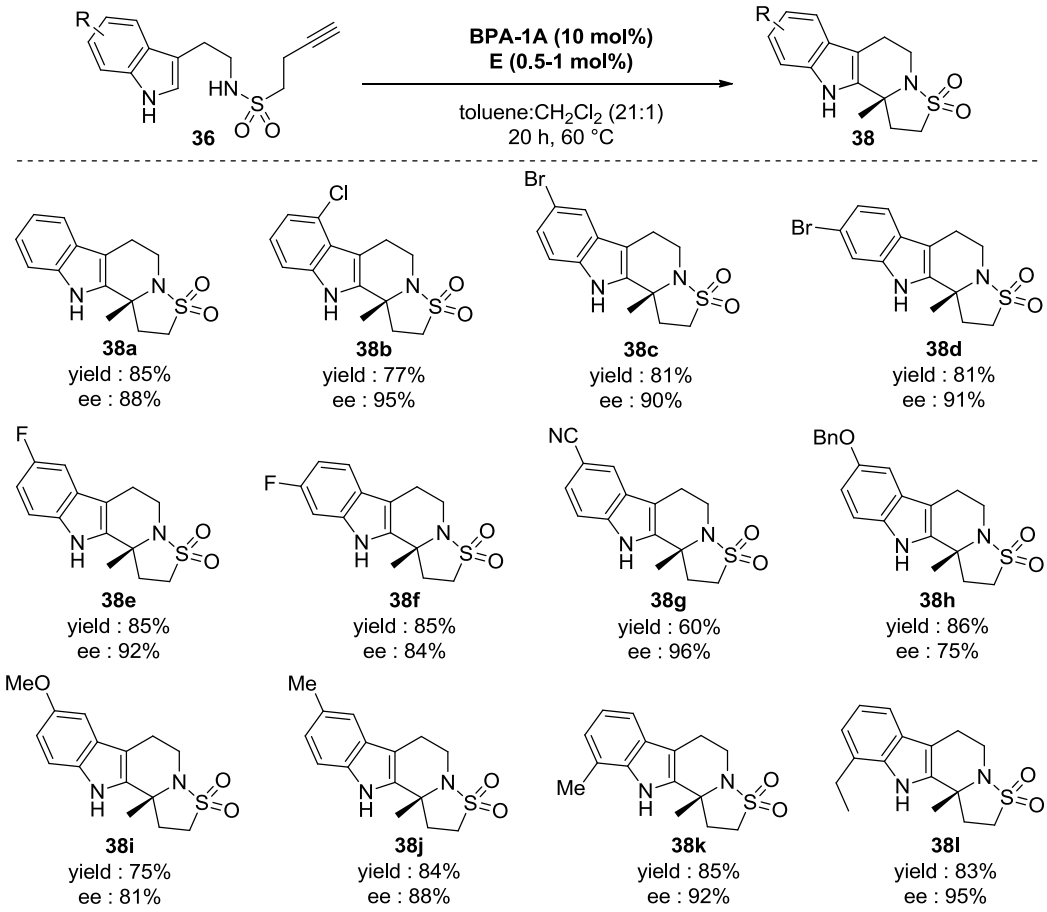

Figure 1.10. Substrate scope.

1.7.2. **Determination of absolute stereochemistry**

The absolute stereochemical configuration was determined by single X-ray crystallography. Multiple attempts to obtain X-ray quality crystals for **38a** proved difficult, whilst single crystals could be formed the nature of the unit cell led to problem when solving the x-ray data. However, derivatisation of **38a** by substitution of the indole-*NH* with a 3-bromobenzyl group gave **50** in 68% yield (Figure 1.11). The 3-bromobenzylated derivative **50** was

recrystallised to >99% e.e. Subsequent crystallisation by slow evaporation of a concentrated diethylether solution resulted in single crystals that could be solved to show that the major enantiomer formed in the cyclisation is the (*R*) enantiomer (Figure 1.11).

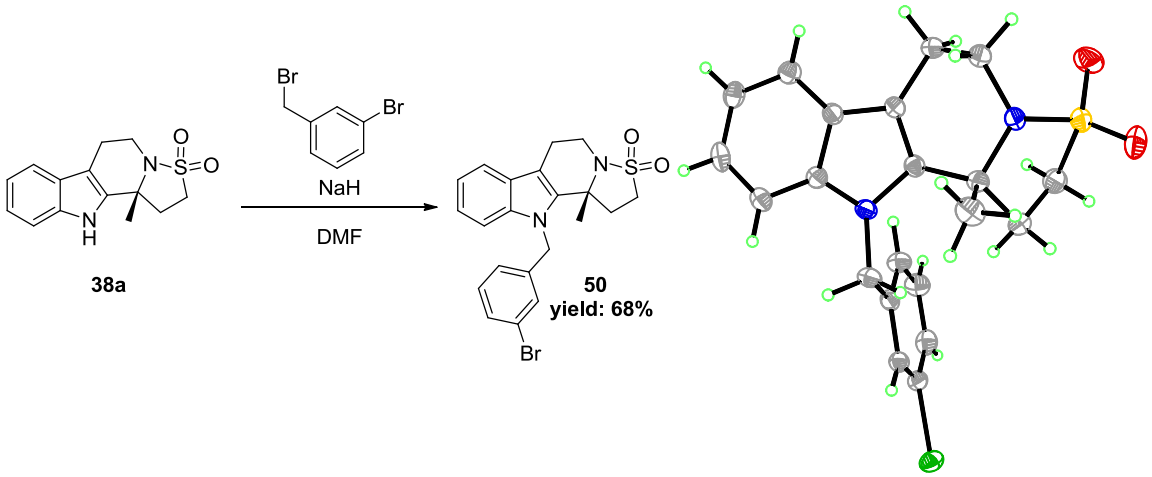

Figure 1.11. Derivitisation of **38a** and thermal ellipsoid plot of **50** determined using single crystal X-ray diffraction data (one equivalent of **50** omitted for clarity). C, gray; Br; green; N, blue; O, red; S; yellow.

1.7.3. **Scope expansion: *N*-acyliminium analogues**

To further test the flexibility of this new methodology, attempts were made to perform the reaction cascade on the chain extended-amide analogue **51** (Scheme 1.17). This set of compounds should again follow the same Au(I) catalysed hydroamination to form either the 6-*exo* (**52**) or 7-*endo* enamide intermediates, which can be protonated to the *N*-acyliminium intermediate (**53**) under acidic conditions and cyclise enantioselectively to form polycyclic lactam products of type **54**.

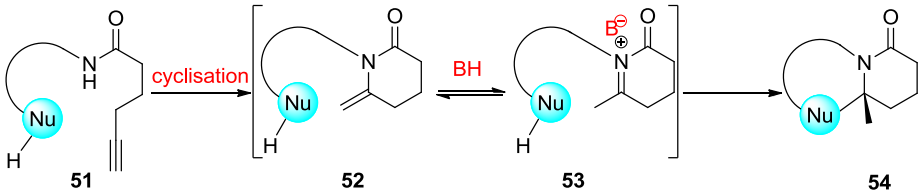

Scheme 1.17. Chain extended amide concept.

The amide analogues **51** were rapidly synthesised by coupling tryptamine derivatives with commercial hex-5-ynoic acid using 1-ethyl-3-(3-dimethylaminopropyl)carbodiimide (EDCI) and 4-dimethylaminopyridine (DMAP) in CH_2Cl_2 (Figure 1.12).

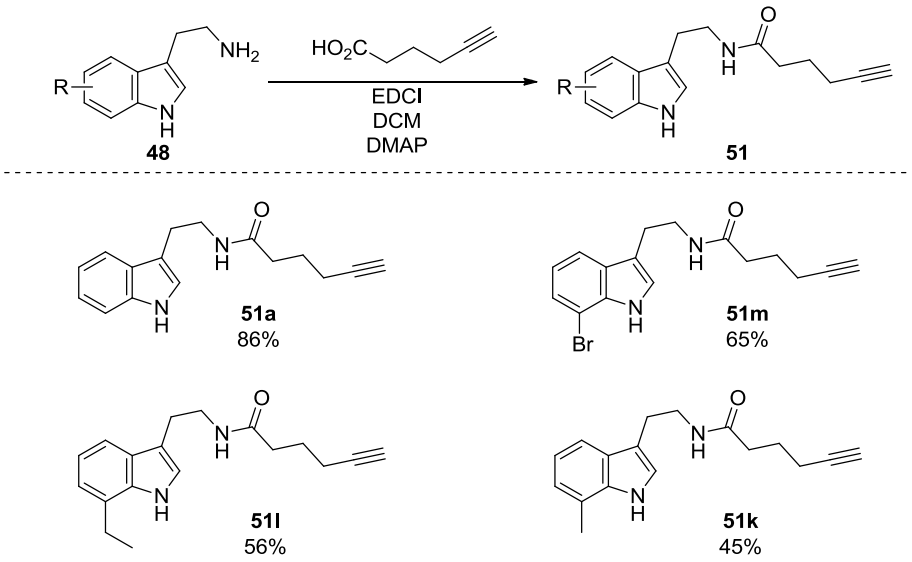

Figure 1.12. Synthesis of amide analogues.

Pleasingly, treating **51a** with 5 mol% of **E** and 10 mol% **BPA-1A** in toluene at 60 °C gave the desired product **54a** in 66% ee and 47% yield as a single regioisomer (6-*exo*) (Table 1.10, Entry 1). This regioisomer is proposed to be favoured because of the unfavourable entropic energy requirements to form the 7-*endo* regioisomer as well as the Au(I) complex being skewed towards the terminal end of the alkyne.[43] The low yield was due to a reduced reaction rate (up to 72 h reaction time), presumably the gold catalyst decomposes before the reaction has reached completion. Raising the temperature to increase the rate of reaction allowed complete conversion (yield 79%) (Table 1.10, Entry 2). Interestingly, in this case the enantioselectivity is reduced. This reduction in enantioselectivity at higher temperatures could be rationalised by the reduced reactivity of the *N*-acyliminium compared to the *N*-sulfonyl iminium ion; therefore at lower temperatures the rate of background Au(I) catalysed

cyclisation is relatively less with respect to the rate of BPA catalysed cyclisation, which ultimately leads to increased enantioselectivity at lower temperatures.

Pleasingly, lowering the loading of the gold catalyst to 3, 1 and 0.5 mol% (Table 1.10, Entries 3-5) resulted in a general increase in the enantioselectivity, but also led to reduced yields. We selected to use 1 mol% of gold catalyst (Table 1.10, Entry 4) as a compromise between yield and enantioselectivity.

Table 1.10. Optimisation of chain extended amide analogues

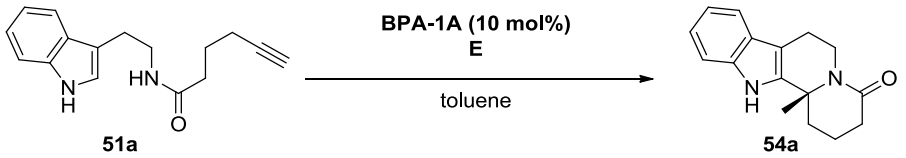

Entry[a]	E (mol%)	Temp (°C)	Yield[b] (%)	e.e. (%)
1	5	60	47	66
2	5	110	79	50
3	3	110	99	62
4	1	110	86	66
5	0.5	110	81	68

[a] All reactions were performed in 38 mg at 7 mM concentration (with respect to 51a). [b] Isolated yield.

1.7.4. *N*-acyliminium cyclisation scope

A collection of examples were examined to test the effects of electron-withdrawing (**51m**) and donating (**51k** and **51l**) substituents in this variant of our cascade process. Pleasingly, the reaction of bromo-substituted indole **51m** proceeded in 93 % e.e. and 99% yield, with no 7-*endo* regioisomer detected. The reactions of the alkylated examples **51k** and **51l** also progressed with good to excellent yields and with enantiomeric excesses up to 93% (Figure 1.13).

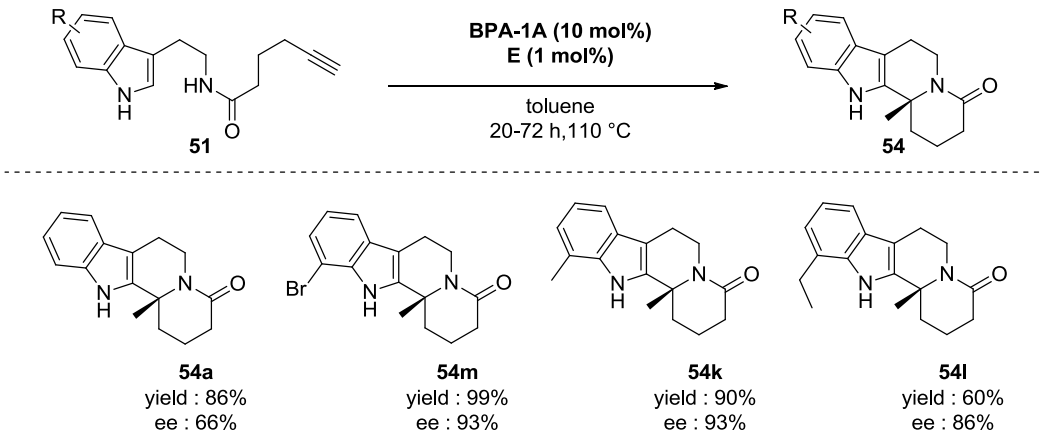

Figure 1.13. *N*-acyliminium cyclisation scope.

1.7.5. **Absolute stereochemistry determination for the *N*-acyliminium cyclisation cascade**

Absolute stereochemical configuration was determined by single X-ray crystallography of **54m**. Recrystalisation by slow evaporation of chloroform provided single crystals of **54m** with >99% e.e (Figure 1.14). Again the enantioselectivity of the reaction was proved to form the (*R*)-enantiomer as the major stereoisomer.

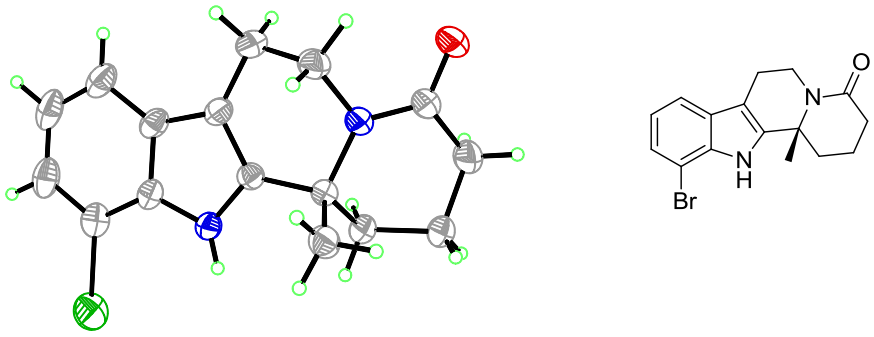

Figure 1.14. Thermal ellipsoid plot of **54m** determined using single crystal X-ray diffraction data (one equivalent of $CHCl_3$ omitted for clarity). C, gray; Br; green; N, blue; O, red; S; yellow.

1.8. Reaction mechanism

From data collected during the development of the cyclisation cascade and literature precedent, we propose that the mechanism of the reaction proceeds through two sequential and independent catalyzed transformations (Scheme 1.18). The Au(I) complex activates alkyne **36** through π acid/base interactions lowering the energy of the alkyne LUMO,[42] which allows the sulfonamide to attack selectively in a 5-*exo* fashion. Presumably the selectivity is due to the gold alkyne bond being skewed towards the terminal end of the alkyne due to the steric interaction with the alkyl chain[43] (as well as the favourable ring size). Protodeauration results in the formation of enesulfonamide **37**. At this juncture, intermediate **37** can take two potential pathways: i) gold catalyzed non-enantioselective *N*-sulfonyliminium cyclisation via **55** (although we cannot rule out Lewis acid assisted Brønsted acid catalysis),[44] or ii) the enantioselective BPA catalyzed *N*-sulfonyliminium cyclisation via **34**. Evidence that the enantioselective reaction pathway passes through an *N*-sulfonyliminium intermediate not by a Au(I) phosphate catalyzed intermediate[45] was supported by the study of ketone **35**. When ketone **35** was treated with **BPA-1A** at 10 mol% in refluxing toluene (Table 1.4, Entry 3), **38a** was obtained in quantitative yield and 92% ee. That the sense and magnitude of the enantioselectivity in this reaction were the same as that in the cascade (Table 1.8, Entry 4) points to a common intermediate **34**.

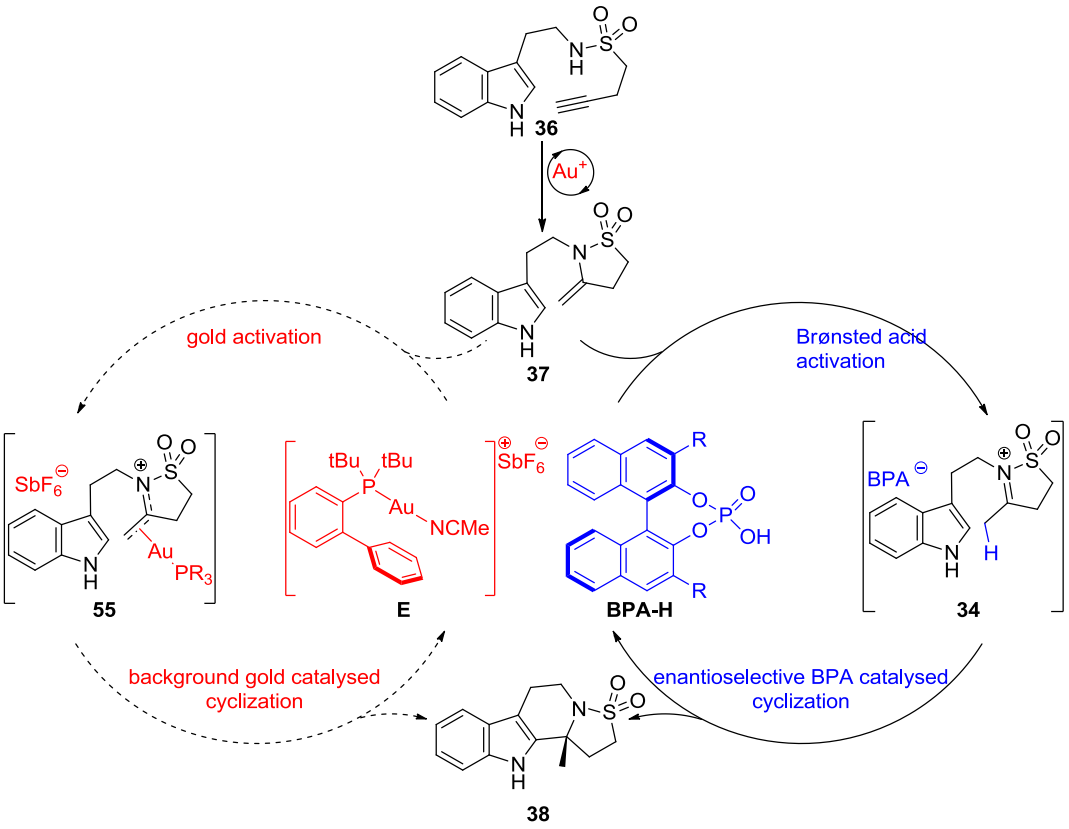

Scheme 1.18. Proposed reaction cascade.

1.9. Conclusion

In conclusion, we have developed a highly enantioselective *N*-sulfonyliminium cyclisation cascade. Mechanistic understanding has allowed us to control the background gold catalyzed reaction and allowed us to access 12 complex and unusual sulfonamide scaffolds in excellent yield (60-85%) and enantioselectivity (75-96%). We have also proven that this methodology can be applied to amide derivatives to create 6 membered ring systems with yields from 60 to 99% and enantiomeric excess up to 93% in 4 examples.

2. Chapter 2: Iridium catalysed nitro-Mannich cyclisation

2.1. Introduction

2.1.1. Metal catalysed silane reduction

Amides are one of the most popular groups in synthesis and provide the key links in many molecules from proteins to drugs and polymers. In many synthetic routes amide formation is employed in joining two halves of a molecule together and may ultimately be reduced to the corresponding amine.

Towards the end of the last century attempts were made to develop catalytic amide reduction methodologies that didn't require the use of stoichiometric metal hydride reagents. To this end, Corriu *et al* showed that bis-hydrosilanes and catalytic [$RhCl(PPh_3)_3$] could reduce N,N-diethylphenylacetamide **60** to the corresponding enamine **61** in 54% yield using the bis-silane reagent as the hydride source (Scheme 2.1).[46]

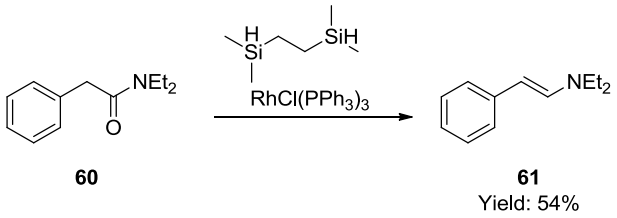

60 **61**
Yield: 54%

Scheme 2.1. Corriu rhodium catalysed amide reduction.

Despite this result, it wasn't until a report by Buchwald *et al* in 1991 that research on silane reduction was popularised.[47] Buchwald showed that a combination of Cp_2TiCl_2, n-BuLi and $(EtO)_3SiH$ would reduce a variety of esters to their corresponding alcohols. Ito and co-workers expanded this methodology using catalytic $RhH(CO)(PPh_3)_3$ and diphenylsilane to reduce a range of tertiary amides in good to excellent yield. The reaction is thought to proceed *via* the following mechanism: oxidative addition of the silane **62** on to the rhodium catalyst forms **63**, subsequent addition of the amide **64** and migratory insertion forms an

alkylrhodium complex **65**. Hydride transfer results in the elimination of siloxane and reductive elimination furnishes the desired amine **66** (Scheme 2.2).[48]

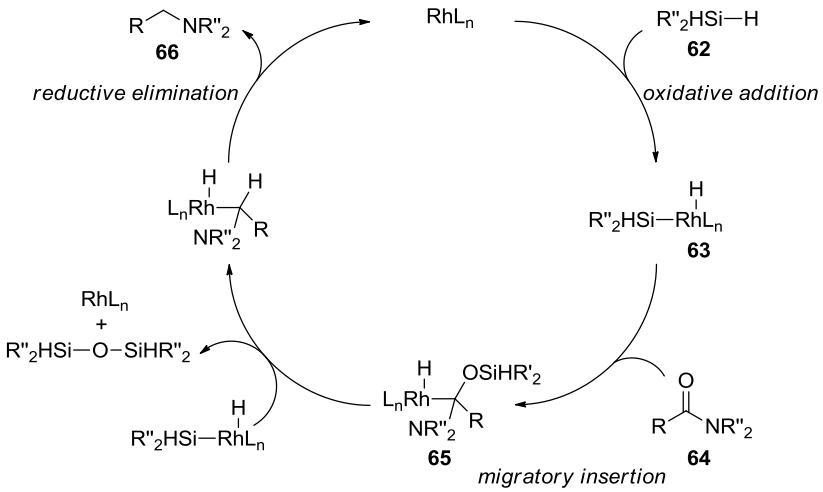

Scheme 2.2. Rhodium catalysed amide reduction

Inspired by this work a wide range of methods have since been developed:[49] Fuchikami *et al* demonstrated that a variety of metal complexes (such as $Mn_2(CO)_{10}$, $RhH(PPh)_4$, $IrCl_3$) and silane combinations can be used for the reduction of tertiary amides.[50] Nagashima and co-workers provided a method with excellent chemoselectivity using a ruthenium cluster catalyst **67** with dimethylphenylsilane. These conditions are able to selectively reduce amides over both esters and ketones (Scheme 2.3).[51]

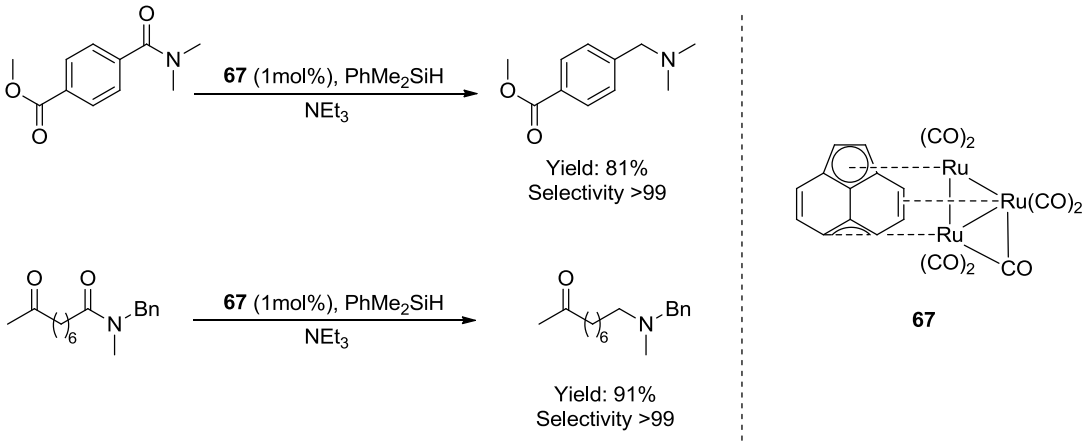

Scheme 2.3. Chemoselective silane reduction using ruthenium cluster complex**.**

Nagashima has also demonstrated that $H_2PtCl_6.H_2O$ and TMDS (tetramethyldisiloxane) can chemoselectively reduce amides in the presence of alkenes, nitro groups, esters and nitriles (Scheme 2.4).[52]

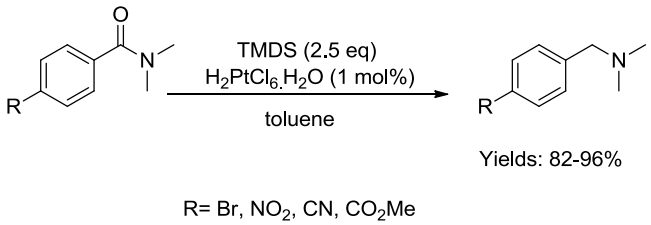

Scheme 2.4. Chemoselective silane reduction using H_2PtCl_6**.**

More recently, focus has shifted to the use of inexpensive metal catalysts and silanes. To this end the Beller group has recently demonstrated that $[Fe_3(CO)_{12}]$ and low cost PHMDS provide a wide range of amines in excellent yield (Scheme 2.5, A).[53] They have also shown that zinc acetate with $(EtO)_3SiH$ reduces amides with excellent chemoselectivity over nitro groups, alkenes, esters and nitriles (Scheme 2.5, B).[54]

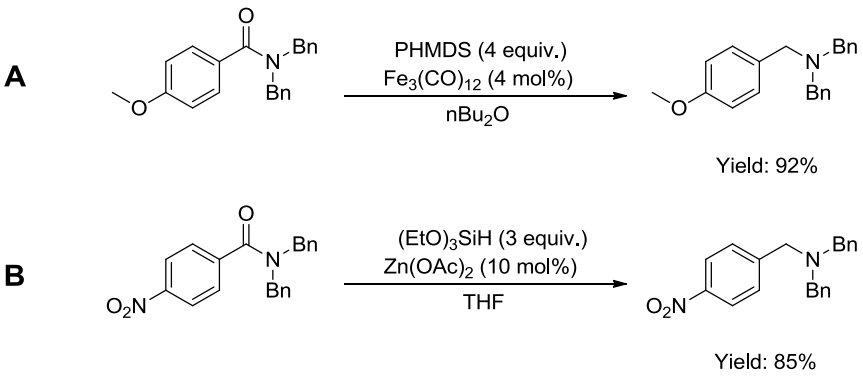

Scheme 2.5. Iron and zinc complex catalysed amide reduction

In summary, a variety of silane/metal catalysed amide reductions have been developed, which offer unprecedented chemoselectivity when compared with traditional metal hydride reagents. The methodologies are generally robust reactions and therefore don't require the rigorous reaction conditions usually associated with metal hydride reductions. Subsequently, metal

complex catalysed silane reduction methodology is becoming increasingly common in synthetic chemistry.

2.1.2. **Partial amide reduction and amide activation**

The partial reduction of amides is a very useful synthetic approach. It allows the formation of a relatively reactive imine/iminium intermediate which theoretically could be attacked by a range of nucleophiles leading to α-substituted amine compounds. However, this field has received relatively little attention even though it has been known for the past 50 years. In 1961 Brown *et al* developed a method that used 0.25 equivalents of lithium aluminium hydride (1 equiv. of hydride) at 0 °C to reduce a range of aziridinones **68** to their corresponding aldehydes **69** in moderate to good yields (Scheme 2.6).[55]

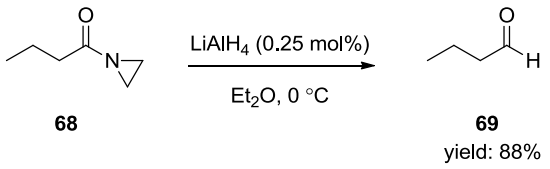

Scheme 2.6. Partial amide reduction to aldehydes

The use of this $LiAlH_4$ reduction methodology was also used to allow the addition of a nitrile to amide **70** *via* KCN attack on the corresponding iminium ion **71**. However, exchanging $LiAlH_4$ with $LiAl(OEt)_3H$ allowed improved yields (**72**) to be achieved (Scheme 2.7).[56]

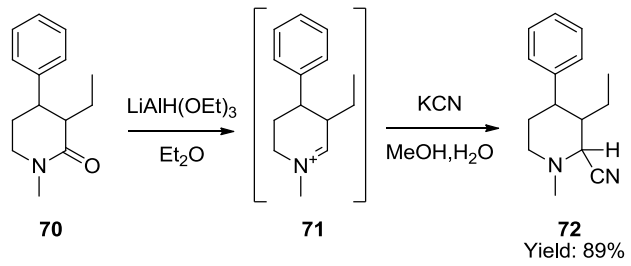

Scheme 2.7. Partial reduction of lactams followed by nitrile addition

Heathcock *et al* also employed this partial reduction route in attempts to synthesise dendrobine. Partial reduction of **73** using lithium aluminium hydride forms iminium **74**, subsequent attack of sodium cyanide allows the formation of tetracycle **75** in good yield (Scheme 2.8).[57]

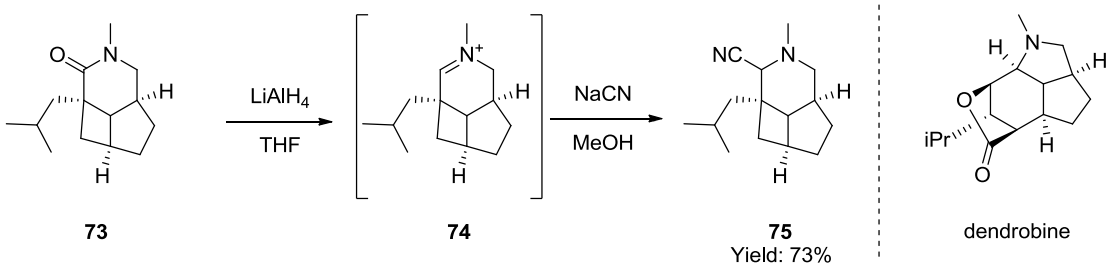

Scheme 2.8. Partial reduction and nitrile addition towards the synthesis of dendrobine

More recently this partial reduction approach was used by the Dixon group in the stereoselective synthesis of (−)-nakadomarin A (Scheme 2.9).[58] Partial reduction of the lactam **76** with DIBAL in the presence of a tethered furan nucleophile provided the pentacyclic core **77** of (-)-nakadomarin A in 41% yield.

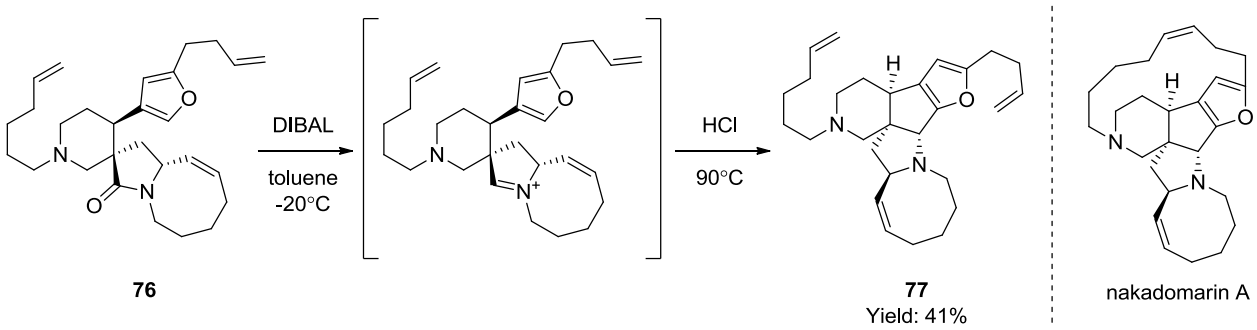

Scheme 2.9. Partial reduction in the synthesis of (-)-nakadomarin A

The above mentioned partial reductions can all be thought of as examples of amide activation. Another approach to amide activation is from dehydration reactions typically using triflic anhydride. Activated amide intermediates have been shown to react with a range of carbon nucleophiles, such as silyl enol ethers, allylsilanes and enamines to form a range of cyclic

structures. For example silyl enol ether lactam **78** can cyclise to form the bicyclic enamine **79** in good yield (Scheme 2.10).[59]

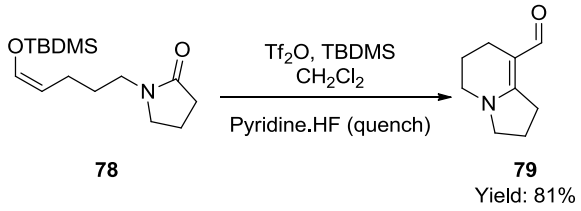

Scheme 2.10. Triflic anhydride activation of amides.

Triflic anhydride has also been used to for the activation of amides in Pictet-Spengler reactions: Nicolaou and co-workers demonstrated this in the total synthesis of aspidophytine (Scheme 2.11).[60] Triflic anhydride activation of the amide **80** allows attack from the indole, rearomatisation provides an iminium intermediate **81**, which is subsequently quenched by sodium borohydride to afford the desired Pictet-Spengler product **82**.

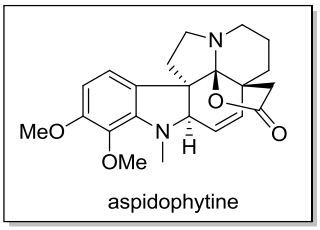

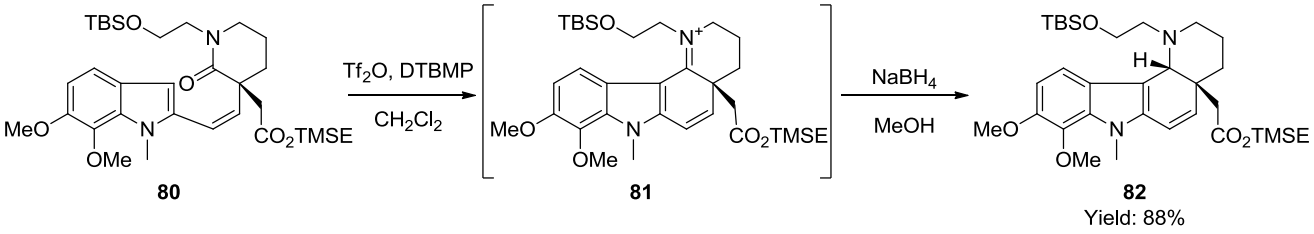

Scheme 2.11. Triflic anhydride in the synthesis of aspidophytine

One of the most powerful amide activation methods employing triflic anhydride is the alkylation of amides with Grignard and organolithium reagents.[61] Huang showed that treating either lactams or amides with triflic anhydride at -78 °C followed by the addition of an organometallic reagent allowed the formation of dialkylation compounds in good yield. By

controlling the stoichiometry of the organometallic reagents two different groups could be added to the amide equivalent by sequential addition. When using chiral α-substituted amides the reaction proved to be highly diastereoselective (Scheme 2.12).

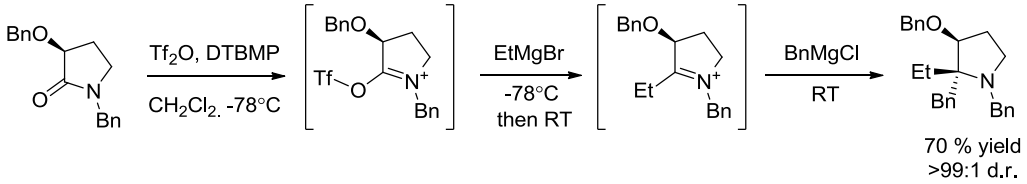

Scheme 2.12. Diastereoselective alkylation of amides with Grignard reagents.

2.1.3. **Nitro-Mannich reaction**

The nitro-Mannich (or aza-Henry) reaction is the C-C bond forming reaction of a nitro-alkane nucleophile with an imine to form β-nitroamine derivatives. The reaction was initially developed by Henry in 1897. Henry showed that treating the piperidine-derived hemiaminal **83** with nitromethane or nitroethane forms the the nitro-triamine **84** and nitro-diamine **85** respectively (Scheme 2.13).[62]

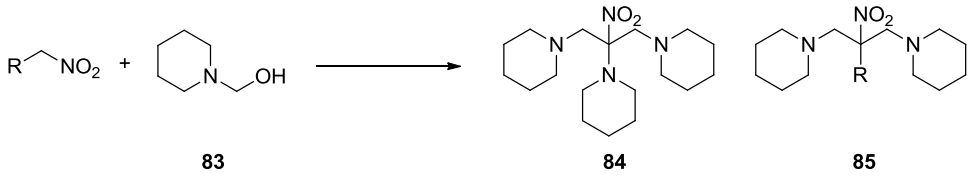

Scheme 2.13. First reported nitro-Mannich reactions by Henry (1987).[62]

However, there was no major advancement in the methodology[63] until Senkus and Johnson independently reported the one-pot, three-componant reaction of formaldehyde, amines **86** (including aromatic and secondary amines) and nitroalkanes **87** to form a range of nitro-Mannich products (scheme 2.14).[64] Secondary nitroalkanes provide the mono-addition product **88** in moderate to good yield and primary nitroalkanes form the double-addition nitro-diamine **89** in good to excellent yields.

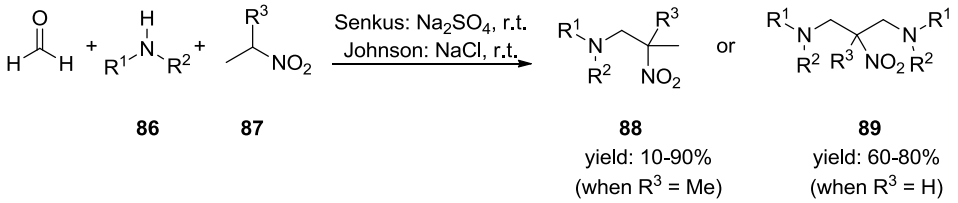

Scheme 2.14. Nitro-Mannich reaction *via in situ* imine formation.

The above mentioned nitro-Mannich reactions have all formed the imine *in situ* from hemiaminal or aldehyde amine combinations. The first use of preformed imines in the nitro-Mannich reaction was demontrated by Hurd and Strong in 1950. They were able to show that reacting *N*-benzylideneaniline **90** with nitromethane formed the mono-addition adduct **91** in 54% yield (Scheme 2.15).[65]

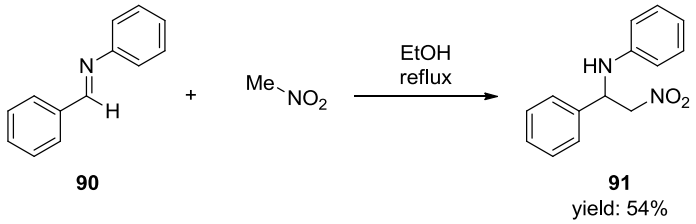

Scheme 2.15. First nitro-Mannich reaction using preformed imines.

However despite these reports it wasn't until the turn of the century that interest in the nitro-Mannich reaction started to increase, this was due to a diastereoselective methodology developed by Anderson and co-workers. They demonstrated the addition of nitronate ions (formed using n-BuLi at -78°C) to a selection of *N*-PMB imines **92**, allowing the formation β-nitroamines (**93**) with diastereoselectivities up to 15:1 (d.r.). Unfortunately the β-nitroamines (**93**) formed were unstable and prone to retro-Mannich reactions, therefore the reaction yield couldn't be calculated until after SmI_2 reduction to 1,2 diamine **94** (Scheme 2.16).

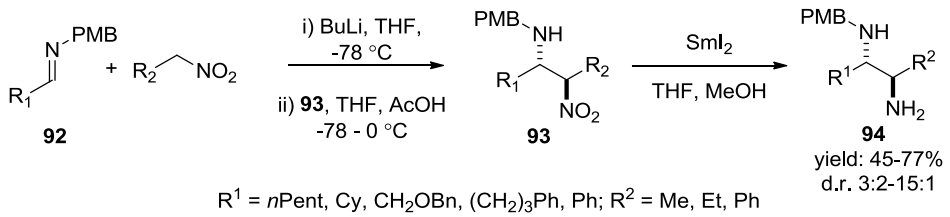

Scheme 2.16. First diastereoselective nitromannich reaction using nitronate nucleophiles.

These results brought the nitro-Mannich reaction to the attention of the synthetic community and subsequently a plethora of nitro-Mannich methodologies have been developed.[66] Particular attention has been paid to stereoselective nitro-Mannich reactions. The two main catalytic methods employ either chiral Lewis acidic metal catalysts or bifunctional organocatalysis. The first enantioselective nitro-Mannich reaction was reported by Shibasaki and co-workers: using a binapthol derived Yb/K complex (**95**) they were able to add nitromethane to *N*-phosphinoyl imines (**96**) in excellent enantioselectivity. However, the reaction times were typically long (2.5–7 days) and the reaction only worked with nitromethane (Scheme, 2.17).

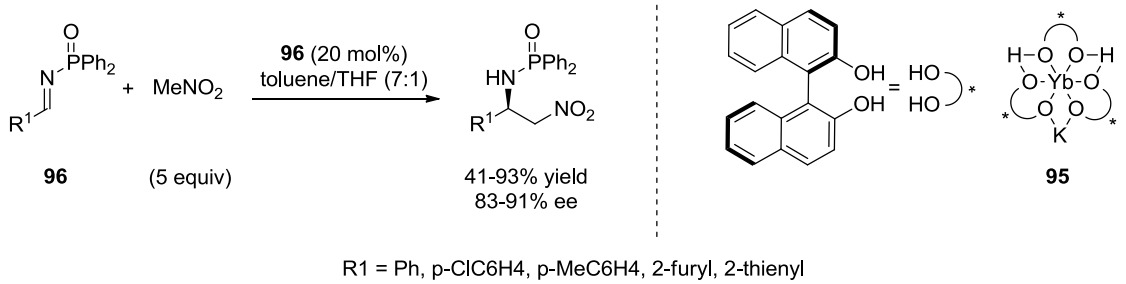

Scheme 2.17. First enantioselective nitro-Mannich reaction.

The first organocatalytic approach to a nitro-Mannich reaction was reported by Takemoto *et al*: employing bifunctional organocatalyst **97**, which possesses both Bronsted base and hydrogen bonding groups they were able to form β-nitroamines with moderate to good enantioselectivity.

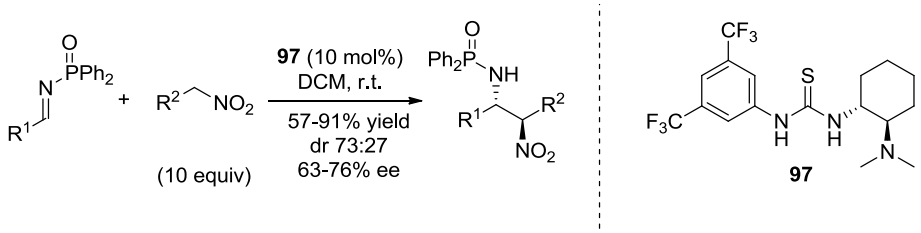

R1 = Ph, p-MeC6H4, p-ClC6H4, 2-napthyl, 2-furyl, 2-pyridyl
2-thienyl, cinnamyl; R2 = H, Me

Scheme 2.18. The first organocatalysed enatioselective nitro-Mannich reaction

In addition to the useful C-C bond forming nature of the nitro-Mannich reaction, the installation of a nitro group into a molecule offers a wide range of reactivity. The nitro group can be removed via radical chemistry,[67] reduced to an amine or converted into a carbonyl. [68] Overall the nitro-Mannich reaction is a useful C-C bond forming tool: it is able to enantioselectively add multiple chiral centres in one step, as well as forming products that possess the useful nitro group, primed for further elaboration.

2.2. Aims

Our success in the *N*-sulfonyliminium methodology left us eager to explore new cascade sequences. Our inspiration for the development of a nitro-Mannich cascade came from a recently published total synthesis of manzamine A within the group.[69] The total synthesis of manzamine A takes advantage of route shortening reaction cascades at various points along the route. One such cascade comprised a previously unknown chemoselective partial reduction: lactam **98** was partially reduced using titanium isopropoxide and diphenylsilane (in the presence of a nitro group, internal and external alkenes and an acetal) to form a transient hemiaminal intermediate. Subsequent elimination forms the complementary iminium intermediate that can undergo nitro-Mannich cyclisation to form the core of manzamine A (**99)** in good yield and diastereoselectivity (Scheme 2.19).

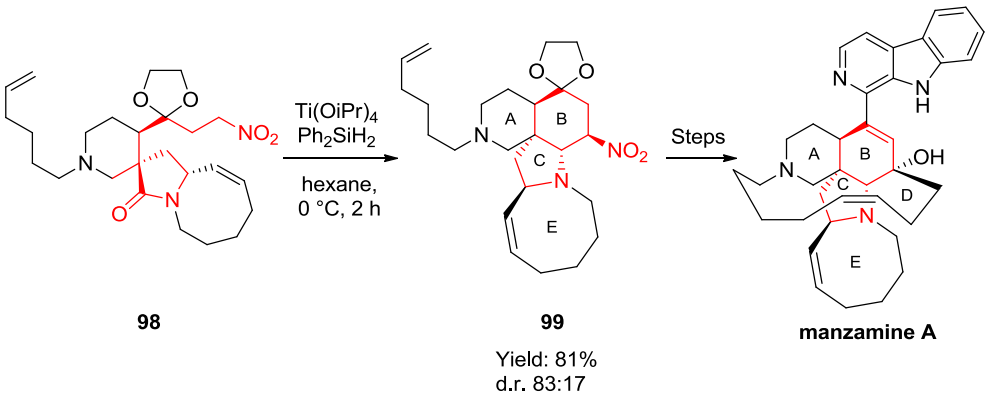

Scheme 2.19. Nitro-Mannich cascade in the total synthesis of manzamine A.

Recognising the synthetic potential of this novel annulation strategy, we wanted to investigate whether an analogous reductive nitro-Mannich cyclisation of *N*-linked lactam substrates of type **100** was feasible.[70] Such chemistry would allow direct access to fused nitrogen containing bicycles of type **101** via reactive iminium ion intermediates **102** (Scheme 2.20).[71] These motifs are abundant in nature, making up major classes of alkaloid natural products which show important biological activity.[72] In addition, the presence of the versatile nitro group could be exploited as a handle to access, for example, ketone[73] and amine functionality. As such the new methodology would be useful for natural product and library synthesis alike.

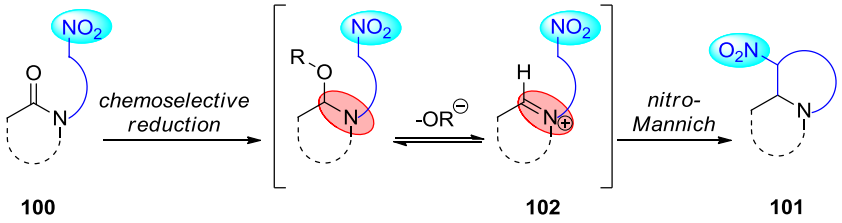

Scheme 2.20. Partial reduction cascade concept.

2.3. Synthesis of model substrate and proof of principle

Caprolactam derived **100a** was selected as our model substrate and was readily accessed in two steps. Caprolactam was *N*-alkylated with 1,4-dibromobutane to form bromide **103a** in

good yield. Treatment of bromide **103a** with sodium nitrite via an S_N2 reaction afforded the nitroalkane tethered lactam **100a** (Scheme 2.21).

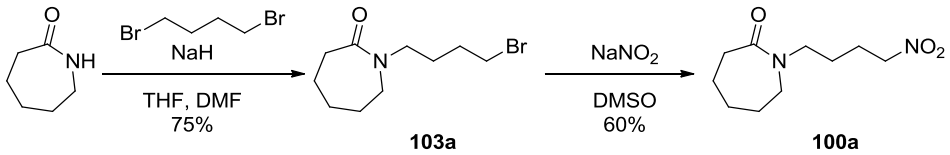

Scheme 2.21. Synthesis of model substrate **100a**.

With our model substrate in hand, nitro-lactam **100a** was subjected to the modified Buchwald conditions used in the synthesis of manzamine A.[74] Pleasingly, the desired bicycle **101a** was isolated 34% yield (Scheme 2.22). However, whilst this provided a good proof of principle, the aim was to develop an efficient catalytic cascade and the use of superstoichiometric quantities of titanium was undesirable so further optimisation was not pursued.

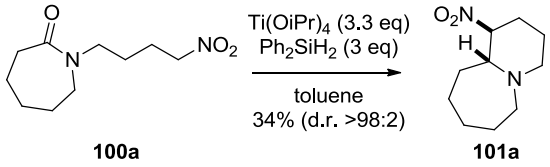

Scheme 2.22. Proof of principle using modified Buchwald conditions.

2.4. Reductive method screen*

Our investigation was subsequently focused on more the recently developed substoichiometric metal catalysed silane reduction methodology.[70,75,76] Unfortunately, following reduction conditions reported by Sakai[77] (using Et_3SiH (4 equiv) and $InBr_3$ (5 mol%) in chloroform) provided only recoved starting material. Investigating the rhodium catalysed reduction methodology developed by Ito[78] (catalytic $RhH(CO)(PPh_3)_3$ (0.1 mol%) and Ph_2SiH_2 (2.1 eq) in THF) it was found that the reaction proceeded cleanly to the undesired tertiary amine **104a** (Table 2.1, Entry 1). Changing the reaction solvent to toluene

* The work reported in reductive method section 2.4 was carried out by Alan Chambers

and lowering the temperature did allowed trace amounts of the desired product **101a** to be isolated, however, due to the low yield and poor selectivity we decided to test further methodologies (Table 4, Entry 3).

Table 2.1. Rhodium catalysed amide reduction

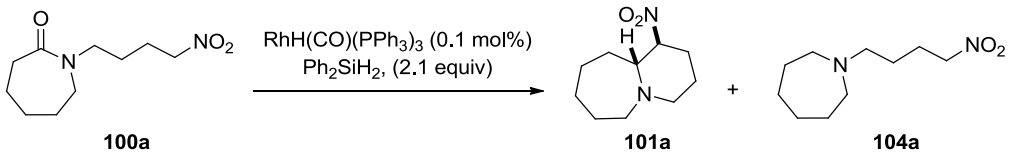

100a **101a** **104a**

Entry[a]	Solvent	Temperature (°C)	Time (h)	Yield[b] 101a(%)	Yield[b] 104a (%)
1	THF	20	0.5	0	90
2	Toluene	20	0.5	0	87
3	Toluene	-20	18	1	37

[a] All reactions performed on 0.100 g scale and at 1 M substrate concentration; [b] Isolated Yields

Nagashima recently developed a method for partially reducing amides to enamines using catalytic $IrCl(CO)(PPh_3)_2$ (Vaska's complex[79]) and TMDS (tetramethydisiloxane) or PMHS (polytetramethyldisiloxane) in excellent yields.[80] However, following the reported conditions failed to yield any product (Table 2.2, Entry 1), although, avoiding the documented basic workup pleasingly yielded both the tertiary amine **104a** and the desired product **101a** (Table 2.2, Entry 2). Using PMHS also worked well but lowering the temperature had a negative effect on the yield. Acidic workup provided no improvement in the yield (Table 2.2, Entries 2-5). Reverting to the TMDS reagent, it was found that in this case using an acidic work up with 1 M HCl afforded the desired product **101a** with a very promising yield (53%) and in high diastereoselectivity (d.r. 88:12) (Table 5, Entry 7). This reagent combination and work up procedure appeared to offer the most potential for optimisation.

Table 2.2. Iridium catalysed amide reduction optimisation

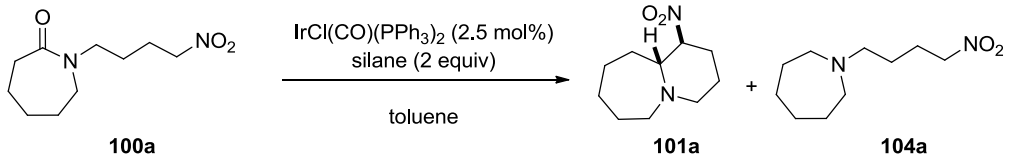

100a 101a 104a

Entry[a]	Temperature (°C)	Silane	Work up	Yield[b] 101a (%)	d.r.	Yield[b] 104a (%)
1	20	TMDS	KOH/MeOH	-	-	-
2	20	TMDS	Silica gel	23	97:3[c]	37
3	20	PMHS	Silica gel	36	88:12	30
4	0	PMHS	Silica gel	28	88:12	18
5	20	PMHS	1 M HCl	19	88:12	20
6	20	TMDS	1 M HCl	53	88:12	2

[a] All reactions performed on 0.100 g scale, 0.05 M substrate concentration, RT, 5 min;[b] Isolated Yields after FCC purification; [c] Further purification of the product by an acid/base extraction may have resulted in a different d.r. compared to other experiments.

2.5. Optimisation of $IrCl(CO)(PPh_3)_2$ and TMDS conditions*

In an attempt to improve the efficiency of the reaction, the loading of Vaska's complex was decreased to 0.5 mol%. This actually resulted in an increased yield (68%) with no significant effect on the diastereoselectivity (Table 2.3, Entry 2). Reducing the loading of Vaska's complex further to 0.1 mol% led to full conversion but gave the product in reduced yield (Table 2.3, Entry 3). Investigating the number of TMDS equivalents required for full conversion was shown to have only a small effect on the reaction yield and diastereoselectivity (Table 2.3, Entries 2,4 and 5).

* The work reported in optimisation of $IrCl(CO)(PPh_3)_2$ and TMDS conditions section 2.5 was carried out by Alan Chambers.

Table 2.3. Effect of catalyst and TMDS equivalents

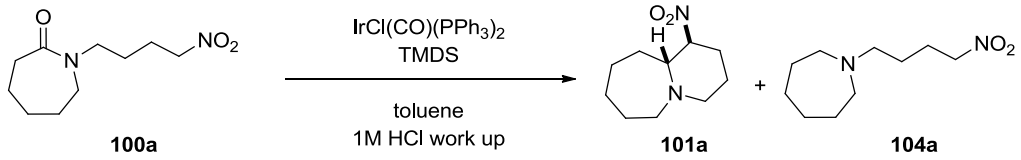

100a 101a 104a

Entry[a]	Catalyst loading (mol%)	TMDS (equiv)	Yield[b] 101a (%)	d.r.	Yield[b] 104a (%)
1	2.5	2.0	53	88:12	2
2	0.5	2.0	68	89:11	14
3	0.1	2.0	50	91:9	14
4	0.5	1.0	55	89:11	9
5	0.5	3.0	65	87:13	12

[a] All reactions performed on 0.100 g scale, 0.05 M substrate concentration, RT, 5 min; [b] isolated yield

A solvent screen was conducted to investigate whether the increased yield could be further improved (Table 2.4). Whilst all the aprotic solvents worked to some extent, toluene was still shown to be the best solvent for the transformation (Table 2.4, Entries 1-4). Reactions performed in ethanol failed to reduce the lactam, which could possibly be due to the ligation of the iridium complex or the consumption of the silane *via* the formation of hydrogen (Table 2.4, Entry 5).

Table 2.4. Solvent screen.

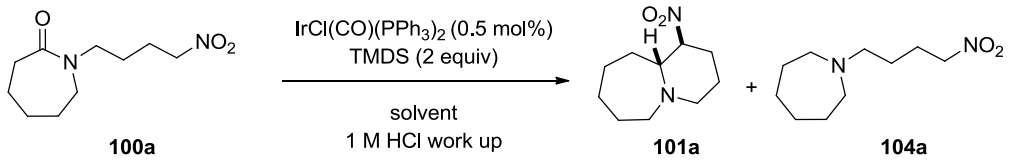

100a 101a 104a

Entry[a]	Solvent	Yield[b] 101a (%)	d.r.	Yield[b] 104a (%)
1	toluene	68	89:11	14
2	hexane	53	91:9	8
3	THF	50	86:14	32
4	DCM	48	88:12	11
5	EtOH	-	-	-

[a] All reactions performed on 0.100 g scale, 0.05 M substrate concentration, RT, 5 min; [b] isolated yield

Due to the cyclisation of the iminium intermediate being an intramolecular process, it was important to see how the substrate concentration would affect the product yield with respect to full reduction to **104a** (Table 2.5). We found that the yield of **101a** decreased with higher substrate concentration (Table 2.5, Entry 1) and increased when the substrate concentration was lowered (Table 2.5, Entry 3). This was potentially due the relative rate of the intermolecular reduction of the iminium intermediate decreasing with increased dilution resulting in slower amine by-product formation.

Table 2.5. Concentration effects.

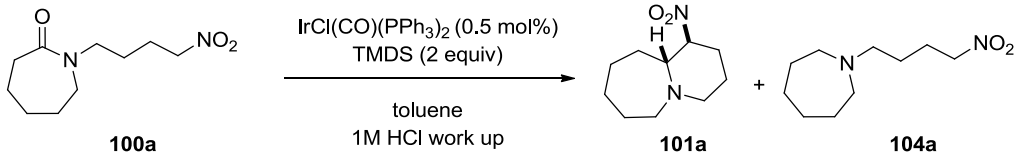

100a **101a** **104a**

Entry[a]	Substrate concentration (M)	Yield[b] 101a (%)	d.r.	Yield[b] 104a (%)
1	0.25	54	91:9	14
2	0.05	68	89:11	14
3	0.01	80	88:12	10

[a] All reactions performed on 0.100 g scale, RT, 5 min; [b] isolated yield.

Finally we wanted to test the optimised conditions on a large scale reaction. Using 2 g of **100a** the desired bicyclic product **101a** was isolated in good yield (71%) and excellent diastereoselectivity (d.r. 98:2). Interestingly, the diastereoselectivity increases and yield decreases with increased scale; this could potentially be attributed to the relative instability of the minor diastereomer on silica gel. As the scale of the reaction is increased a larger quantity of silica gel is required for purification, therefore the minor diastereomer experiences prolonged contact with the silica gel, which subsequently decreases the quantity of isolated minor diastereomer.

2.6. Reaction scope

With the optimisation complete we sought new structures to submit to our reaction conditions. Changing the size of the lactam would not only provide new structures it would also test the partial reductive reactivity of the Vaskas's complex system and the relative stability of the corresponding enamine/iminium intermediates (see mechanism section).

2.6.1. **Synthesis of starting materials**

The first point of variation to be tested was the size of the lactam ring, this would test the reactivity of both the partial reduction and the nitro-Mannich cyclisation as well as providing a range of new scaffolds. Following analogous conditions to those used in the synthesis of model system **100a** (Scheme 2.21) lactam substrates possessing 5 membered rings up to 8 membered rings were obtained in modest yield (Figure 2.1).

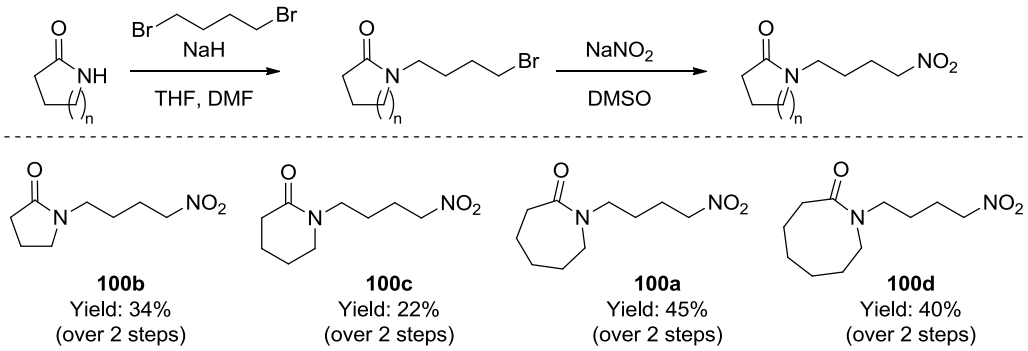

Figure 2.1. Nitro-butyl tethered lactam variation.*

The addition of an ether group into the lactam ring system would not only provide new structures but would also demonstrate the functional group tolerance of the reaction. *N*-Alkylation of 1,4-oxazepan-5-one proceeded well affording the bromide **103e** in 86% yield. Nitration of **103e** using silver nitrite provided the desired nitroalkane **100e** in 42% yield.

* Compounds **100b** and **100d** synthesised by Alan Chambers.

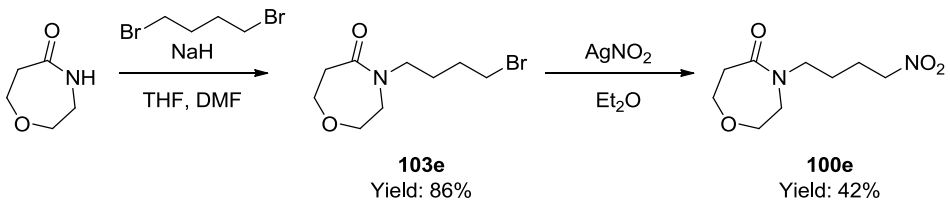

Scheme 2.23. Synthesis of oxazepanone derivatives.

The next point of variation was the length of the nitro alkane tether, this variation would not only provide a new range of bicyclic scaffolds but also test the effect of tether length on the reaction. Again following analogous conditions to those used for model substrate **100a** piperidinone and caprolactam were *N*-alkylated with 1,5-dibromopentane, Kornblum nitration of (**103f** and **103g**) provided piperidone and caprolactam derivatives **100f** and **100g** (Figure 2.2).

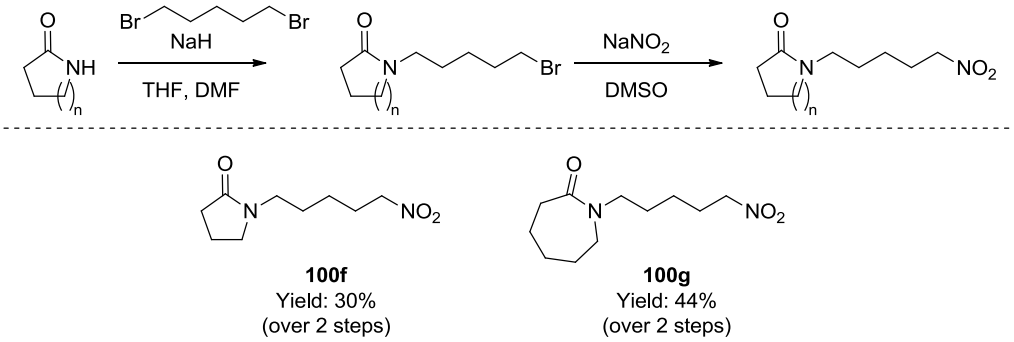

Figure 2.2. Extended nitro-alkane tethered analogues.*

Interestingly, when attempting to synthesise the shortened tethered examples following the same alkylation conditions with 1,3-dibromopropane no bromo-lactam was formed. Instead the alkylated allyl-lactam was recovered, presumably due to elimination of the tethered bromide lactam intermediate. Changing the electrophile to 1-bromo-3-chloro-propane allowed effective formation of the chloro-propane tethered lactams **103h** and **103i** due to the relatively less reactive chloride group (Figure 2.3).

* Compound **100f** was synthesised by Alan Chambers.

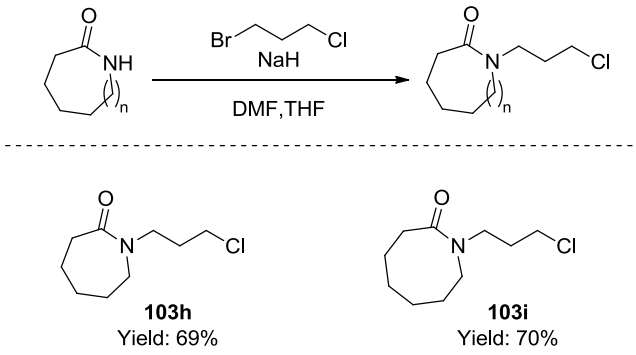

Figure 2.3. Shortened chloro-propane tethered analogues.

A range of nitration methods were screened in an attempt to substitute the chloride **103h** (Table 2.6). Modified Kornblum conditions using phloroglucinol as an additive in an attempt consume the nitrite ester by-product, provided only the corresponding nitrite ester, alcohol and alkene (Table 2.6, Entry 1). Switching the solvent to acetone in the absence of phloroglucinol showed poor reactivity with only 10% conversion to the alkene (Table 2.6, Entry 2). Switching the solvent back to DMSO and using substoichiometric amounts of potassium iodide to impart an *in situ* Finkelstein reaction afforded 9% of the desired nitroalkane (Table 2.6, Entry 3). Increasing the equivalents of sodium nitrite increased the yield of the desired product (21%) (Table 2.6, Entry 4).

Table 2.6. Screen of reagents for the nitration of chloro-alkane **103h**.

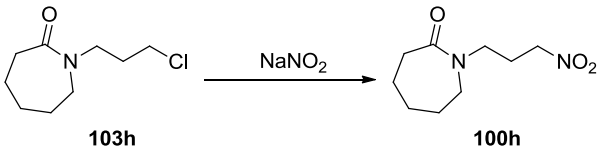

Entry[a]	Concentration [b] (M)	Additive	Solvent	$NaNO_2$ (Equiv.)	Yield[c] (%)
1	0.1	phloroglucinol	DMSO	2.1	0
2	0.1	-	acetone	1.5	0
3	1.0	KI	DMSO	1.3	9
4	1.0	KI	DMSO	3.6	21

[a] All reactions performed on 0.200 g scale at 20 °C; [b] Substrate 103h concentration; [c] isolated yield.

Applying the optimised conditions to the azocanone derived chloride **103i** resulted in the formation of the desired nitroalkane in a comparable yield to **100i** (Figure 2.4).

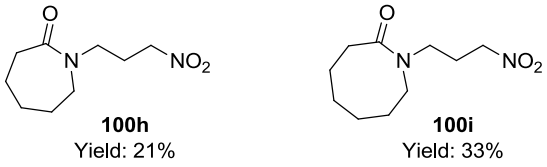

Figure 2.4. Nitro-propane tethered lactam derivatives.

2.6.2. **Synthesis of starting material with an aryl linked nitroalkane tether**

An aryl-linked tether was designed to test the effect of having both benzylic nitro- and amide-groups as well as the presence of the aromatic group itself on the reaction. Alkylation of valerolactam, caprolactam and azacan-2-one with 1,2-bis(bromomethyl)benzene afforded the desired aryl-linked bromides in moderate yield (Figure 2.5).

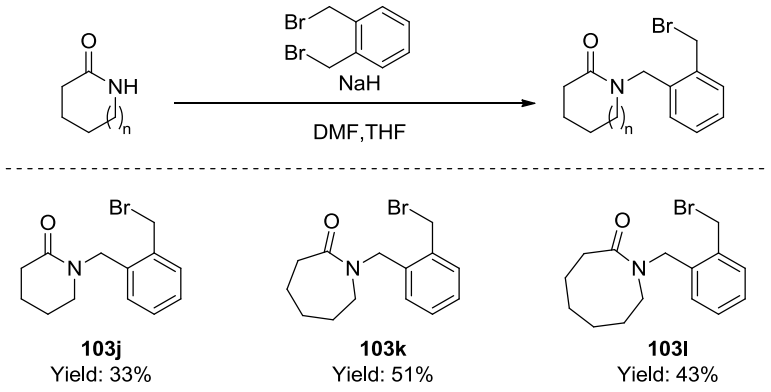

Figure 2.5. Synthesis of aryl-linked bromo-tethered lactam.

The caprolactam derived bromide **103k** was effectively converted to the complementary nitroalkane **100k** using the silver nitrite method used for **100e** in 24% yield-the low yield was due to large amounts of alcohol and nitrite ester by-products. When the same method was applied to the valerolactam and azacan-2-one derived bromides (**103j** and **103l**) the desired nitrated products were observed but only in poor yield and purity. Following the

phloroglucinol additive method also failed to provide any of the desired nitro-compound. Finkelstein reaction of bromides **103j** and **103l** formed their respective iodides and treatment of the crude iodides with sodium nitrite at −20 °C in DMF allowed the formation of the desired nitro-analogues **100j** and **100l** (Figure 2.6).

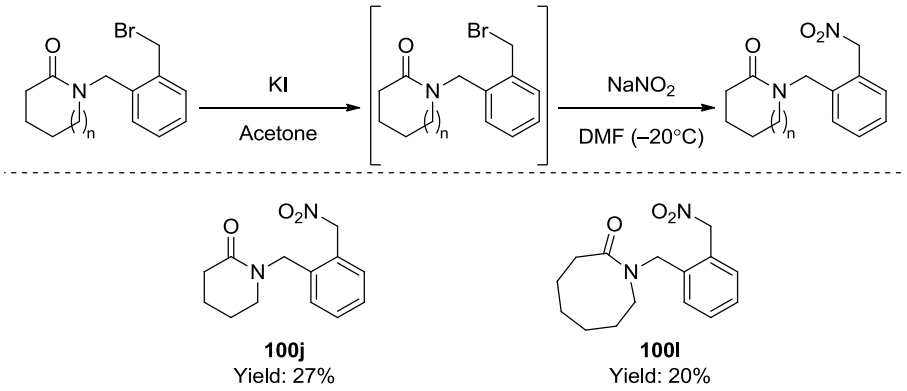

Figure 2.6. Synthesis of aryl linked nitro-lactam.

We can propose a number of theories as to why nitration of this family of compounds is so tricky. It is known that benzylic halides can be oxidised to the relevant carboxylic acid (under Kornblum nitration conditions). This is thought to proceed by the formation of nitrolic acid intermediate **105** from the nitrosation of the benzylic nitro product **100** with nitrite ester **106.** Subsequent hydrolysis of the nitrolic acid **105** affords the undesired carboxylic acid by-product (Scheme 2.24).[81]

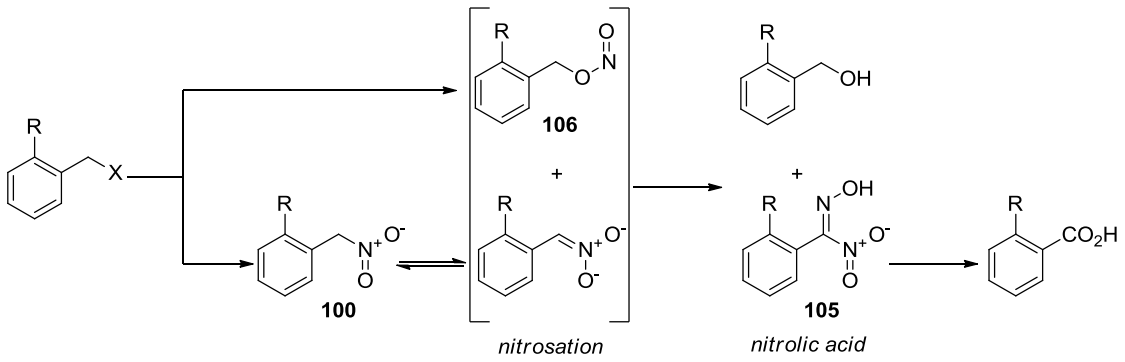

Scheme 2.24. Proposed decomposition of benzylic nitro-products.

Therefore, the increased acidity of the benzylic protons increases the rate of nitro decomposition. Thus, when nitrating benzylic halides of type **103(j/k/l)** the reaction time is crucial, to bring about full conversion but at the same time limit product decomposition. For this reason nitration of the preformed iodides at reduced temperature allows cleaner, better yielding reactions due to the relative faster reaction rate compared to the rate of product decomposition. It is also suspected that some neighbouring group participation (from the amide) may increase the rate of decomposition of **100(j/k/l)**. It is likely that this is the reason for the difficulty in forming the shorter nitropropane tethered examples (**100(h/i)**), the amide can form a 6-membered ring transition state **107** that can result in the elimination of the iodide forming the undesired alkene by-product **108**.

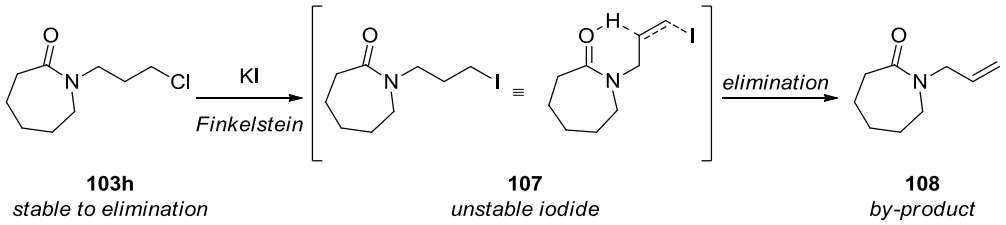

Scheme 2.25. Neighbouring group participation in the nitration of **103h**.

2.6.3. **Iridium catalysed nitro-Mannich cyclisation reaction scope**

With the desired starting materials prepared we were able to test the scope of the methodology. The size of the lactam ring was shown to very important for the reaction to work well. The smaller pyrrolidone and piperidone derived substrates **100b** and **100c** provided the desired bicycles **101b** and **101c** in only modest yield. It was proposed that this may be due to the relative instability of the enamine intermediate present in the reaction mixture (see mechanistic section 2.8). However, the cyclisation of azacanone-derived lactam **100d** resulted in **101d** in good yield and excellent diastereoselectivity. The reaction was shown to also tolerate the ether functionality present in **100e**; treating **100e** with the reaction conditions provided oxazapane **101e** with excellent diastereoselectivity albeit in reduced

yield. With all the 6-membered nitro-Mannich ring closing reactions working well we tested the extended- and shortened- tethered nitro-alkane analogues. The lengthened nitroalkane tethered examples provided access to 7-membered rings upon ring closure, exemplified by **100f** and **100g** in both proceeding in acceptable yields and good diastereoselectivity. Testing the reaction on shortened nitroalkane tethered substrates to generate 5 membered ring bicycles **101h** and **101i** again proceeded in good yield. Unfortunately, with these examples a reduction in diastereoselectivity was observed (Figure 2.6).

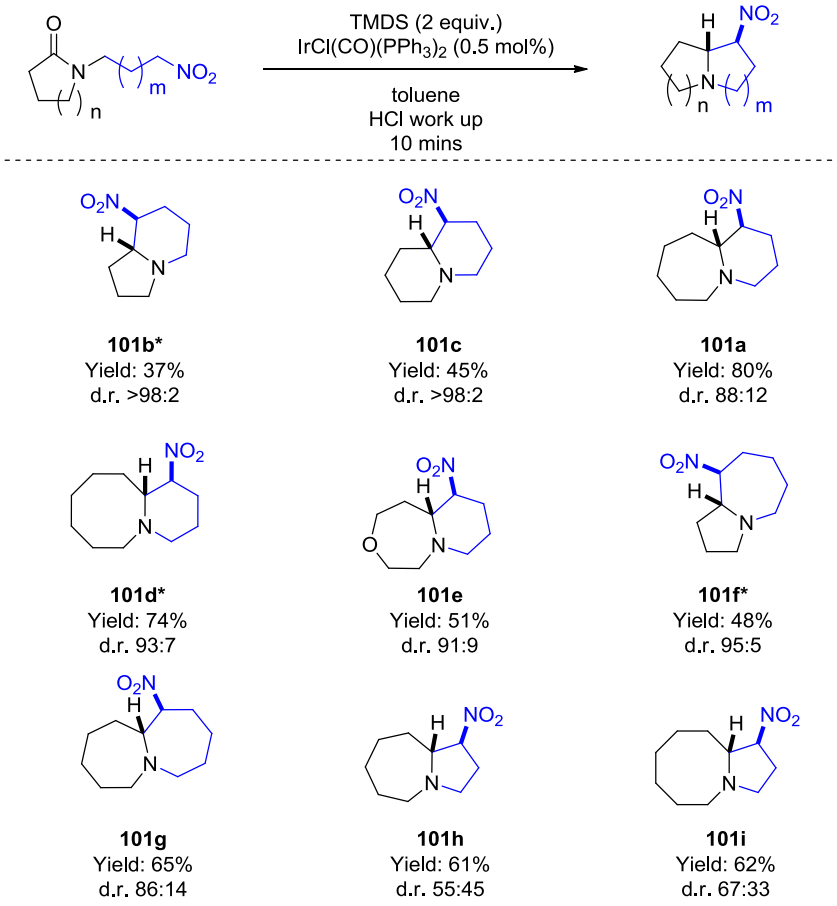

Figure 2.6. Scope of the iridium catalysed nitro-Mannich cyclisation.*

* Compounds **101b**, **101d** and **101f** were synthesised and characterised by Alan Chambers.

Substrates possessing an arene group in the nitroalkane tether pleasingly cyclised to their respective tricyclic products (**101k**, **101k** and **101l**) in good to excellent yields (52-81%) and diastereoselectivities up to 98:2 (Figure 2.7).

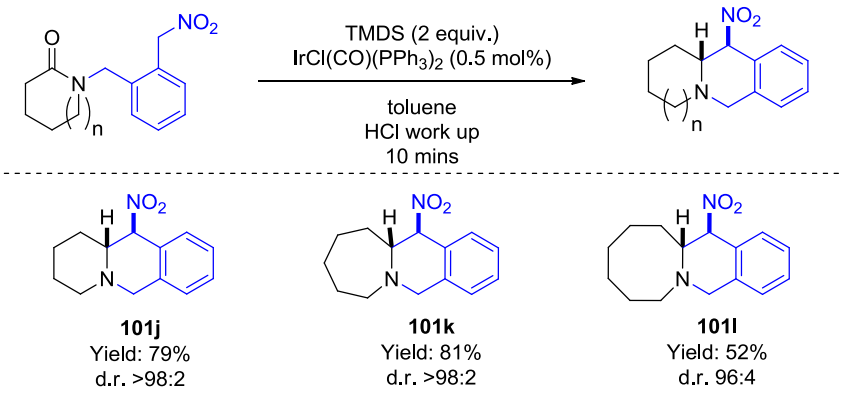

Figure 2.7. Scope of the iridium catalysed nitro-Mannich cyclisation.

2.7. Reaction Mechanism

In an attempt to gain understanding of the reaction mechanism and therefore help explain some of the results observed in the reaction scope, we designed a series of NMR experiments to elucidate the intermediate structures present at each stage of the reaction, thereby revealing the reaction mechanism (Figure 2.8). We began by taking the ^{1}H NMR spectrum of our model system **100a** in d_8-toluene (Figure 2.8. Spectrum **A**). Addition of TMDS and mesitylene as an internal standard is shown in Spectrum **B** (Figure 2.8) and shows that there is no change to the lactam starting material **100a**. Addition of Vaska's catalyst to the reaction mixture shows rapid conversion (5 mins) to the enamine compound **109** in quantitative yield (Figure 2.8, spectrum **C**). This enamine was shown to be relatively stable, decomposing slowly over more than 24 h. In a separate reaction we were able to investigate the intermediate present in the acidic work up; enamine intermediate **109** was formed following our standard conditions, after which 1 M HCl was added and the reaction mixture was subsequently extracted. Simply concentrating the aqueous solution furnished essentially pure iminium **110,** which could be

fully characterised (Figure 2.8, Spectrum **D**). Only after basification (K_2CO_3) of the aqueous layer and subsequent extraction were we able to recover our desired cyclised bicycle **101a** (Figure 2.8, spectra **E**).

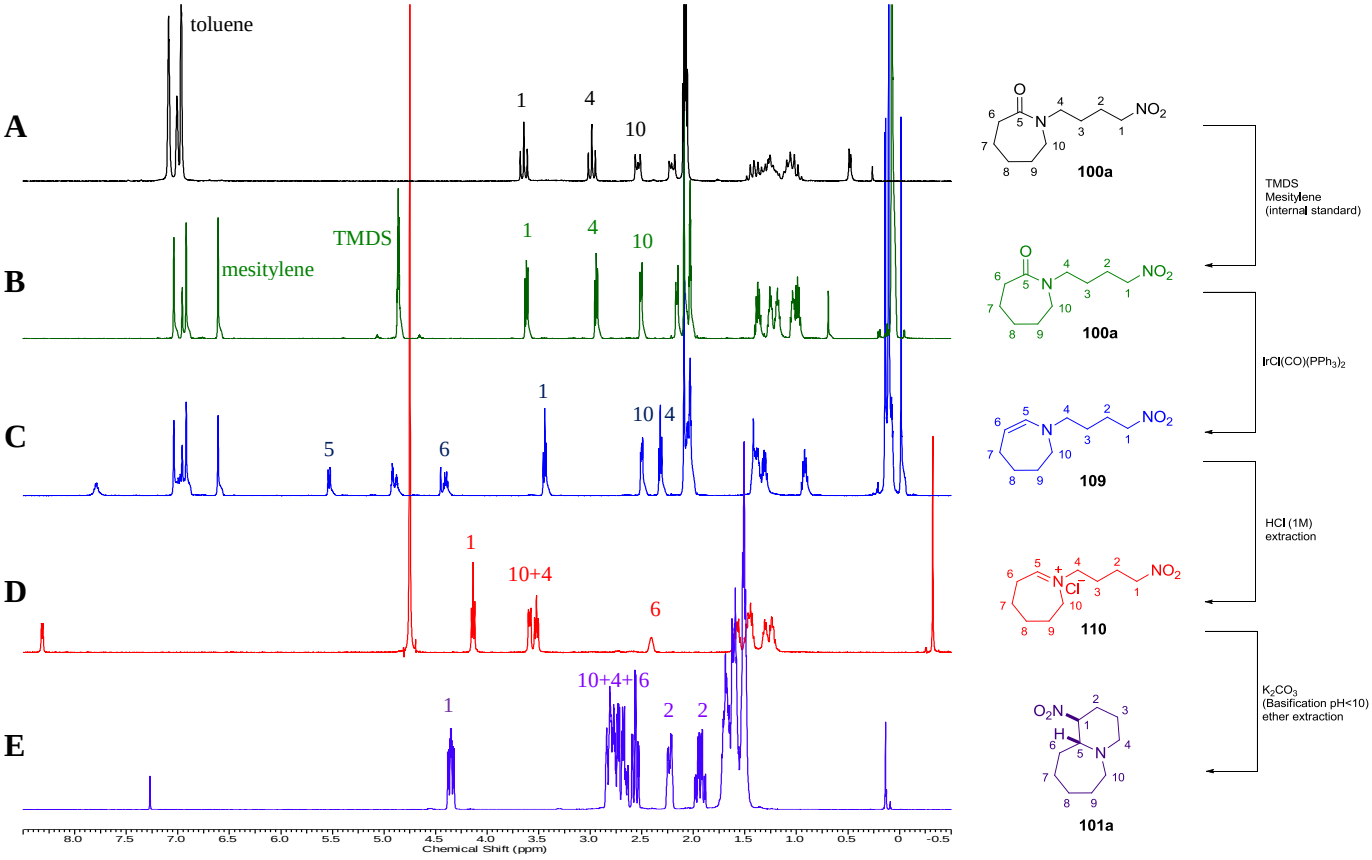

*Spectra **A**, **B**, and **C** were measured in d_8-toluene. Spectrum **D** was obtained in D_2O and spectra **E** was measured in $CDCl_3$.*

Figure 2.8. ^{1}H NMR spectra of starting material, intermediates and the desired product at selected phases of the reaction.*

Given the direct evidence for the presence of each intermediate at their respective phases in the reaction we postulated that the reaction proceeds *via* the mechanism shown in Figure 2.9. The iridium complex catalyses the partial reduction of amide **100a** to the siloxy intermediate **111**,[19] elimination and subsequent deprotonation reveals enamine **109**. Only upon acidic workup is the enamine re-protonated to give the stable water soluble iminium ion **110**. Upon

* The NMR data for the enamine intermediate **109** and iminium **110** was gathered by Alan Chambers.

addition of solid potassium carbonate, the resulting rise in pH to >10 facilitates smooth cyclisation of the putative nitronate **112** to form product bicycle **101a** (Figure 2.9).

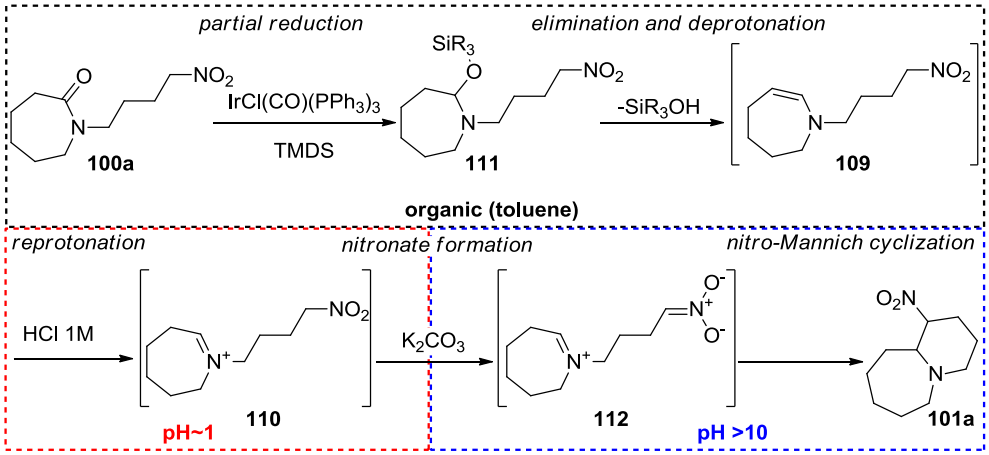

Figure 2.9. Postulated reaction mechanism.

2.8. Total synthesis of (±)-*epi*-epiquinamide

Epiquinamide was isolated in 2003 from the Ecuadorean poison dart frog *Epipedobates tricolour* (Figure 2.10) by Daly and co-workers.[82] Initially, they found that epiquinamide was an agonist for nicotinic acetylcholine receptors. However, when the Daly group synthesised epiquinamide and its diastereomer epi-epiquinamide they found neither were active with against these receptors and subsequently concluded that the activity comes from an impurity epibatidine.[83]

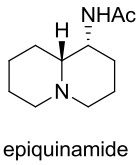

epiquinamide

Figure 2.10. A picture of *Epipedobates tricolour* and epiquinamide.

Retro-synthetic analysis clearly showed (±)-epi-epiquinamide could be synthesised *via* the quinolizidine product **101c** by reduction and acetylation. quinolizidine **101c** was accessed from simple commercial starting materials, valerolactam and dibromobutane as previously described.

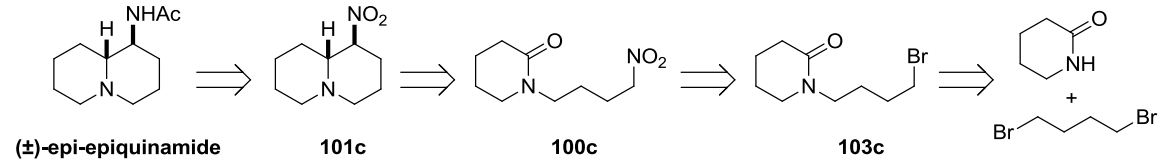

Scheme 2.26. Retrosynthetic analysis of (±)-epi-epiquinamide

Alkylation of valerolactam with dibromobutane provided the tethered bromide **103c** in 60% yield. Nitration afforded the nitroalkane tether **101c** in 36% yield. Iridium catalysed nitro-Mannich cyclisation provided the key step of the synthesis in 45% yield and excellent diastereoselectivity. A one pot reduction and acetylation completed the synthesis of (±)-epi-epiquinamide in 75% yield with an overall yield of 8% over the 4 steps (Scheme 2.27).

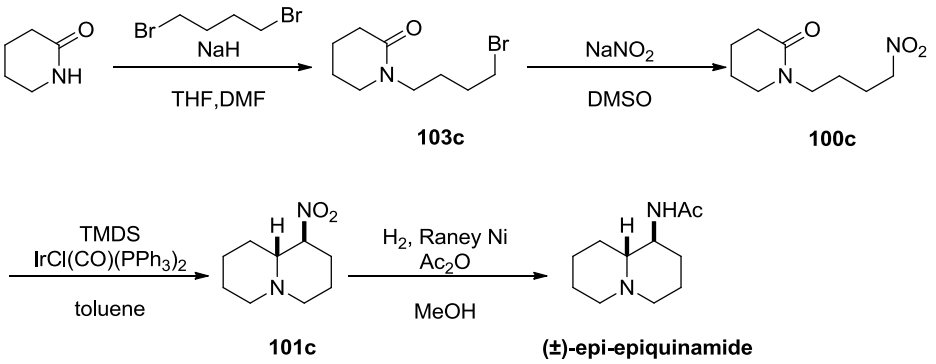

Scheme 2.27. Total sysnthesis of (±)-epi-epiquinamide.

2.9. Proof of relative stereochemistry.

The synthesis of (±)-*epi*-epiquinamide confirms the relative stereochemistry of **101c** as (*R**,*S**) by comparison with literature data.[20] Compounds **101f** and **101g** (formed by a seven

membered ring cyclisation) were also assigned as (*R**,*S**) by NOE spectroscopy data from compound **101g (**Figure 2.11): Spectra **B** and **E** (Figure 2.11) show the irradiation of the minor diastereomer protons 15_{minor} and 13_{minor} respectively, a clear NOE interaction can be seen between proton 15_{minor} and 13_{minor} (Spectrum **B**) and 13_{minor} and 15_{minor} (Spectrum **E**). However, irradiation of the corresponding major diastereomer protons 15_{major} and 13_{major} shows interaction through zero quantum coherence with 15_{major} and 13_{major} (Spectra **C**) as well as 13_{major} and 15_{major} (Spectrum **D**, Figure 2.11).[84] All other compounds were assigned as (*R**,*S**) by analogy to **101c** and **101g**.

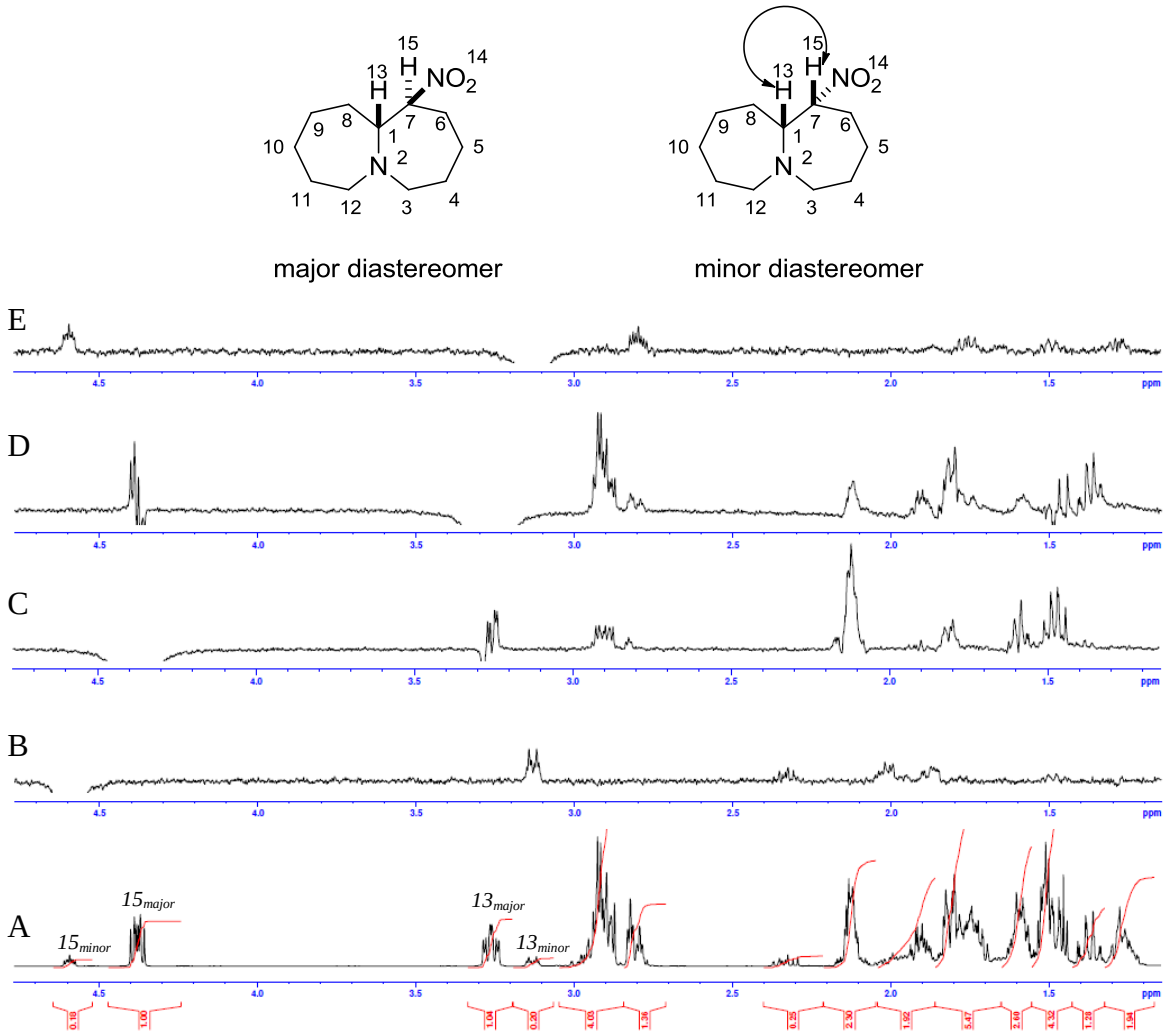

Figure 2.11. NOE analysis of 101g.

2.10. Conclusion

In conclusion, we have developed a novel chemoselective reductive cyclisation. The process is unprecedented, fast, efficient and stereoselective and provides heterocyclic compounds with cores that are abundant in nature and make up classes of alkaloids that show potent biological activity. We have gained a thorough understanding of the reaction mechanism through NMR studies and have applied the new methodology to the total synthesis of (±)-*epi*-epiquinamide in 4 steps. This methodology is potential very attractive for use in target synthesis. The relatively stable lactam has the capacity to be carried through a vast range of synthetic steps only to be "activated" at the desired moment using this methodology. Activation (partial reduction) forms a highly electrophilic iminium intermediate under mild conditions, which in theory could be quenched any chosen nucleophile.

3. Chapter 3: Iridium Catalysed Reductive interrupted Pictet-Spengler Cyclisation

3.1. Aims

Recognising the power of the iridium-catalysed partial reduction in the nitro-Mannich cyclisation cascade, we wanted to investigate the use of different tethered nucleophiles to quench the iminium ion formed in the reaction. One option was to use our previous knowledge of the Pictet-Spengler reaction to form compounds of type **120** from indole tethered lactams (**121**) *via* an iminium intermediate **122** (Scheme 3.1). Whilst these compounds have been previously documented,[85] this would constitute a new and direct strategy to access this family of compounds and furthermore would provide another proof of principal for the trapping of the partially reduced amide.

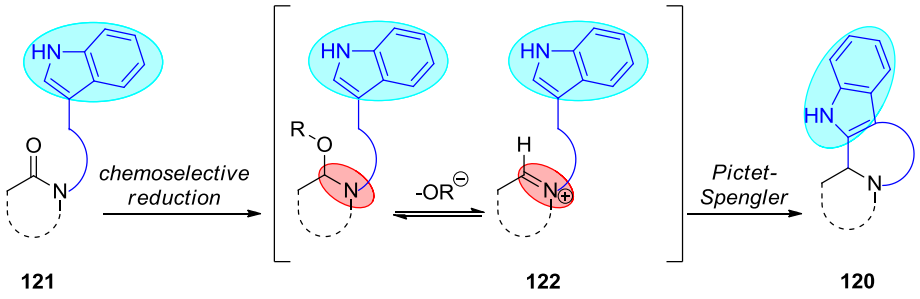

Scheme 3.1. Partial reductive Pictet-Spengler cyclisation concept.

3.2. Proof of principal and model substrate synthesis

A piperidone-derived two-carbon-tethered indole **123c** was selected as our model substrate and was readily synthesised by coupling commercial tryptamine with 5-bromopentanoyl chloride (synthesised from the corresponding acid and used crude) affording bromo-amide **124c**. Treating **124c** with potassium hydride in hot THF, allowed cyclisation to our desired indole tethered lactam **123c** in 25% yield over three steps (Scheme 3.2).

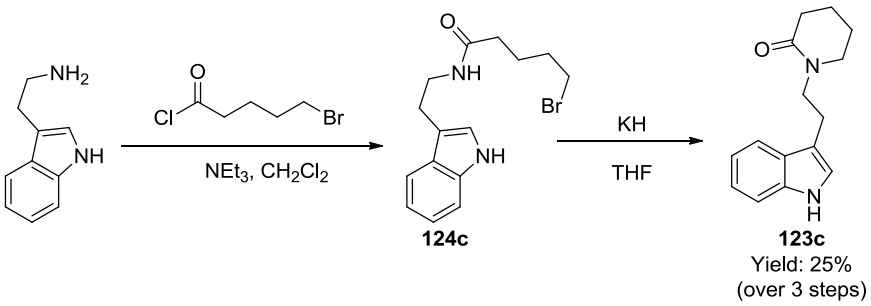

Scheme 3.2. Synthesis of model substrate **123c**

We wanted to test the compatibility of the partial reduction methodology used in the nitro-Mannich cascade with our model substrate. However, due to the highly reactive intermediates involved in these partial reduction methodologies and our positive experience of using ^{1}H NMR monitored reactions to deduce the mechanism in the nitro-Mannich cascade we opted to use this method to monitor the reaction. This method provided a direct view of the compounds present in the reaction mixture without risking the decomposition of transient intermediates or the promotion of side reactions upon work up or purification. Accordingly, **123c** was subjected to similar conditions to those employed in the iridium catalysed reductive nitro-Mannich reaction; **123c** (1 eq), TMDS (3eq) and mesitylene were dissolved in d_8-toluene and an NMR spectrum was recorded. Vaska's complex (2 mol%) was then added and a further ^{1}H NMR spectrum was taken. This showed complete consumption of starting material **123c** to a proposed enamine intermediate as well as other by-products. Unfortunately, due to the poor solubility of the starting material in d_8-toluene we were unable to get a NMR yield on this conversion. Changing the solvent to d_2-DCM and repeating the reaction had dramatic effect on the reaction, giving near quantitative conversion to a new compound **125c** (NMR yield: 90%, Figure 3.1).

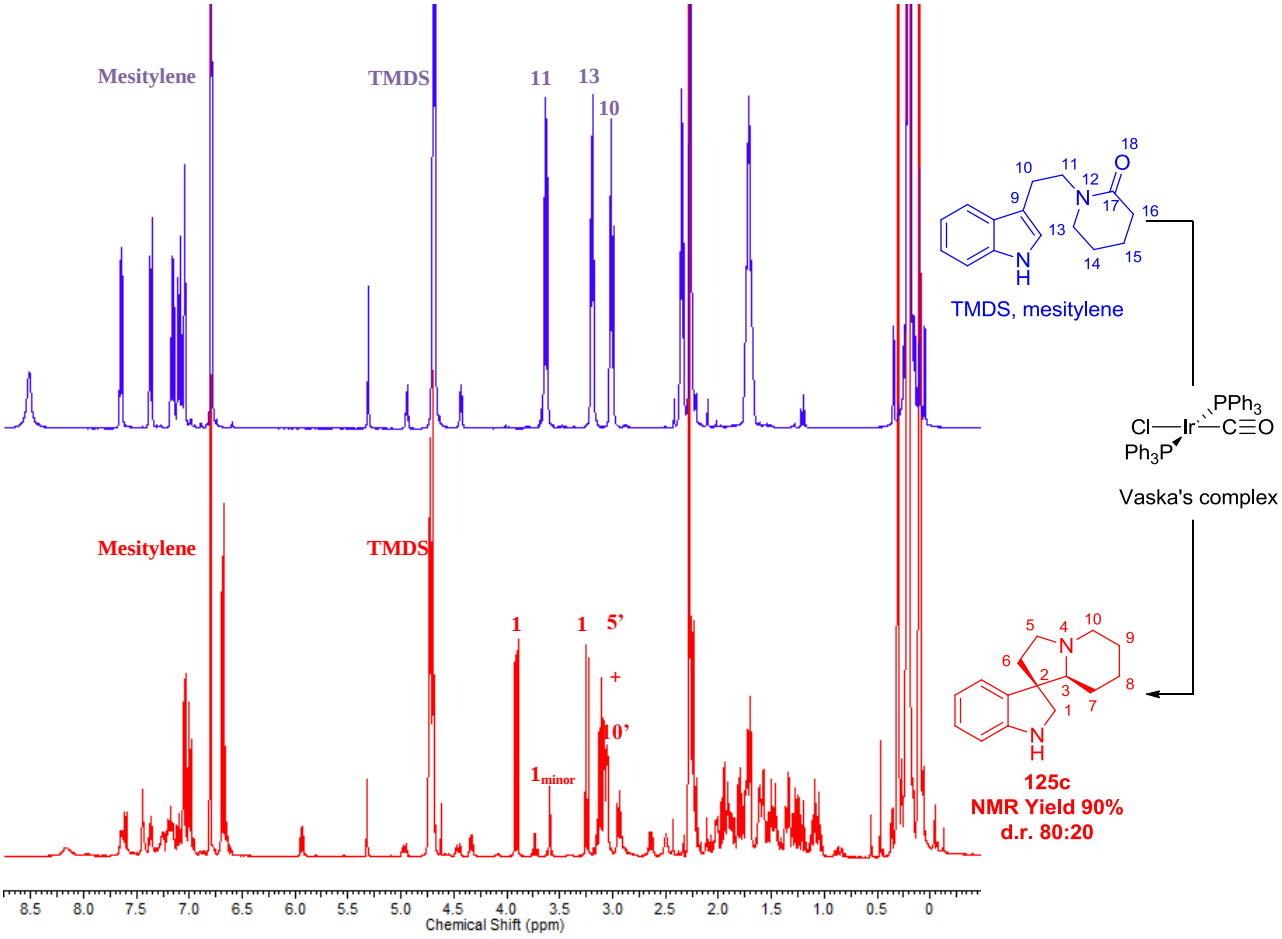

Figure 3.1. ^{1}H NMR reaction showing lactam **123c** and product **125c**

Repeating the reaction in a round bottom flask (concentration (6.5 mM), TMDS (3 equiv.), $IrCl(CO)(PPh_3)_2$ (2 mol%)), again showed complete consumption of the starting material. Subsequent purification of the unknown compound pleasingly revealed a novel spirocyclic indoline **125c** in 91% yield (d.r. 72:28). The formation of the spiro-indoline product can be rationalised by intramolecular indole attack on iminium ion **126** *via* the indole-C3 carbon to form the spiro-indolium ion **127**. The excess silane equivalent subsequently traps the indolium ion **127** and provides the stable indoline spirocycle **125c** (Scheme 3.3).

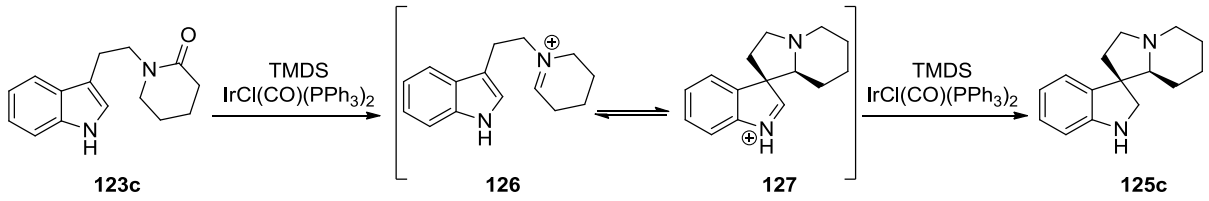

123c 126 127 125c

Scheme 3.3. Proposed route to novel spirocyclic compound **125c**

These novel structures could prove to be a very important family of compounds; owing to their abundance in many natural product cores, for example in the *strychnos* family of compounds,[86] as well as potential drug compounds.[87] The relative stereochemistry of **123c** was assigned as the (*exo*-S*,S*) diastereomer by NOE and NOESY analysis (see Appendix A and section 3.7).

3.3. Reaction optimisation

Although the yield of this novel reaction was already high, we wanted to screen the reaction parameters to ensure the methodology was fully optimised. Investigating the effects of concentration on the reaction showed that high dilution resulted in a mild improvement in the reaction yield but with a slight reduction in diastereoselectivity (Table 3.1, Entries 1-4). As a compromise between both reaction yield and diastereoselectivity 40 mM was chosen as the concentration for further optimisation. The loading of Vaska's complex and TMDS could be lowered to 1 mol% and 3 equivalents respectively with no noticeable effect on yield or diastereoselectivity (Table 3.1, Entries 4-6).

Table 3.1. Optimisation of reaction concentration and catalyst/TMDS loading.

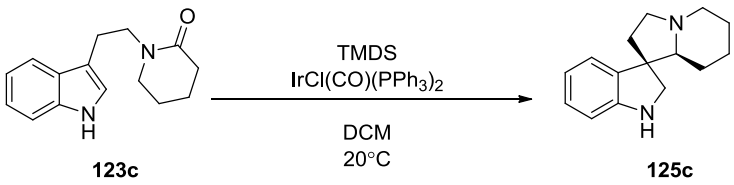

Entry[a]	TMDS (equiv.)	Cat (mol%)	Conc. (nM)	Yield[b] (%)	d.r.[c]
1	4	3	80	82	86:14
2	4	3	8	92	79:21
3	4	3	16	92	80:20
4	4	3	40	91	84:16
5	3	3	40	96	80:20
6	3	1	40	96	82:18

[a] All reactions performed on 0.060 g scale. Reaction time 20 mins; [b] Isolated yields; [c] calculated from crude ^{1}H NMR peaks.

In an attempt to improve the diastereoselectivity of the reaction, we wanted to investigate the reaction at reduced temperature (Table 3.2, Entry 2). Pleasingly, lower temperatures did indeed lead to vastly improved diastereoselectivity (d.r. >98:2). Lowering the temperature further to −20 and −78 °C also gave excellent yields and diastereoselectivity (Table 3.2, Entries 3-4).*

Table 3.2. Reaction temperature optimisation.

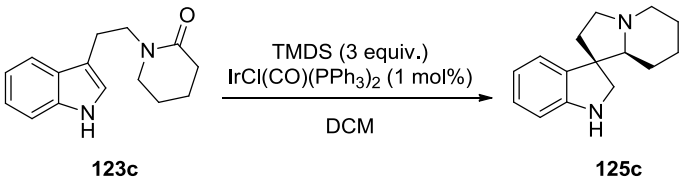

Entry[a]	Temperature[b] (°C)	Yield[c](%)	d.r.[d]
1	20	96	82:18
2	0	94	>98:2
3	-20	93	>98:2
4	-78	84	>98:2

[a] All reactions performed on 0.012 g scale and 40 mM concentration. Reaction time 90 mins; [b] Temperatures given are the temperatures of the pre-cooled solution of 123c, TMDS and mesitylene in a sealed tube. Vaska's complex was subsequently added through a septum as a stock solution in DCM. [c] NMR Yields (mesitylene internal standard); [c] Calculated from crude ^{1}H NMR peaks.

* although we cannot rule out the possibility that these reactions took place at a higher temperature than that quoted before the ^{1}H NMR could be measured and the yield and diastereoselectivity could be calculated.

With the reaction optimised, a range of substrates were required to analyse the effects of the lactam size and the length of the indole tether on the reaction.

3.4. Synthesis of substrates for the reaction scope

The key step in the synthesis of the model substrate was the formation of the lactam ring *via* a potassium hydride activated cyclisation. Concerns about our ability to form larger lactam rings *via* this method and the linear nature of the synthesis led us to investigate new methods of synthesising the desired indole-lactams. Starting the synthesis with the desired lactam and subsequently building the indole tether onto the lactam would remove the lactam formation problem and also provide us with a handle for late stage variation. With this in mind, retrosynthetic analysis of **123a** (Scheme 3.4) showed that Fischer indole synthesis methodology could be used on the corresponding aldehyde **128c**, which in turn could be formed from the bromo-tethered lactam **103a** following Kornblum-type oxidation conditions.[88] The formation of these bromides has already been demonstrated in the nitro-Mannich methodology (Chapter 2, section 2.6.1).

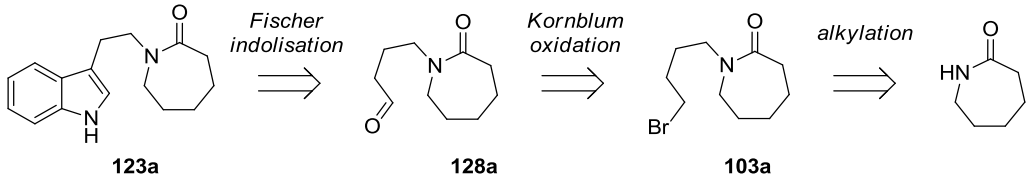

Scheme 3.4. Retrosynthesis of indole tethered lactam **125a** to parent lactam.

3.4.1. **Kornblum oxidation**

Following modified Kornblum oxidation conditions developed by Ganem and co-workers[89] the desired aldehyde **128a** was isolated, albeit with impurities and in poor yield (Table 3.3, Entry 1). Heating the reaction mixture did not improve the reaction and resulted in a lower yield (Table 3.3, Entry 2). Using TMANO as the *N*-oxide oxidising agent and following

methodology also developed by Ganem furnished aldehyde **128a** with improved purity but still in modest yield (Table 3.3, Entry 3).[90] Pleasingly, replacing the relatively expensive TMANO with NMO provided aldehyde **128a** in good yield (Table 3.3, Entry 4).

Table 3.3. Optimisation of Ganem oxidation conditions.

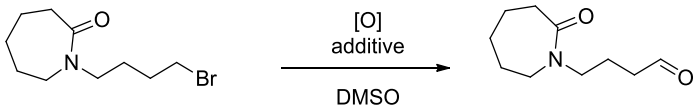

Entry[a]	[O]	[O] (equiv.)	Additives[b]	Temperature (°C)	Concentration (M)	Yield[c](%)
1	DMSO	-	$AgBF_4/NEt_3$	20	0.5	33
2	DMSO	-	$AgBF_4/NEt_3$	80	0.15	6
3	TMANO	4	-	20	0.5	26
4	NMO	4	-	20	0.5	65

[a] All reactions performed on 0.260 g scale. Reaction time 20 h; [b] $AgBF_4$ (1.5 equiv.), NEt_3 (1.5 equiv.); [c] Isolated yield.

3.4.2. **Optimisation of the Fischer indolisation**

With an effective method developed towards aldehyde tethered lactams in hand, our efforts turned to building the indole onto our tethered lactam. As there are a vast number of conditions for performing the Fischer indole reaction, a wide screening of conditions and reagents was undertaken for the indolisation of aldehyde **128a** (Table 3.4). Using acetic acid as both the reaction solvent and acid catalyst did lead to product formation, however, the product was highly contaminated with by-products (Table 3.4, Entry 1). Changing the solvent to methanol and using sulfuric acid again led to product formation along with inseparable impurities (Table 3.4, Entry 2). Using zinc chloride as a Lewis acid in ethanol failed to provide any product (Table 3.4, Entry 3). A breakthrough came when using sulfuric acid in THF; these conditions provided pure indole lactam **123a** in an acceptable yield (Table 3.4, Entry 4). Adding the sulfuric acid as a solution in THF provided no enhancement in yield and stirring neat aldehyde and phenylhydrazine at 100°C to encourage condensation to the hydrazine adduct before the addition of the acidic THF solution again showed no

improvement in reaction yield (Table 3.4, Entries 5-6). However, increasing the equivalents of hydrazine pleasingly improved the yield to 63% (Table 3.4, Entry 7)

Table 3.4. Optimisation of Fischer indole synthesis

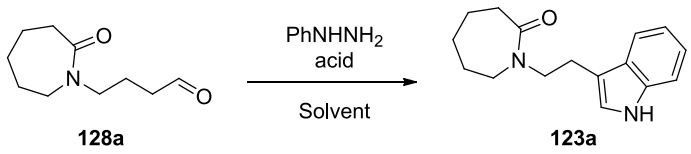

128a **123a**

Entry[a]	Acid	Acid (equiv.)	$PhNHNH_2$ (Equiv.)	Solvent	Temperature (°C)	Concentration (M)	Yield[b] (%)
1	AcOH	-	2.5	AcOH	110	0.06	<55[f]
2	H_2SO_4	4	1	MeOH	reflux	0.3	<29[f]
3	$ZnCl_2$	1.8	1	EtOH	reflux	0.8	-
4[c]	H_2SO_4	7	1	THF	reflux	0.1	40
5[d]	H_2SO_4	7	1	THF	reflux	0.1	41
6[e,d]	H_2SO_4	7	1	THF	reflux	0.1	42
7[d]	H_2SO_4	7	4	THF	reflux	0.1	63

[a] All reactions performed on 0.185 g scale. Reaction time 3 h; [b] Isolated yield unless stated; [c] H_2SO_4 was added to the mixture of aldehyde 128a, phenylhydrazine and THF. [d] pre mixed sulphuric acid in THF was added to a neat mixture of aldehyde 128a and phenyl hydrazine; [e] aldehyde and hydrazine stirred together for 1 h at 100°C before THF/ acid was added; [f] Product was highly contaminated with by-products so actual yield is much lower than that stated.

Following the optimised oxidation and indolisation conditions a library of indole tethered lactams were synthesised. These varied in lactam ring size ranging from 5-9 membered rings as well as in the length of the fully saturated linker from two to four carbon linked systems (Figure 3.2).

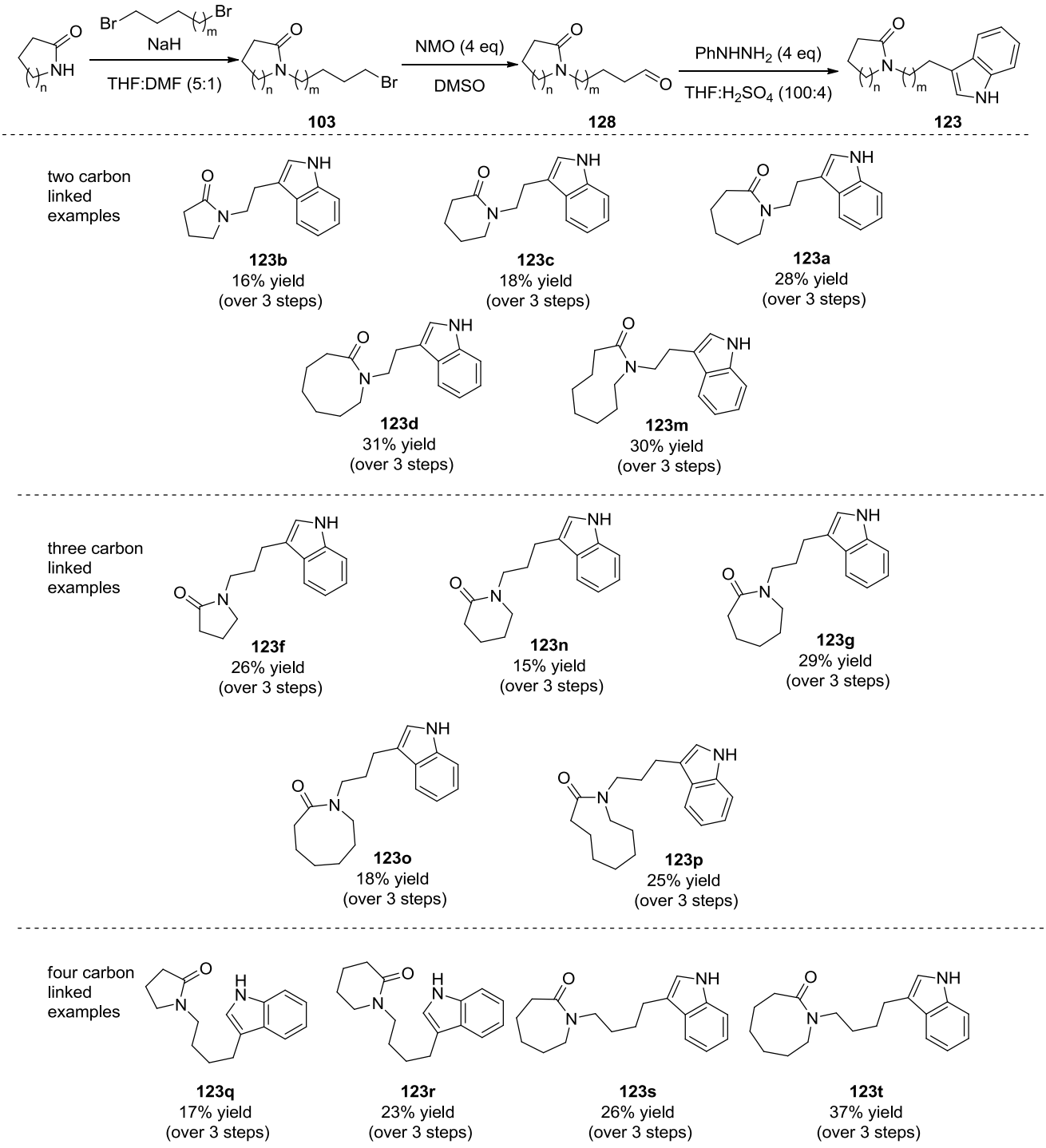

Figure 3.2. Library of indole linked lactam substrates.

3.5. Scope of the reaction methodology on lactam derived substrates

With a range of substrates available for cyclisation we began to test the scope of the reaction cascade on the two carbon linked analogues (Figure 3.3). Pyrrolidone-derived substrate **123b**

failed to form any cyclisation products and only fully reduced amine was observed in the reaction mixture. This may be due to a number of reasons: the increased ring strain in the pyrrolium intermediate may lead to an increased rate of reduction to the amine. Alternatively, the internal bond angles in the iminium intermediate (111 ° at nitrogen)[*] are much smaller than those of the six-membered analogue (121 ° at nitrogen),[*] which results in a relatively more strained angle of attack by the indole upon the iminium intermediate, and therefore the cyclisation process is out-competed by the reduction of the iminium to the amine product.

Increasing the size of the lactam to 7 and 8 membered rings provided the desired spirocycles **125a** and **125d** albeit in reduced yield with respect to the model substrate **125c**. This again was due to the increased quantity of fully reduced amine formed by the competing iminium reduction[†]. Pleasingly, 9 membered ring lactam **123m** cyclised in 72% yield with good diastereoselectivity. Interestingly, performing the reaction at 0 °C for the 7 to 9 membered ring lactams (**123a**, **123d** and **123m**) had a much reduced effect on the diastereoselectivity of the reaction when compared to model subtrate **123c**. The relative stereochemistry of **123(a/d/m)** was assigned by comparison to **123c**, which was confirmed to be the (*exo*-S*,S*) diastereomer by NOE and NOESY analysis (see Appendix A and section 3.7).

[*] Angles calculated using ChemBio3D ultra after MM2 energy minimisation.
[†] ^{1}H NMR reactions of substrate **123a** and **123b** show that the high quantities of amine formation is an inherent characteristic of **123a** and **123b**. the ratio of cyclisation and full reductions is stable within 5 mins (or the time taken to run the ^{1}H NMR after the addition of Vaska's complex).

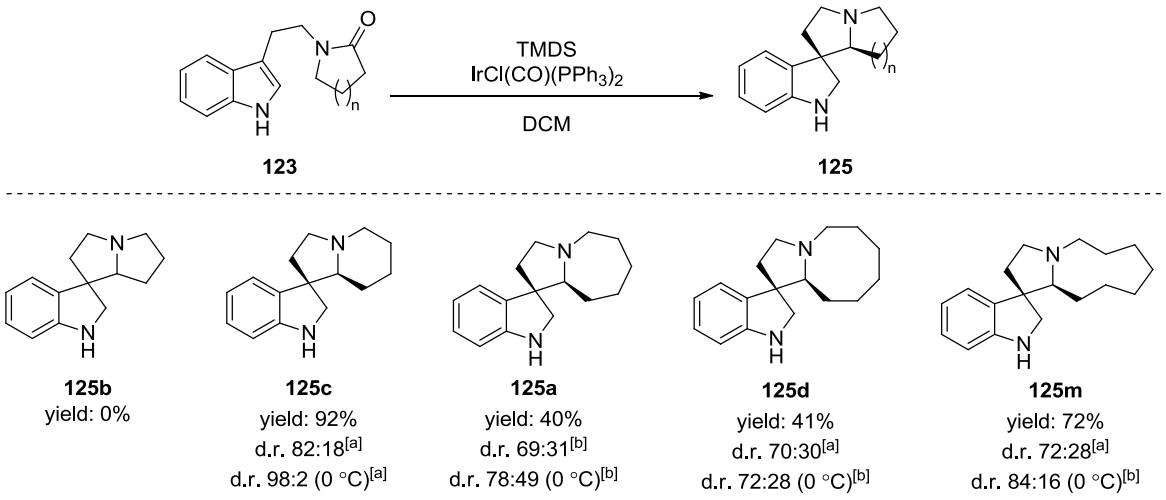

[a] d.r. calculated from isolated yields. [b] d.r. calculated from crude HNMR.

Figure 3.3. Cyclisation of two-carbon linked indole lactams.

With general success in the two-carbon linked compounds we were keen to investigate the reaction methodology on the three-carbon linked systems (Figure 3.3). Exposing pyrrolidone derivative **123f** to the reaction conditions, pleasingly, resulted in the desired spiro-indoline product being formed in 54% yield, but with poor diastereoselectivity. We propose that the increased tether length allows an improved angle of attack between the indole and iminium species when compared to that of **123b**, therefore in this case cyclisation is able to take place.

The three-carbon linked valerolactam derived system **123n** cyclises but in much reduced yield and diastereoselectivity to that witnessed with the shortened tethered system **123c**. This was again due to an increased proportion of the reaction undergoing full reduction to form the undesired indole tethered piperidine. The three-carbon linked caprolactam derived analogue **123g** worked poorly (28% yield) with the major product being the fully reduced amine. Increasing the lactam size further to the 8 and 9 membered ring systems (**123o** and **123p**) only provided full reduction, and no cyclised product could be detected.[*]

[*] Reactions on **123o** and **123p** were carried out in an NMR tube with no cyclised product being detected in the crude ^{1}H NMR.

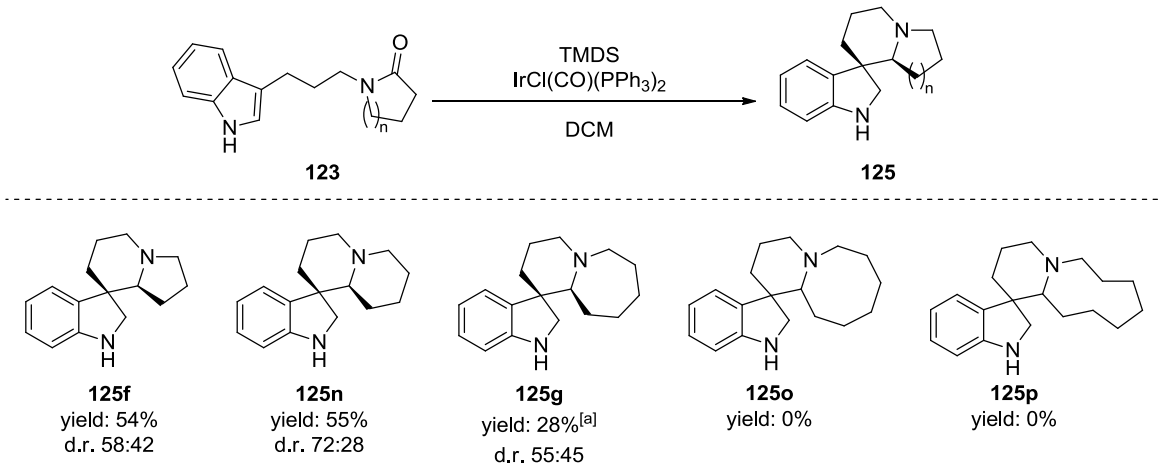

[a] calculate by NMR conversion of the crude reaction and couldn't be isolated.

Figure 3.3. Cyclisation of ethyl-linked indole lactams.

With the three-carbon tethered systems tending towards full reduction, we expected that the four-carbon linked moieties (**123q**–**123t**) would also proceed to the fully reduced tethered indole-amine products. The investigations of the four-carbon tethered substrates were carried out in ^{1}H NMR reactions to conveniently test the reactivity of these systems. The pyrrolidine substrate **123q** formed only a complex mixture. However, treatment of **123r**, **123s** and **123t** with the reaction conditions all showed complete consumption of the starting material to their corresponding enamine structures, with no detectable cyclisation product (Figure 3.4, Appendix B).

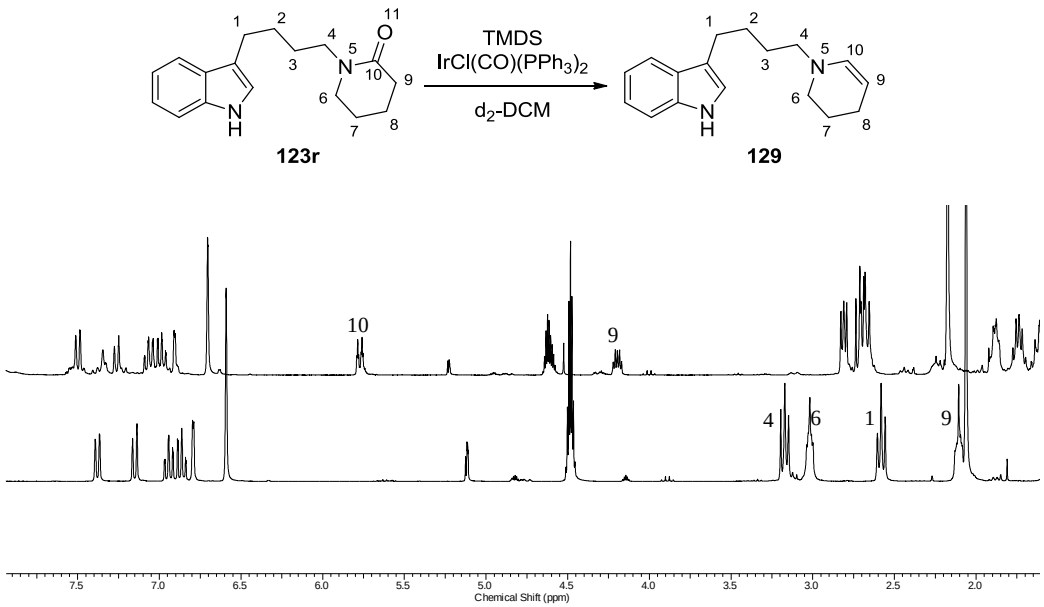

Figure 3.4. ^{1}H NMR reaction of **123r**, showing full conversion to enamine **129**.

These results are surprising because we assumed the only by-product available to the reaction cascade was full reduction to the amine. This suggests that the reduction of the iminium is influenced by neighboring group participation of the indole group (see mechanism section 3.7).

3.6. Acyclic amide examples

In an attempt to expand the methodology further we wanted to test our partial reduction on acyclic-tertiary-amide structures of type **130**. These compounds can be readily accessed by coupling *N*-methyl tryptamine **131** with the corresponding carboxylic acid/acyl chloride-derivative **132** (Scheme 135). *N*-Methyl tryptamine **131** was synthesised in 83% yield (over two steps) *via* the formation of the ethylcarbamate under Schotten-Baumann conditions and subsequent $LiAlH_4$ reduction[91] (Scheme 3.5).

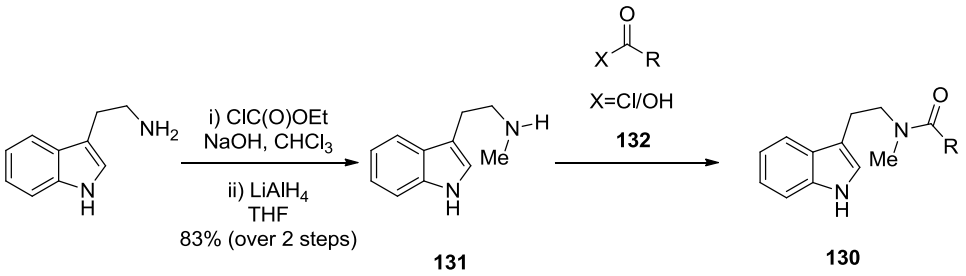

Scheme 3.5. Synthesis of acyclic indole tethered amides.

Using commercially available acyl chlorides we were able to form a wide range of acyclic amide substrates. Adding premixed *N*-methyl tryptamine **131** and triethylamine in DCM to a solution of the appropriate acid chloride in DCM in an ice bath afforded the phenyl (**130a**), cyclohexyl (**130b**), *iso*-propyl (**130c**), *tert*-butyl (**130d**), adamantyl (**130e**) and furanyl (**130f**) amides in acceptable to good yields (Figure 3.5).

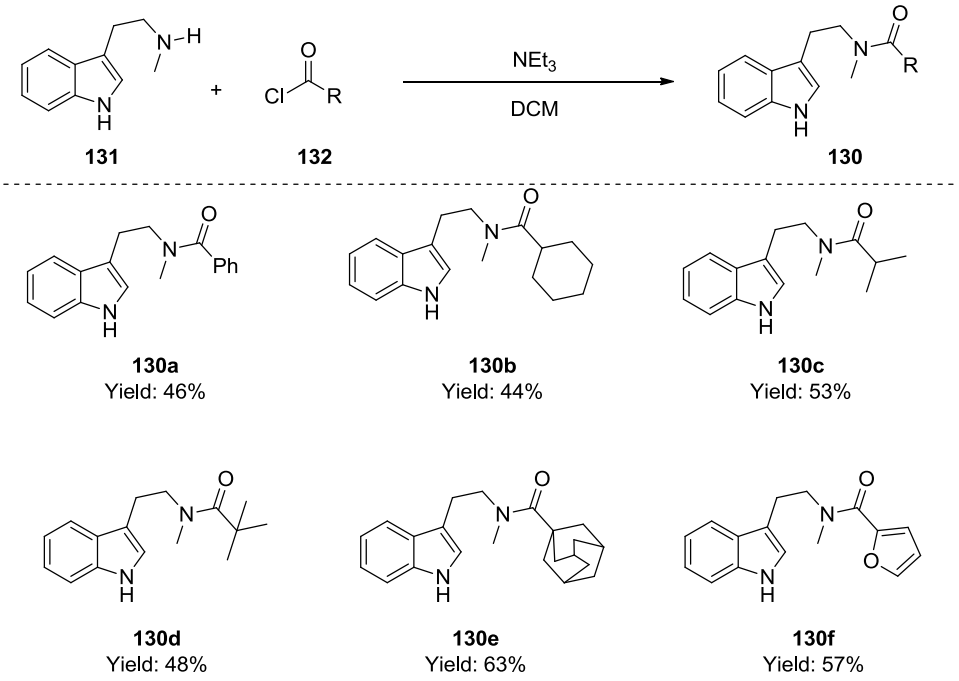

Figure 3.5. Synthesis of acyclic amide substrates from acyl chlorides.

With our acyclic amide substrates in hand we began testing them on our reaction conditions (Figure 3.6). Pleasingly, when phenyl substituted amide derivative **130a** was exposed to the

reaction conditions, the desired spirocyclic-indoline **133a** was isolated in excellent yield, albeit with low diastereoselectivity. For cyclohexyl and *iso*-propyl substituted examples **130b** and **130c** cyclisation again proceeds in excellent yield and with an increased diastereoselectivity with respect to **130a**. Pleasingly, these two examples demonstrate that the reaction can be performed in the presence of potentially acidic α-protons (to the carbonyl/iminium group). The presence of a proton in this position can lead to the formation of relatively stable enamines that cannot undergo cyclisation, however, in these examples no enamine was witnessed. When the sterically hindered *tert*-butyl and adamantyl substituted examples **130d** and **130e** were subjected to the reaction conditions, spirocylces **133d** and **133e** were very pleasingly isolated as single diastereomers, albeit with a reduced yield. The reduced yield and high diastereoselectivity could be an indicator that the increase in d.r. is due to the minor diastereomer decomposing upon purification but evidence from the crude ^{1}H NMR, ^{1}H NMR experiments and the stability of the minor diastereomers in the other examples would suggest that the selectivity is controlled by the diastereoselective attack of the indole on the iminium (see mechanism section 3.7). The probable reason for the reduced yields in these examples is due to the extended reaction times; in both cases the reactions took 24 h to reach completion[*] and this may result in a larger amounts by-product formation.

[*] Reactions were monitored by TLC analysis, and judged to be complete upon the complete consumption of starting material.

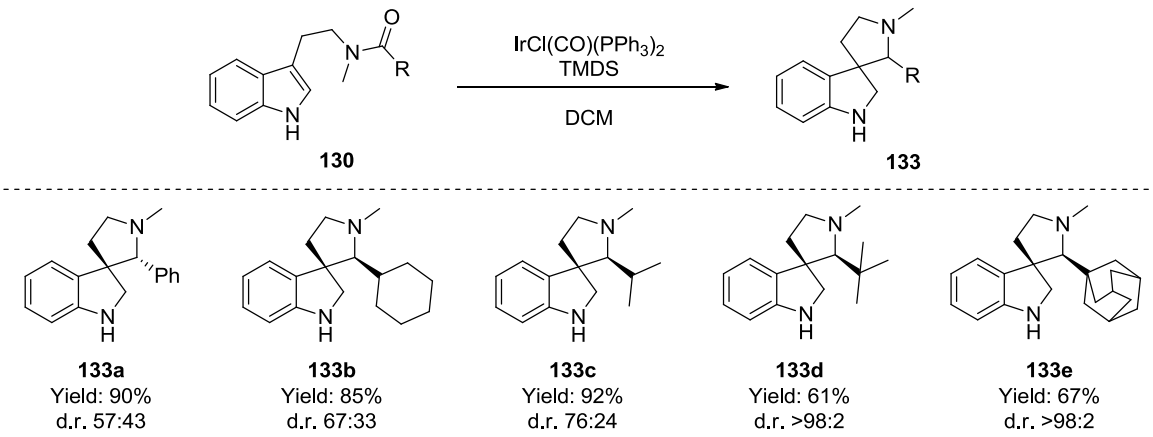

Figure 3.6. Cyclisation of acyclic amide substrates.

The furan substituted example **130f** was an interesting example to investigate because not only would it test the reactions ability to work in the presence of a nucleophilic heteroaromatic substituent, it also had the potential to form a new ring by attacking the indolium intermediate **134**, which could form a pentacyclic structure of type **135** (Scheme 3.6). However, when we treated **130f** under our optimised cyclisation conditions we only isolated the spiro-indolene product **133f** in excellent yield as a mixture of diastereomers (Scheme 3.6).

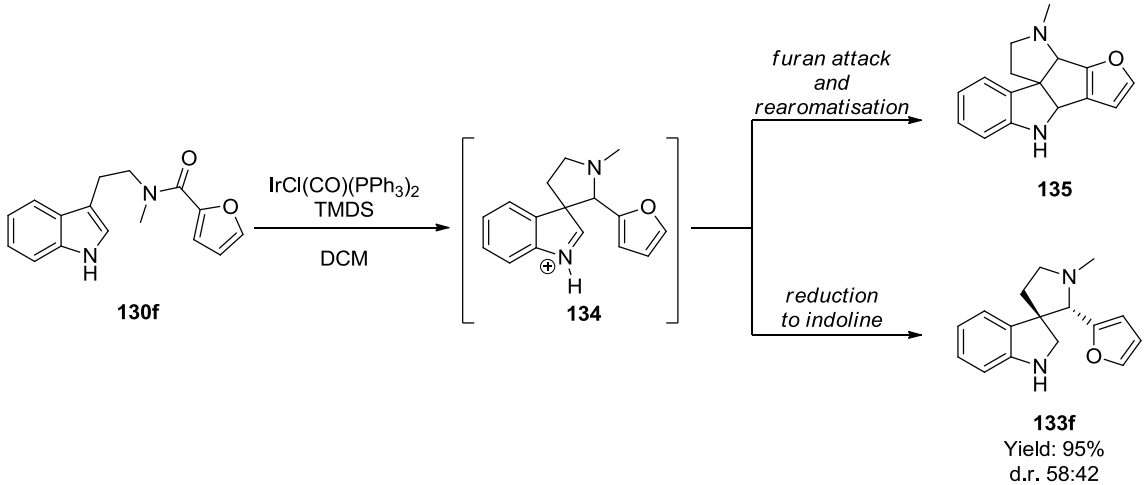

Scheme 3.6. Cyclisation of acyclic furan substituted example **130f**.

The relative stereochemistry of **133b** and **133e** was assigned by comparison to the compounds **133c** and **133d**, which were both confirmed to be the (*exo*-S*,S*)-diastereomers by NOESY experiments (Appendicies C and D). However, for aromatic compound **133a** and **133f** (by analogy) the stereochemistry of the major diastereomers was deemed to be the opposite diastereomer by NOESY analysis (*endo*-R*,S* for 133a and *endo*-S*,S* for **133f**) (Appendix E).

With the success of the reaction in the presence of a heterocyclic substituent, a range of acyclic heterocyclic substituted amide structures were synthesised. For these heterocyclic examples, the carboxylic acid groups are more readily available so the amide coupling was performed using the carbodiimide coupling reagent EDAC with DMAP catalyst (Figure 3.7).

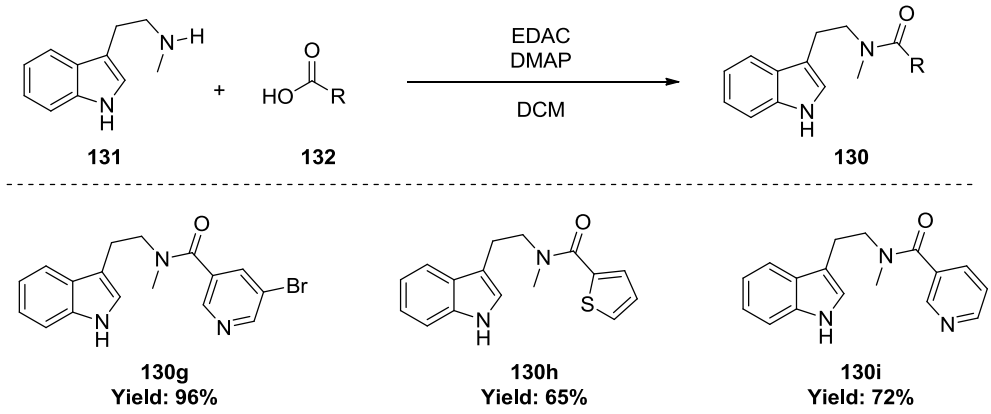

Figure 3.7. Synthesis of acyclic amide substrates from carboxylic acids.

Disappointingly, when we tested the bromo-substituted pyridine example **130g** no spiro-indoline product was observed, instead only a complex mixture resulted. However, treating the thiophene substituted amide with the reductive cyclisation conditions formed the desired indoline **133h** in excellent yield but poor diastereoselectivity (Figure 3.8). The relative stereochemistry for **133h** was assigned by comparison to **133a** (Appendix E). Interestingly, the pyridyl example **130i** cyclises to form the desired spirocycle **133i** as a single diastereomer in excellent yield. The relative stereochemistry of **133i** was assigned by NOESY analysis

(Appendix F) and appears to show the opposite selectivity to that shown for the other aromatic analogues.

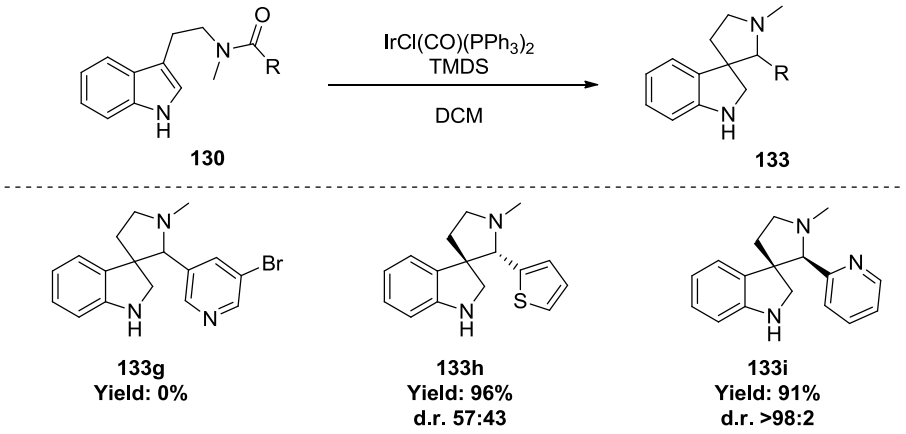

Figure 3.8. Cyclisation of acyclic amide substrates.

The excellent diastereoselectivity also appears to not fit the trend set up by the other sp^2 substituted examples, with **133a**, **133f** and **133h** all showing poor diastereoselectivity. The key piece of evidence for the increased and opposite selectivity can be found in the crude ^{1}H-NMR of the reaction mixture: this shows a d.r. of 74:26 with the minor diastereomer matching that of the major isolated diastereomer (See appendix G). One hypothesis to explain this is that the spirocyclic indoline **133i** can equilibrate on silica to form the more thermodynamically stable diastereomer. In fact calculating the relative energies of both diastereomers shows an energy difference of 3.6 kcal mol^{-1},[*] this provides the driving force for equilibration to convert to the *exo*-product. A possible mechanism for this equilibration could be *via* protonation of the pyridine substituent **136**, which is able to promote an indoline assisted ring cleavage forming a transient enamine structure **137**. A change in conformation of **137** and re-cyclisation allows **133i** to be isolated with a reversal in diastereoselectivity and as a single diastereomer (Scheme 3.7).

[*] Relative energies calculated using ChemBio3D ultra after MM2 energy minimisation.

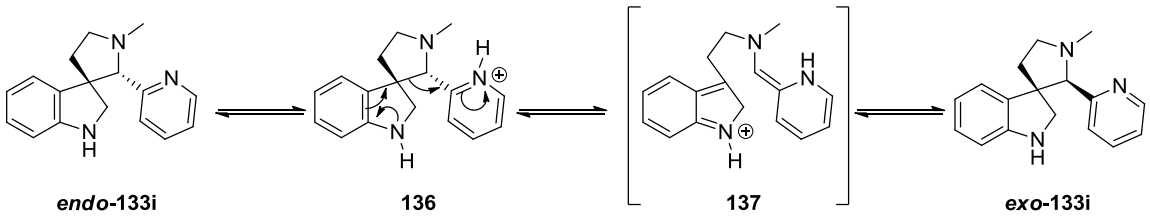

Scheme 3.7. Equilibration mechanism for pyridine example **133i**

3.7. Reaction mechanism and diastereoselectivity

The mechanism for this reductive interupted Pictet-Spengler cyclisation cascade is proposed to go by an initial reduction of the lactam **139** to form the hemiaminal **140**; elimination of siloxide then forms the key iminium intermediate **141**. At this point three options are available: 1) deprotonation forms enamine **142**; 2) reduction forms the undesired amine **143** or 3) indole attack forms **144**, which can be rapidly reduced to the desired spirocyclic indoline **145** (Figure 3.9). ^{1}H NMR reactions of multiple examples have shown us that the reaction doesn't proceed *via* a stepwise enamine intermediate, which converts to the cyclised product on work up or purification as was the case in the reductive nitro-Mannich cyclisation. When monitoring the reaction of **123c** over time we noticed there was no increase in the reaction product as well no decrease in the quantity of enamine. This implies that the enamine is not an intermediate towards the spirocyclic indoline product; instead it can be thought of as a by-product formed by irreversible deprotonation. Thus, for the reaction to be high yielding the speed of cyclisation (k_2) must be faster than the rate of deprotonation to enamine (k_1). Further evidence for this is that examples with no α-protons are often the most high yielding reactions due to their inability to form enamine intermediates.

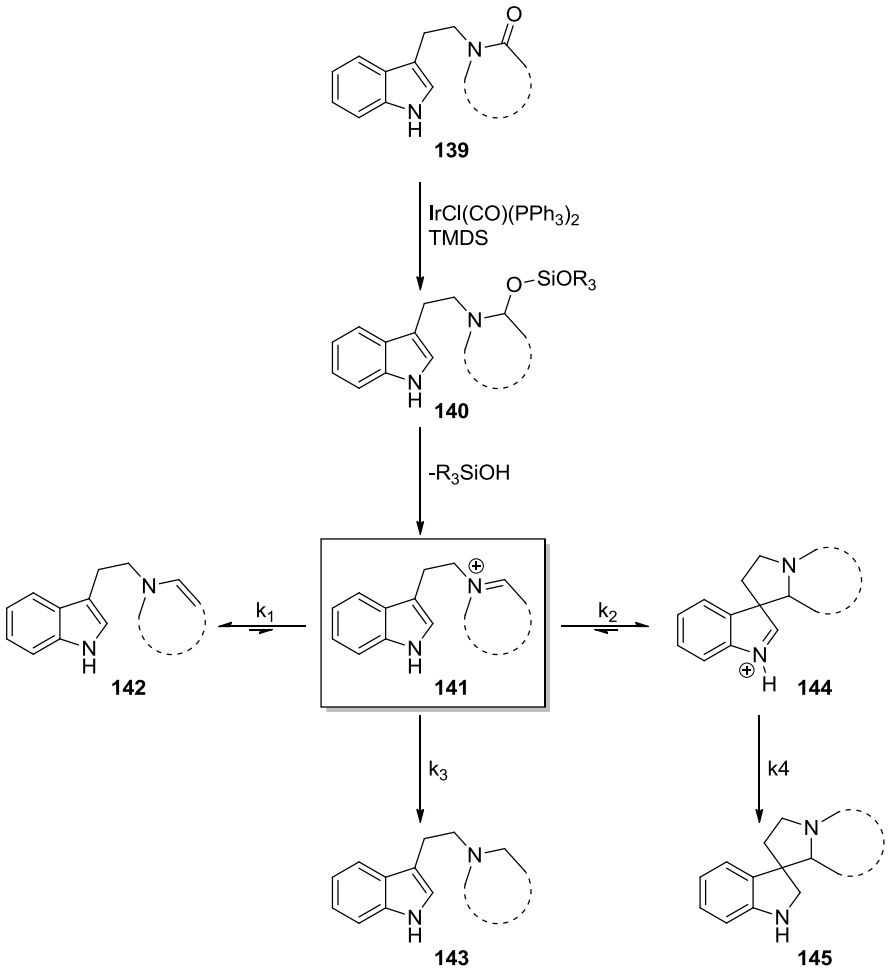

Figure 3.9. Proposed reductive interrupted Pictet-Spengler cyclisation mechanism

The relative rate of cyclisation (k_2) compared with the rate of full reduction (k_3) seems to be based on the length of the indole tether. Comparing the reactions of the valerolactam-derived examples **123c**, **123n** and **123r** we can see a clear decrease in the yield of spiroindoline formation as the length of the tether increases; this initially seems to be due to the competing reduction of the iminium to the undesired amine. However, with the butyl tether no cyclisation or amine formation was witnessed, only the enamine was formed. We can potentially explain this observation through neighboring group participation of the indole to promote the reduction of the iminium before deprotonation to the enamine can occur; so as the distance increases between the indole and iminium the rate of both cyclisation (k_2) and reduction (k_3) are reduced and therefore deprotonation dominates to form the enamine. This

hypothesis is also supported by the attempted cyclisation of *N*-methylated indole example **146**. An NMR reaction was carried out to see if **146** could cyclise and form the spiro-indoline product **147** (Figure 3.10). Spectrum **A** shows the starting material **146**, TMDS and mesitylene (as an internal standard). Spectrum **B** shows the reaction mixture 5 mins after the addition of Vaska's complex. This shows complete consumption of the starting material, and the only visible product is the enamine **148** in excellent yield (no amine **149** could be detected) (Figure 3.10).

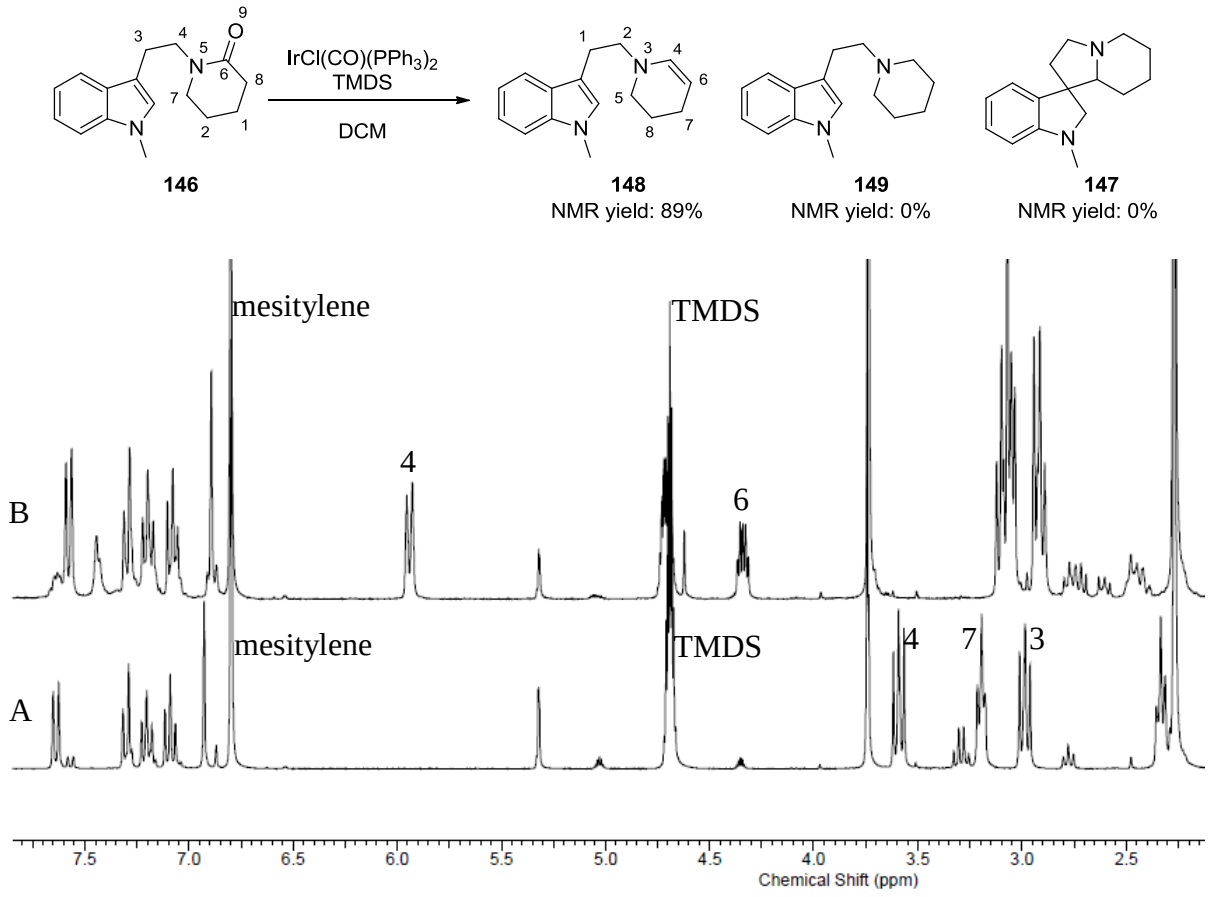

Figure 3.10. Partial reduction of *N*-methyindole **146** to enamine **148**

This implies that the indole-*NH* is crucial to both the cyclisation and reduction of the iminium intermediate. An explanation of why *N*-methyl-indole **146** doesn't cyclise may be twofold: the increased steric bulk on indole ring could lower the rate of cyclisation (k_2) to form the indolium intermediate. Also, the rate of indolium reduction (k_4) may be lower because of the

extra steric demands placed upon the indolium intermediate and may result in retro-cyclisation. Therefore the cyclisation reaction is out competed by the unaffected competing irreversible deprotonation (k_1) to form enamine product **148**.

The fact that the partial reduction of *N*-methylated indole **146** shows no full reduction product **149**, suggests that not only is the relative distance of the indole from the iminium crucial in the reduction of iminium, but the indole-*NH* is also required. There has been a substantial amount of research carried out on the insertion of Ir(I) complexes into N-H bonds including indole-*NH* bonds by oxidative addition, these Ir(III)(N)(H) complexes have then been shown to perform hydroamination reactions on a variety of alkenes.[92] We tentatively propose that the reductive reagent responsible for iminium reduction may be some as of yet unknown *N*-linked iridium complex, which can deliver a hydride in an intra-molecular fashion to the intermediate iminium (Figure 3.11).

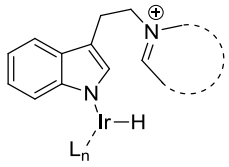

Figure 3.11. *N*-linked iridium complex reduction of the iminium intermediate

In summary: substrates with a short two-carbon tethers and no α-protons (to the carbonyl) are generally the best substrates for this methodology due to the rate of indole attack being key to gaining good product yields.

The diastereoselectivity of the reaction was assigned by NOE and NOESY analysis of **125c** as well as NOESY analysis of **133a**, **133c**, **133d** and **133i** (Appendices A, E, C, D, and F). The selectivity appears to be controlled by the attack of the tethered indole on the iminium intermediate. The major compound in most cases is the *exo*-product which is formed *via* the transition state with the substituted position *exo* to the indole (Figure 3.12). This can be

rationalised by considering the steric interaction of the bulky substituent with the indole ring itself. However, as the steric bulk of the substituent decreases for example *iso*-propyl (**130c**) and aryl examples (**130a**, **130f** and **133a**) the selectivity decreases due to the reduced steric interaction. The fact that the pyridine substituted example **133i** equilibrates from the *endo* diastereomer to the *exo* product also suggests that this is the thermodynamic product.

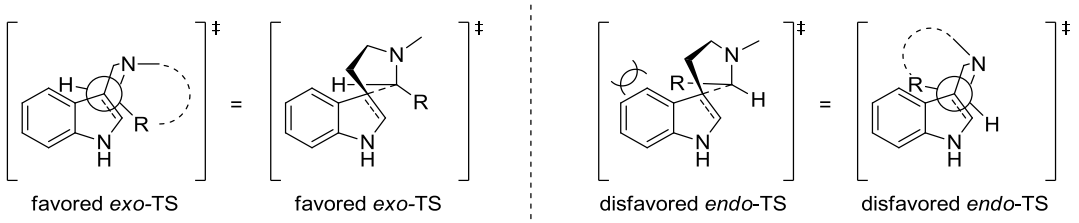

Figure 3.12. *exo* and *endo* transition states of indole attack on the iminium intermediate.

3.8. Scope expansion: 2-substituted indole tethered lactams

In an attempt to expand the scope of the product scaffolds created by this methodology we decided to investigate substrates that are tethered *via* the indole-C2 position (**150**). These compounds could be accessed by the Larock style indole formation[93] and potentially, could allow the formation of tetracyclic indoline products of type **151**.

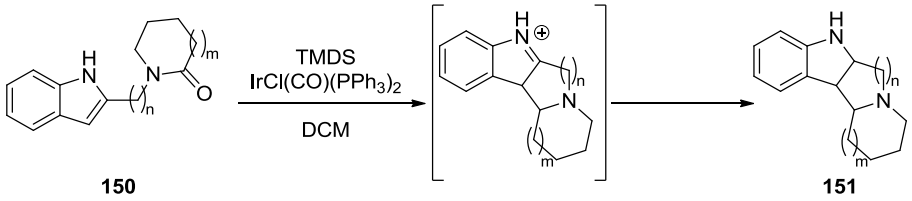

Scheme 3.8. Partial reduction concept for C2-substituted indole substrates.

3.8.1. **Synthesis of starting material.**

The synthesis of 2-substituted indole substrates *via* Larock indole synthesis first required the alkylation of our chosen lactam with 4-bromobutyne. However, this reaction proved to be

very difficult, the alkylation of caprolactam with 4-bromobutyne repeatedly failed to yield any alkylated product (Table 3.4). A literature search also revealed reactions of this type were rare. We proposed this is due to the relative high basicity of the deprotonated lactam and the ease of E2 elimination of the bromo-alkyne, whilst sodium hydride deprotonates caprolactam readily the speed of base assisted E2 elimination is much faster than alkylation, resulting in reprotonated caprolactam and the conjugated but-3-ene-1-yne (Table 3.4, Entries 1-2). Weaker bases such as potassium and cesium carbonate failed to deprotonate the lactam and therefore show no reaction; even at elevated temperatures the reactions still show only starting material (Table 3.4, Entries 3-5).

Table 3.4. Alkylation of caproplactam with 4-bromobutyne.

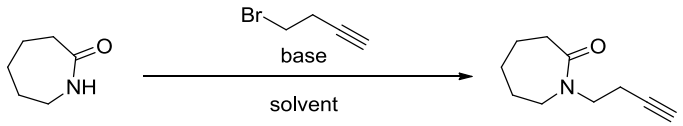

Entry[a]	Base	Base (equiv.)	Alkyne (equiv.)	Solvent	Temperature (°C)	Concentration (M)	Yield (%)
1	NaH	1.25	1.25	THF/DMF[b]	20[c]	0.2	-
2	NaH	1.25	2	THF/DMF[b]	20[c]	0.2	-
3	Cs_2CO_3	2	2	MeCN	70	0.2	-
4	K_2CO_3	1.8	2	acetone	Reflux	0.2	-
5	Cs_2CO_3	1	2	DMF/THF[b]	20	0.14	-

[a] All reactions performed on 0.325 g scale; [b] THF/DMF ratio is 5:1; [c] NaH added to caprolactam at 0 °C and stirred for 1 h before 4-bromobutyne was added and given reaction temperature reached.

If the undesired reactivity of 4-bromobutyne was due to the conjugation developed with its eliminated product, then extending the chain to 5-bromo-pentyne should provide more favourable reactivity. Pentyne-5-tosylate **152** was synthesised in 85% yield from 5-hydroxypentyne **153** (as 5-bromo-pentyne is not commercially available). Alkylation of caprolactam provided alkyne **154a** in 65% yield. Larock style coupling of alkyne **154a** with *o*-iodo-tosylaniline **155** (which was preformed in 99% yield from pentyn-5-ol) proceeded in good yield (**156a**) (77%). Removal of the tosyl group with magnesium and ammonium

chloride afforded the desired 2-substituted indole linked lactam **157a** in 76% yield (Scheme 3.9).

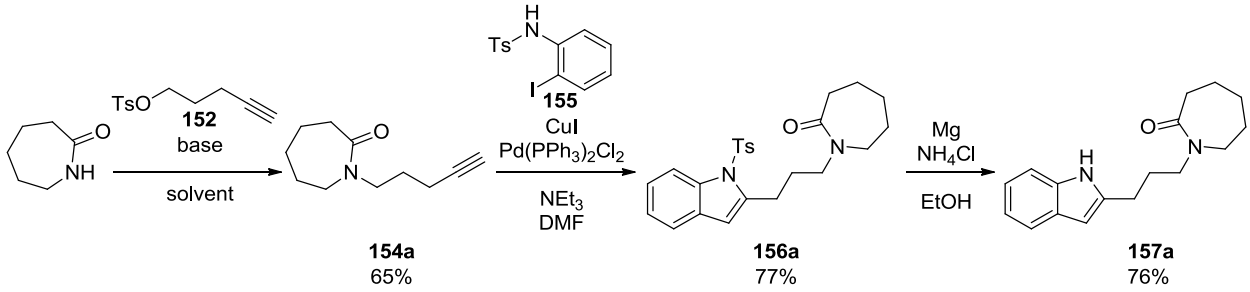

Scheme 3.9. Larock style synthesis of 2-substituted indoles.

Using the same method, we were able to form analagous stuctures with 6- membered ring lactam (**157b**) as well as a shortened tether example **157c** formed using propargyl bromide (Figure 3.13).

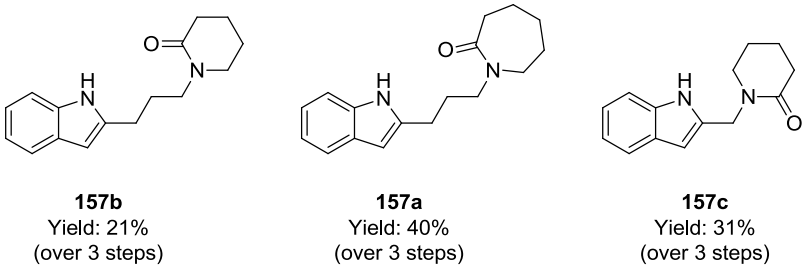

Figure 3.13. 2-substituted indole substrates.

Treating the 3-carbon linked examples **157b** and **157a** with the reaction conditions failed provide the proposed indoline products of type **151** (Scheme 3.10). Instead, trace amounts of Pictet-Spengler products could be seen (**158(b/c)**); unfortunatly these couldn't be isolated. The major product formed were the corresponding indole tethered amines **159b** and **159a** *via* full reduction of the lactam.

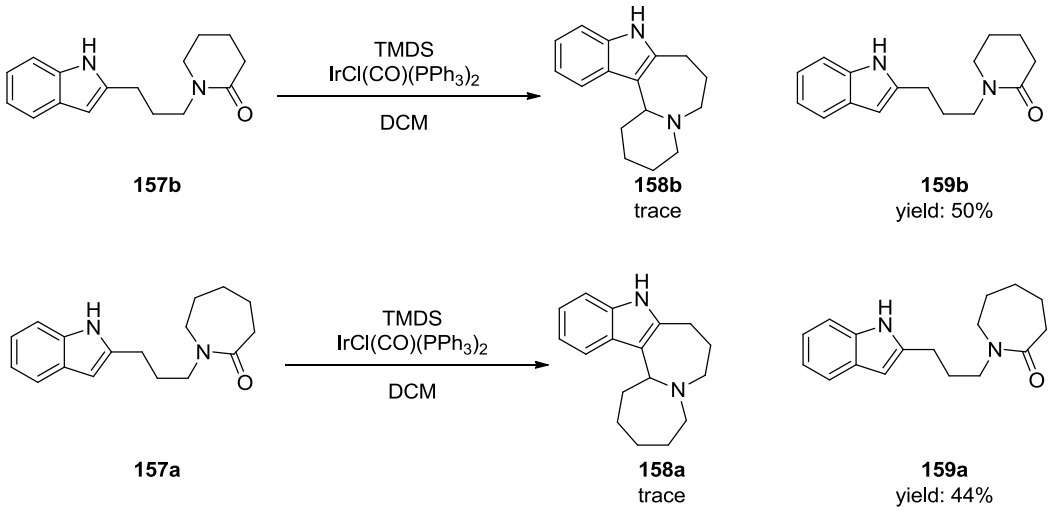

Scheme 3.10. Reductive Pictet-Spengler cyclisation of 2-substituted indole linked lactams.

However, subjecting the shortened chain example **157c** to reaction conditions provided the novel Pictet-Spengler product **158c** in good yield. The reason this example was able to work well was presumably due to the relative rate of cyclisation being faster than the rate of full reduction because of the smaller ring forming size (Scheme 3.11).

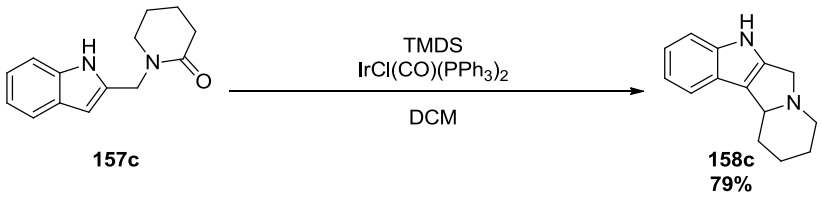

Scheme 3.11. Reductive Pictet-Spengler cyclisation of 2-substituted indole linked lactams.

In all the above mentioned *C*2-indole linked examples the only cyclised products formed were the rearomatised Pictet-Spengler products, no indoline products were detected. A plausible explanation for this change in reactivity with respect to the *C*3-indole linked examples could be attributed to the mechanism of rearomatisation, *C*2-indole linked examples only require deprotonation to achieve rearomatisation, whereas *C*3-indole linked examples require an initial rearrangement before deprotonation can afford the rearomatised product.

Another variable in these examples is the steric hindrance at the C2 position of the indolium intermediate **160**, which could slow the rate of indolium reduction (Scheme 3.12).

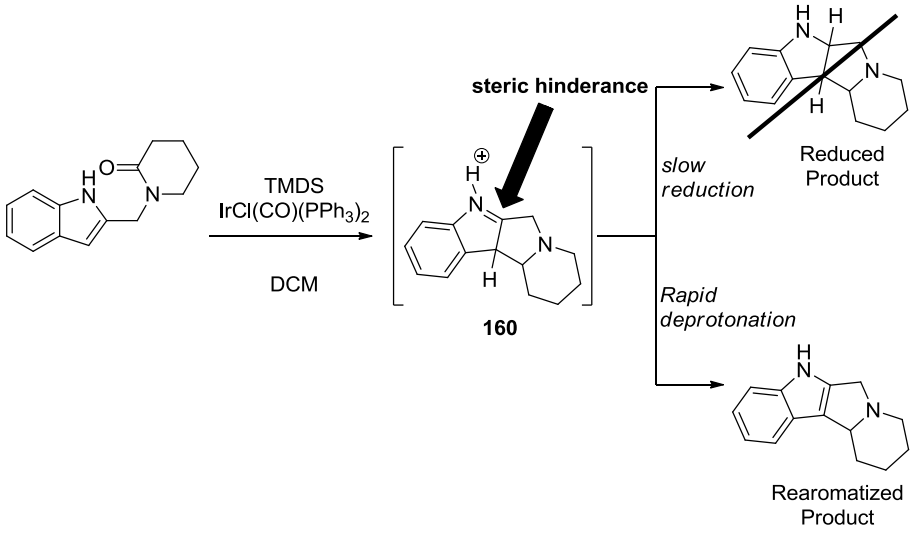

Scheme 3.12. Proposed selectivity for rearomatisation vs reduction of indolinium.

These results offer a very promising proof of principle for the formation of tetracyclic indole products. There are still a substantial amount of examples that could be investigated by varying the size of the lactam on the one-carbon tethered substrate as well as the potential to form a selection of two-carbon linked substrates.

3.9. Conclusion

A novel methodology towards the synthesis of spiro-indoline structures has been developed. By exploiting the partial reduction of both lactams and amides to their respective iminium intermediates, a library of spiro indoline structures has been formed: both 5,5 and 5,6 spiro-ring systems have been created and the reaction has been proven to tolerate a wide range of functional groups. In total we have synthesised 15 novel spirocyclic-indoline compounds with yields up to 95% and diastereoselectivity up to >98:2. A proof of principle has also been developed for a reductive Pictet-Spengler cyclisation on C2-substituted indole tethered lactams.

4. Summary and Future Work.

Investigating novel cyclisation cascades that pass through reactive iminium intermediates has revealed a rich area of synthetic methodology. Logical reaction design and serendipitous discoveries have enabled the development of three novel reaction cascades which allow the synthesis of a range of unprecedented molecular scaffolds.

A highly enantioselective hydroamination/*N*-sulfonyliminium cyclisation cascade has allowed access to 12 complex and unusual sulfonamide scaffolds in excellent yield (60-85%) and enantioselectivity (75-96%). The methodology was extended to include amide derivatives which allows 6-membered ring systems to be accessed with yields ranging from 60 to 99% and enantiomeric excess up to 93%. Further work in this area would centre around the use of novel tethered aromatic nucleophiles **161** such as dimethoxy-phenyl-,[94] pyrrole-[95] and imidazole-derivatives[96] resulting in **162**, **163**, **164** (Scheme 4.1). Another area that could provide a range of interesting structures would be the use of a sulfamide **165** linker instead of the sulfonamide used in this work (Scheme 4.1).

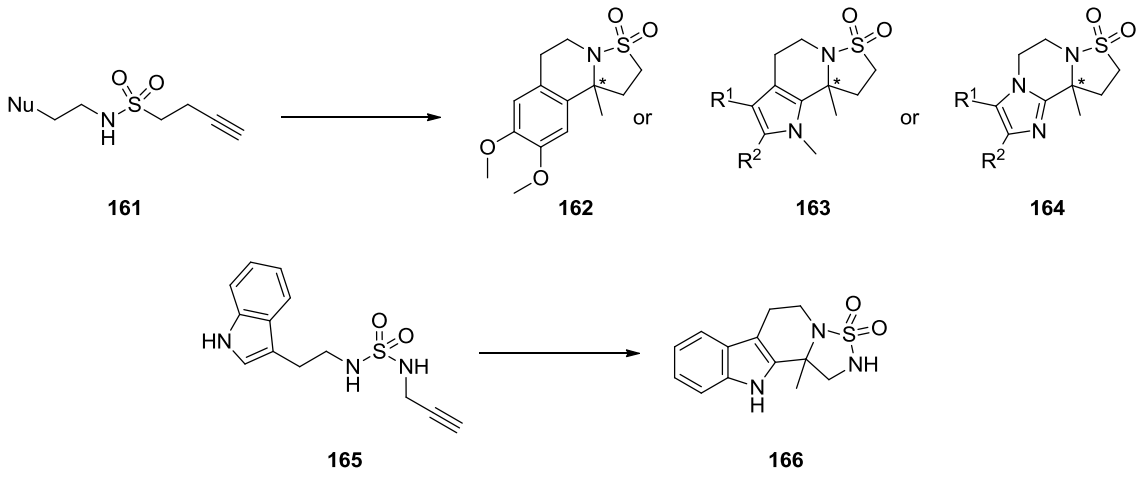

Scheme 4.1. Potential future work using Gold(I) and BPA catalysed cyclisation cascades.

The partial amide reduction methodology has provided a novel approach to synthesising C-C bonds. This thesis has demonstrated that lactams and acyclic amides can be activated to iminium intermediates, which can subsequently be quenched by a tethered nucleophile. Using this method a range of complex novel polycyclic products have been formed in a single step from readily available starting materials (Scheme 4.2). Nitro-Mannich cyclisation affords heterocyclic compounds (**101a** and **101j**) with cores that are abundant in nature and make up classes of alkaloids that show potent biological activity. Interrupted Pictet-Spengler cyclisation provides a host of novel spirocyclic indoline products including **125m** and **133i**, which would be formidable targets via standard synthetic methods. Partial reduction of 2-substituted indole tethered lactam **157c** provides a proof of principle for further research into Pictet-Spengler cyclisation products of type **158c**.

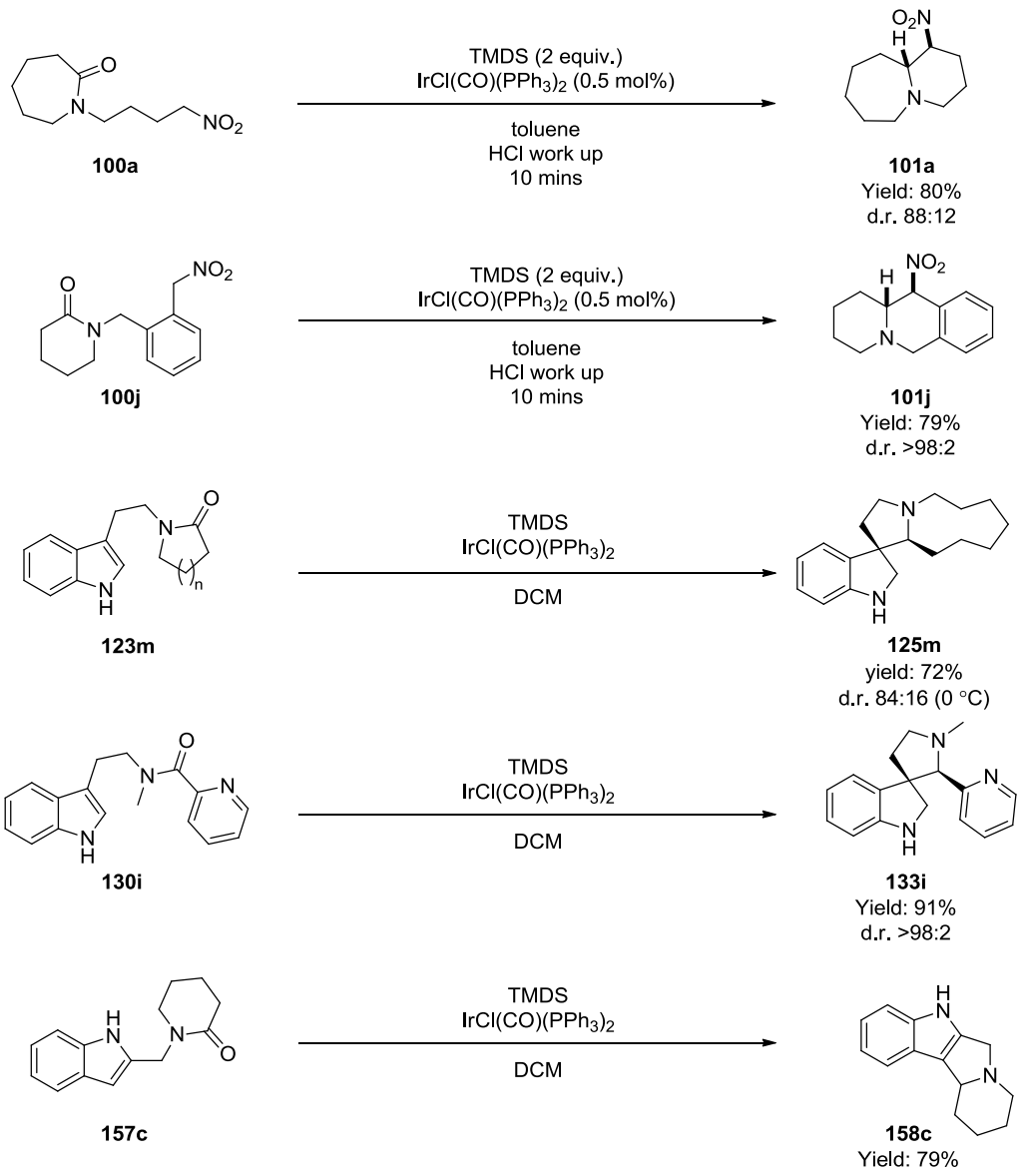

Scheme 4.2. Selection of cyclisation products available *via* partial amide reduction.

This work provides an excellent proof of principle for further reaction development. Such future work could centre around the testing of new tethered nucleophiles for example, silyl-enol-ethers, vinyl-silanes or nucleophilic heterocycles. However, it would be highly attractive to use the partial amide reduction methodology to allow the formation of enamine intermediates (**167**) and subsequently exploit their reactivity (Scheme 4.3). This research, so far suggests that the enamine intermediates are the most favourable intermediate formed *via* the iridium catalysed partial reduction. These intermediates could potentially react with an

appropriate electrophile **168** and in turn cyclise back onto the iminium intermediate **169**. This would allow the formation of cyclohexene products of type **170** (Scheme 4.3).[97]

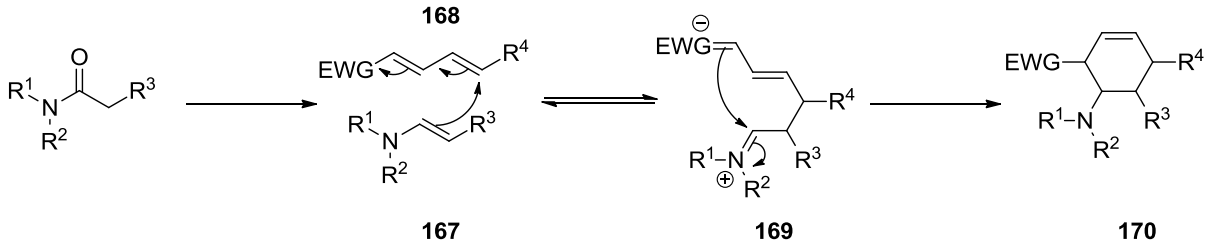

Scheme 4.3. Potential use of the enamine intermediate as a nucleophile.

Another potential use of an enamine intermediate would in a Diels-Alder reaction; partial reduction of β,γ-unsaturated amide **171** to diene **172** may allow this to take place with an appropriate dieneophile **173**, which would afford polysubstituted cyclohexenes of type **174** (Scheme 4.4)**.**[98]

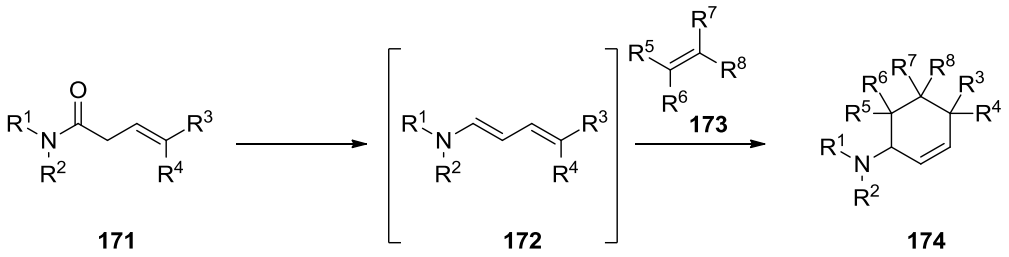

Scheme 4.4. Diels-Alder reaction of diene intermediate form the partial reduction of β,γ-unsaturated amides.

The beauty of this work arises from the ease of amide synthesis as well as its robust nature to a wide range of reagents. This therefore lends the methodology towards total synthesis whereby an amide can be readily formed and carried through a synthesis until it is activated by partial reduction to be used as an iminium intermediate, or potentially as an enamine intermediate.

Investigation into these areas may confirm that partial reduction methodology is a powerful new tool in organic synthesis and provides a novel approach to the use of iminium and enamine intermediates in organic synthesis.

5. Bibliography

[1] Liebig, J. *Liebigs Ann. Chem.* **1860**, *113*, 246.

[2] Bredig, G.; Fiske, P. S. *Bichem. Z,* **1912**, *46*, 7.

[3] (a) Pracejus, H. *Liebigs Ann. Chem.* **1960**, *634*, 9. (b) Pracejus, H. *Liebigs Ann. Chem.* **1960**, *634*, 23.

[4] Hajos, Z. G.; Parrish, D. R. *J. Org. Chem.* **1974**, *39*, 1615.

[5] Ahrendt, K. A.; Borths, C. J.; MacMillan, D. W. C. *J. Am. Chem. Soc.* **2000**, *122*, 4243.

[6] (a) Jen, W. S.; Wiener, J. J. M.; MacMillan, D. W. C. *J. Am. Chem. Soc.* **2000**, *122*, 9874. (b) Karlsson, S.; Hogberg, H. E. *Tetrahedron: Asymmetry* **2002**, *13*, 923.

[7] Paras, N. A.; MacMillan, D. W. C. *J. Am. Chem. Soc.* **2001**, *123*, 4370.

[8] Brown, S. P.; Goodwin, N. C.; MacMillan, D. C. W. *J. Am. Chem. Soc.* **2003**, *125*, 1192.

[9] a) Dalko, P.I.; Moisan, L. *Angew. Chem., Int. Ed*. **2004**, *43*, 5138; b) Dalko, P.I.; Moisan, L. *Angew. Chem., Int. Ed*. **2001**, *41*, 3726; c) Bertelsen, S.; Jørgensen, K. A. *Chem. Soc. Rev.* **2009**, *38***,** 2178.

[10] a) Trost. B. M.; *Science*. **1991**, *254*, 1471; b) Trost. B. M.; *Angew. Chem., Int. Ed*. **1995**, *34*, 259.

[11] a) Tietze, L. F.; *Chem. Rev.* **1996**, *96*, 115; b) Nicolaou, K. C.; Chen, J. S. *Chem. Soc. Rev.* **2009**, *38*, 2993.

[12] Paterson, I.; Tillyer, R. D.; Smaill, J. B. *Tetrahedron Lett.* **1993**, *34*, 7137.

[13] B. E. McCarry, R. L. Markezich, W. S. Johnson, *J. Am. Chem. Soc.* **1973**, *95*, 4416

[14] a) Taylor, M. S.; Jacobsen, E. N. *Angew. Chem., Int. Ed.* **2006**, *45*, 1520; b) Schreiner, P, R.; Wittkopp, A. *Org. Lett*. **2002**, *4*, 217; c) Schreiner, P, R.; Wittkopp, A. *Chem.--Eur. J*. **2003**, *9*, 407.

[15] a) Kampen, D.; Ladépêche, A.; Clasen, G.; List, B. *Adv. Synth. Catal.* **2008,** *350*, 962; b) Hatano, M.; Maki, T.; Moriyama, K.; Arinobe, M.; Ishihara, K. *J. Am. Chem. Soc.* **2008,** *130*, 16858; c) Pan, S. C.; List, B. *Chem. Asian J.* **2008,** *3*, 430; d) Hatano, M.; Ishihara, K. *Synthesis*, **2010,** 3785.

[16] Akiyama, T.; Itoh, J.; Yokota, K.; Fuchibe, K. *Angew. Chem., Int. Ed.* **2004**, *43*, 1566.

[17] Uraguchi, D.; Terada, M. *J. Am. Chem. Soc.* **2004**, *126*, 5356.

[18] (a) Rueping, M.; Nachtsteim, B. J.; Ieawsuwan, W.; Atodiresei, I. *Angew. Chem., Int.Ed.* **2011**, *50*, 6706. (b) Terada, M. *Synthesis*. **2010**, *12*, 1929. (c) Terada, M. *Chem. Commun.* **2008**, 4097. (d) Akiyama, T. *Chem. Rev.* **2007**, *107*,5744. (e) Akiyama, T.; Itoh, J.; Fuchibe,

K. *Adv. Synth. Catal.* **2006**, *348*, 999. (f) de Vries, J. G.; Mrsic, N. *Catal. Sci. Technol.* **2011**, *1*, 727.

[19] Terada, M.; Machioka, K.; Sorimachi, K. *Angew. Chem., Int. Ed.* **2006**, *45*, 2254.

[20] Akiyama, T.; Tamura, Y.; Itoh, J.; Morita, H.; Fuchibe, K. *Synlett.* **2006**, 141.

[21] a) Uraguchi, D.; Sorimachi, K.; Terada, M. *J. Am. Chem. Soc.* **2004**, *126*, 11804. b) Kang, Q.; Zhao, Z.-A.; You, S.-L. *J. Am. Chem. Soc.* **2007**, *129*, 1484.

[22] a) Rueping, M.; Sugiono, E.; Azap, C.; Theissmann, T.; Bolte, M. *Org. Lett.* **2005**, *7*, 3781. b) Hoffmann, S.; Seayad, A. M.; List, B. *Angew. Chem., Int. Ed.* **2005**, *44*, 7424.

[23] a) Simon, L.; Goodman, J. M. *J. Org. Chem.* **2011**, 76, 1775; b) Grayson, M. N.; Pellegrinet, S.C.; Goodman, J. M. *J. Am. Chem. Soc.* **2012**, 134, 2716; c) Simon, L.; Goodman, J. M. *J. Org. Chem.* **2010**, 75, 589; d) Simon, L.; Goodman, J. M. *J. Am. Chem. Soc.* **2008**, 130, 8741; e) Simon, L.; Goodman, J. M. *J. Am. Chem. Soc.* **2009**, 131, 4070.

[24] Wakchaure, V. N.; Zhou, J.; Hoffmann, S.; List, B. *Angew. Chem., Int. Ed.* **2010**, *49*, 4612.

[25] Uraguchi, D.; Terada, M. *J. Am. Chem. Soc*. **2004**, *126*, 5356.

[26] Jia, Y.-X.; Zhong, J.; Zhu, S.-F.; Zhang, C.-M.; Zhou, Q.-L. *Angew. Chem., Int. Ed*. **2007**, *46*, 5565.

[27] Dagousset, G.; Drouet, F.; Masson, G.; Zhu, J. *Org. Lett.* **2009**, *11*, 5546.

[28] For recent reviews on cascade and dual catalysis, see: (a) Rueping,M.; Koenigs, R. M.; Atodiresei, I. *Chem.--Eur. J.* **2010**, *16*, 9350; (b)Shao, A.; Zhang, H. *Chem. Soc. Rev.* **2009**, *38*, 2745; (c) Parra, A.; Reboredo, S.; Martin Castro, A. M.; Aleman *J. Org. Biomol. Chem.***2012**, *10*, 5001; (d) Zhong, C.; Shi, X. *Eur. J. Org. Chem.* **2010**, *16*, 2999; (e) Loh, C. C. G.; Enders, D. *Chem.--Eur. J.* **2012**, *18*, 10212; (f) Grondall, C.; Jeanty, M.; Enders, D. *Nat. Chem*. **2010**, *2*, 167; (g) Du,Z.; Shao, Z. *Chem. Soc. Rev*. **2013**, *42*, 1337.

[29] Ibraham, I.; Cordova, A. *Angew. Chem., Int. Ed*. **2006**, *45*, 1952

[30] (a) Hashmi, S. K. *Chem. Rev*. **2007**, *107*, 3180. (b) Li, Z.; Brouwer, C.; He, C. *Chem. Rev*. **2008**, *108*, 3239; (c) Arcadi, A. *Chem. Rev*. **2008**, *108*, 3266; (d) Gorin, D. J.; Sherry, B. D.; Toste, F. D. *Chem. Rev*. **2008**, *108*, 3351; (e) Corma, A.; Leyva-Perez, A.; Sabater, M. J. *Chem. Rev*. **2011**, *111*, 1657; (f) Rudolph,M.; Hashmi, A. S. K. *Chem. Commun*. **2011**, *47*, 6536; (g) Hashmi, A. S. K.; Hutchings, G. J. *Angew. Chem., Int. Ed.* **2006**, *45*, 7896; (h)Toste, F. D. *Nature*. **2007**, *446*, 395. (i) *Modern Gold Catalyzed Synthesis*; Hashmi, A. S. K., Toste, F. D., Eds.; WILEY-VCH: Weinheim, **2012**. (j) Furstner, A. *Chem. Soc. Rev*. **2009**, *38*, 3208.

[31] Liu, X.-Y.; Che, C.-M. *Org Lett.* **2009**, *11*, 4204.

[32] Han, Z.-Y.; Xiao, H.; Chen, X.-H.;Gong, L.-Z. *J. Am .Chem. Soc.* **2009**, *131*, 9182.

[33] Muratore, M. E.; Holloway, C. A.; Pilling, A. W.; Storer, I.; Trevitt, G.; Dixon, D. J. *J. Am. Chem. Soc.* **2009**. *131*, 10796

[34] a) Alemán, J.; Solar, V.; Alvarez-Valdés, A.; Ríos-Luci, C.; Padrón, J. M.; Navarro-Ranninger C. *Med. Chem. Commun.* **2011**, *2*, 789; b) Supuran, C. T.; Scozzafava, A. *Expert Opin. Ther. Pat.* **2002**, 12, 217

[35]http://cbc.arizona.edu/njardarson/group/sites/default/files/Top200%20Pharmacetical%20Products%20by%20US%20Retail%20Sales%20in%202012_0.pdf

[36] Franzen, V. *Chem. Berich.* **1954**, *87*, 1219

[37] Cheung, F. K.; Hayes, A. M.; Morris, D, J.; Wills, M. *Org. Biomol. Chem.* **2007**, *5*, 1093.

[38] Leyva, A.; Corma, A. *J. Org. Chem.* **2009**, *74*, 2067.

[39] a) Jacobi, P.; Rajeswari. *Tetrahedron Lett.* **1992**, *33*, 6231; b) Jacobi, P.; Rajeswari. *Tetrahedron Lett.* **1992**, *33*, 6235; c) Jacobi, P. A.; Brielmann, H, L.; Hauck, S, I. *Tetrahedron Lett.* **1995**, *36*, 1193; d) Jacobi, P. A.; Guo, J.; Zheng, W. *Tetrahedron Lett.* **1995**, *36*, 1197; e) Yasuhara, A.; Kanamori, Y.; Kaneko, M.; Numata, A.; Kondo, Y.; Sakamoto, T. *J. Chem. Soc. Perkin Trans. 1*. **1999**. 529.

[40] Hiroya, K.; Jouka, R.; Kameda, M.; Yashara, A.; Sakamoto, T. *Tetrahedron* **2001**, *57*, 9697.

[41] Brak, K.; Jacobsen, E. N. *Angew. Chem., Int. Ed.* **2013**, *52*, 534.

[42] Schmidbaur, H.; Schier, A. *Organometallics*, **2010**, *29*, 2.

[43] a) Soriano, E.; Marco-Contelles, J. *Chem.--Eur. J.* **2008**, *14*, 6771; b) Soriano, E.; Marco-Contelles, J. *Acc. Chem. Res.* **2009**, *42*, 1026; c) Li, G. T.; Zhang, G. Z.; Zhang, L. M. *J. Am. Chem. Soc.* **2008**, *130*, 3740.

[44] a) LaLonde, R. L.; Brenzovich Jr, W. E.; Benitez, D.; Tkatchouk, E.; Kelley, K.; Goddard III, W. A.; Toste. F. D.; *Chem. Sci.* **2010**, *1*, 226; b) Liu, L.; Hammond, G. B. *Chem. Soc. Rev.* **2012**, *41*, 3129.

[45] Raducan, M.; Moreno, M.; Boura, C;. Echavarren, A. M. *Chem. Commun.* **2012**, *48*, 52.

[46] Corriu, R. J. P.; Moreau, J. J. E.; Pataud-Sat, M. *J. Organomet. Chem.* **1982**, *228*, 301.

[47] a) Berk, S. C.; Kreutzer, K. A.; Buchwald, S. L.; *J. Am. Chem. Soc.* **1991**, *113*, 5093; b) Berk, S. C.; Buchwald, S. L.; *J. Org. Chem.* **1992**, *57*, 3751; c) Barr, K. J.; Berk, S. C.; Buchwald, S. L.; *J. Org. Chem.* **1994**, *59*, 4323; d) Reding, M. T.; Buchwald, S. L.; *J. Org. Chem.* **1995**, *60*, 7884; e) Verdaguer, X.; Hansen, M. C.; Berk, S. C.; Buchwald, S. L.; *J. Org. Chem*. **1997**, *62*, 8522.

[48] Kuwano, R.; Takahashi, M.; Ito, Y. *Tetrahedron Lett*. **1998**, *39*, 1017.

[49] Addis, D.; Das, S.; Junge, K.; Beller, M. *Angew. Chem., Int. Ed*. **2011**, *50*, 6004.

[50] Igarashi, M.; Fuchikami, T. *Tetrahedron Lett*. **2001**, *42*, 1945.

[51] Sasakuma, H.; Motoyama, Y.; Nagashima, H. *Chem. Commun*. **2007**, 4916.

[52] Hanada, S.; Tsutsumi, E.; Motoyama, Y.; Nagashima, H. *J. Am. Chem. Soc*. **2009**, *131*, 15032.

[53] Zhou, S.; Junge, K.; Addis, D.; Das, S.; Beller, M. *Angew. Chem. Int. Ed*. **2009**, *48*, 9507.

[54] Das, S.; Addis, D.; Zhou, S.; Junge, K.; Beller, M. *J. Am. Chem. Soc*. **2010**, *132*, 1770.

[55] Herbert, C.; Tsukamoto, A. *J. Am. Chem. Soc.* **1961**, 4549,

[56] Rapoport, H.; Gless, R. D. *J. Org. Chem.* **1979**, *44*, 1324.

[57] Connolly, P. J.; Heathcock, C. H. *J. Org. Chem*. **1985**, *50*, 4135.

[58] Jakubec, P. J.; Cockfield, D.; Dixon, D.J. *J. Am. Chem. Soc.* **2009,** *131*, 16632

[59] Belanger, G.; Larouche-Gauthier, R.; Menard, F.; Nantel, M.; Barabe, F. *Org. Lett.* **2005**. *7*, 4431.

[60] Nicolaou, K. C.; Dalby, S. M.; Majumder, U. J. Am. Chem. Soc. **2008**, *130*, 14942.

[61] Xiao, K.–J.; Luo, J.-M.; Ye, K.-Y.; Wang, Y.; Huang, P.-Q. *Angew. Chem. Int. Ed*. **2010,** *49*, 3037.

[62] Henry, L. *Bull. Acad. Roy. Belg.* **1897**, *33*, 412.

[63] a) Mousset, T. *Bull. Acad. Roy. Belg.* **1901**, 622; b) Duden, P.; Bock, K.; Reid, H. J. *Ber.* **1905**, *33*, 2036; c) Cerf de Mauny, H. *Bull. Soc. Chim.* 1**931**, *4*, 1451; d) Cerf de Mauny, H. *Bull. Soc. Chim.* **1931**, *4*, 1460.

[64] a) M. Senkus, *J. Am. Chem. Soc.* **1946**, *68*, 10; (b) H. G. Johnson, *J. Am. Chem. Soc.* **1946**, *68*, 12; (c) H. G. Johnson, *J. Am. Chem. Soc.* **1946**, *68*, 14.

[65] Hurd, C. D.; Strong, J. S. *J. Am. Chem. Soc.* **1950**, *72*, 4813.

[66] Noble, A.; Anderson, J. C. *Chem. Rev.* **2013**, *113*, 2887.

[67] Ono, N.; Kaji, A. *Synthesis*. **1986**, *9*, 693.

[68] Ballini, R.; Petrini, M. *Tetrahedron*. **2004**, *60*, 1017.

[69] Jakubec, P.; Hawkins, A.; Felzmann, W.; Dixon, D. J. *J. Am. Chem. Soc.* **2012**, *134*, 17482.

[70] For a selection of metal catalysed silane reductions see: a) Hanada, S.; Tsutsumi, E.; Motoyama, Y.; Nagashima, H. *J. Am. Chem. Soc.* **2009**, *131*, 15032; b) Sakai, N.; Fujii, K.; Konakahara, T. *Tetrahedron Lett*. **2008**, *49*, 6873; c) Matsubara, K.; Iura, T.; Maki, T.; Nagashima, H. *J. Org. Chem.* **2002**, *67*, 4985; d) Hanada, S.; Ishida, T.; Motoyama, Y.; Nagashima, H. *J. Org. Chem.* **2007**, *72*, 7551; e) Igarashi, M.; Fuchikami, T. *Tetrahedron*

Lett. **2001**, *42* 1945; f) Das, S.; Addis, D.; Zhou, S.; Junge, K.; Beller, M. *J. Am. Chem. Soc*. **2010**, *132*, 1770. g) Connolly, P. J.; Heathcock, C. H. *J. Org. Chem.* **1985**, *50*, 4135; h) Sanders, E. B.; DeBardeleben, J. F.; Osdene, T. S. *J. Org. Chem.* **1975**, *40*, 2848; i) Gless, R. D.; Rapoport. H. *J. Org. Chem.* **1979**, *44*, 1324.

[71] Walser, A.; Benjamin, Sr, L. E.; Flynn, T.; Mason, C.; Schwartz, R. *J. Org. Chem*, **1978**, *43*, 937; b) Kim, H. Y.; Li, J.-Y.; Kim, S.; Oh, K. *J. Am. Chem. Soc.* **2011**, *133*, 20750; c) Jia, Z.–X.; Luo, Y.–C.; Xu, P.–F. *Org. Lett*, **2011**, *13*, 832. d) Anderson, J. C.; Noble, A.; Torres, P. R. *Tetrahedron Lett*, **2012**, *53*, 5707.

[72] Daly, J. W. *J. Nat. Prod.* **1998,** *61*, 162; (b) Pronin, S. V.; Tabor, M. G.; Jansen, D. J.; Shenvi, R. A. *J. Am. Chem. Soc.* **2012,** *134*, 2012. a) Charette, A. B.; Chua, P. J. *J. Org. Chem.* **1998,** *63*, 908; b) Belanger, G.; Larouche-Gauthier, R.; Menard, F. Nantel, M. Barabe, F. *Org. Lett*. **2005**, *7*, 4431; c) Nicolaou, K. C.; Dalby, S. M.; Majumder, U. *J. Am. Chem. Soc*. **2008**, *130*, 14942; d) Xiao, K.–J.; Luo, J.-M.; Ye, K.-Y. Wang, Y.; Huang, P.-Q. *Angew. Chem., Int. Ed*. **2010,** *49*, 3037.

[73] Ballini, R.; Petrini, M. *Tetrahedron*. **2004**, *60*, 1017.

[74] Laval, S.; Dayoub, W.; Favre-Reguillon, A.; Demonchaux, P.; Mignani, G.; Lemaire, M. *Tetrahedron Lett.* **2010,** *51*, 2092.

[75] a) P. J. Connolly, C. H. Heathcock, *J. Org. Chem.* **1985**, *50*, 4135; b) E. B. Sanders, J. F. DeBardeleben, T. S. Osdene, *J. Org. Chem.* **1975**, *40*, 2848; c) R. D. Gless, H. Rapoport. *J.* Org. *Chem.***1979**, *44*, 1324.

[76] Reviews on metal catalysed silane reduction: D. Addis, S. Das, K. Junge, M. Beller, *Angew. Chem., Int. Ed.* **2011**, *50*, 6004.

[77] Sakai, N.; Fujii, K.; Konakahara, T. *Tetrahedron Lett.* **2008,** *49*, 6873.

[78] Kuwano, R.; Takahashi, M.; Ito, Y. *Tetrahedron Lett.* **1998,** *39*, 1017.

[79] Vaska, L.; DiLuzio, J. W. *J. Am. Chem. Soc.* **1961,** *83*, 2784.

[80] Motoyama, Y.; Aoki, M.; Takaoka, N.; Aoto, R.; Nagashima, H. *Chem. Commun.* **2009,** *13*, 1574.

[81] Kornblum. N.; Weaver. W. M. J. Am. Chem. Soc. **1958**, *80*, 4333

[82] a) R. W. Fitch, H. M. Garraffo, T. F. Spande, H. J. C. Yeh, J. W. Daly, *J. Nat. Prod*. **2003**, *66*, 1345.

[83] Fitch, R. W.; Sturgeon, G. D.; Patel, S. R.; Spande, T.F.; Garraffo, H.M.; Daly, J. W.; Blaauw, R. H. *J. Nat. Prod.* **2009,** *72*, 243.

[84] Thrippleton, M. J.; Keeler, J. *Angew. Chem., Int. Ed*. **2003**, *42*, 3938.

[85] a) Hoefgen, B.; Decker, M.; Mohr, P.; Schramm, A. M.; Rostom, S. A. F.; El-Subbagh, H.; Schweikert, P. M.; Rudolf, D. R.; Kassack, M. U.; Lehmann, J. *J. Med. Chem.* **2006**, *49*, 760. b) Sanaboina, C.; Jana, S.; Chidara, S.; Patro, B.; Raolji, G. B.; Eppakayala, L. *Tetrahedron. Lett*, **2012**, *53*, 5027. c) Szawkalo, J.; Czarnocki, S. J.; Zawadzka, A.; Wojtasiewicz, K.; Leniewski, A.; Maurin, J. K.; Czarnocki, Z.; Drabowicz, J. Tetrahedron: Asymmetry. **2007**, *18*, 406.

[86] a) Gan, C. Y.; Low, Y.-Y.; Etoh, T.; Hayashi, M.; Komiyama, K.; Kam, T.-S. *J. Nat. Prod.* **2009**, *72*, 2098; b) Tan, S.-J.; Low, Y.-Y.; Choo, Y.-M.; Abdullah, Z.; Etoh, T.; Hayashi, M. Komiyama, Kam, T.-S. *J. Nat. Prod.* **2010**, *73*, 1891; c) Mizoguch, H.; Oikawa, H.; Oguri, H. *Nat. Chem*. **2014**, *6*, 57.

[87] Li, J.; Wu, N.; Tian, Y.; Zhang, J.; Wu, S. *ACS Med. Chem. Lett.* **2013**, *4*, 806; b) Powell, N. A.; Kohrt, J. T.; Filipski, K. J.; Kaufman, M.; Sheehan, D.; Edmunds, J. E.; Delaney, A.; Wang, Y.; Bourbonais, F.; Lee, D.-Y.; Schwende, F.; Sun, F.; McConnell, P.; Catana, C.; Chen, H.; Ohren, J.; Perrin, L. A. *Bioorg. Med. Chem. Lett.* **2012**, *22*, 190; c) Sluder, A.; Shah, S.; Cassayre, J.; Clover, R.; Maienfisch, P.; Molleyres, L. P.; Hirst, E, A.; Flemming, A. J.; Shi, M.; Cutler, P.; Stanger, C.; Roberts, R. S.; Hughes, D. J.; Flury, T.; Robinson, M. P.; Hillesheim, E.; Pitterna, T.; Cederbaum, F.; Worthington, P. A.; Crossthwaite, A. J.; Windass, J. D.; Currie, R. A.; Earley, F. G. P. *PLOS. ONE*. **2012**, *7*, 1 d) Patchett, A. A.; Nargund, R. P.; Tata, J. R.; Chen, M.-H.; Barakat, K. J.; Johnston, D. B. R.; Cheng, K.; Chan, W. W.-S.; Butler, T. B.; Hickey. G.; Jacks, T.; Schleim, K.; Pong, S.-S.; Chaung, L.-Y. P.; Chen, H. Y.; Frazier, E.; Leung, K. H.; Chiu, S,-H. L.; Smith, R, G. *Proc. Natl. Acad. Sci. USA*, **1995**, *92*, 7001; e) Abdel-Rahman, A. H.; Keshk, E. M.; Hannab, M. A.; El-Bady, S. M. *Bioorg. Med. Chem.* **2004**, *12*, 2483.

[88] a) Ly, T. W.; Liao, J.-H.; Shia, K.-S.; Liu, H.-J. *Synthesis.* **2004**, *2*, 271; b) Kornblum, N.; Jones, W. J.; Anderson, G. J. *J. Am. Chem. Soc.* **1959**, *81*, 4113; c) Kornblum, N.; Powers, J. W.; Anderson, G. J.; Jones, W. J.; Larson, H. O.; Levand, O.; Weaver, W. M. *J. Am. Chem. Soc.* **1957**, *79*, 6562.

[89] Ganem, B. *Tetrahedron. Lett*. **1974**, *11* ,917.

[90] Godfrey, A. G.; Ganem, B. *Tetrahedron. Lett*. **1990**, *131*, 4825.

[91] Jenkins, P. R.; Wilson, J.; Emmerson, D.; Garcia, M. D.; Smith, M. R.; Gray, S. J.; Britton, R. G.; Mahale, S.; Chaudhuri, B. *Bioorg. Med. Chem.* **2008**, *16*, 7728.

[92] a) Casalnuovo, A. L.; Calabrese, J. C.; Milstein, D. *J . Am. Chem. Soc.***1988**, *110*, 6738; b) Sevov, C. S.; Hartwig, J. F. *J. Am. Chem. Soc.* **2013**, *135*, 2116; c) Sevov, C. S.; Zhou, J. S.;

Hartwig, J. F. *J. Am. Chem. Soc.* **2014**, *136*, 3200; d) Zhou, J. S.; Hartwig, J. F. *J. Am. Chem. Soc.* **2008**, *130*, 12220.

[93] a) Zeni, G.; Larock, R. C. *Chem. Rev.* **2006**, *106*, 4644; b) Grigg, R.; Sridharan, V, Sykes, D. A. *Tetrahedron*. **2008**, *64*, 8952.

[94] a) Pouilhès, A.; Baltaze, J-. P.; Kouklovsky, C. *Synlett*. **2013**, *24*, 1805; b) Gómez-SanJuan, A.; Sotomayor, N.; Lete, E. *Tetrahedron Lett*, **2012**, *53*, 2157.

[95] He, Y.; Lin, M.; Li, Z.; Liang, X.; Li, G.; Antilla, J. C. *Org, Lett*, **2011**, *13*, 4490.

[96] Sifferlen, T.; Koberstein, R.; Cottreel, E.; Boller, A.; Weller, T.; Gatfield, J.; Brisbare-Roch, C.; Jenck, F.; Boss, C. *Bioorg. Med. Chem. Lett.* **2013**, *23*, 2212.

[97] Padwa, A.; Gareau, Y.; Harrison, B.; Rodriguez, A. *J. Org. Chem*, **1992**, *57*, 3540.

[98] a) Kozmin, S. A.; Rawal, V. H. J. Am. Chem. Soc, **1999**, *121*, 9562; b) Kozmin, S. A.; Iwama, T.; Huang, Y.; Rawal, V. H. J, Am, Chem. Soc, **2002**, *124*, 4628.